DEVELOPMENT AND EVALUATION OF A RADAR SYSTEM FOR GROUND SURFACE DETECTION IN WILD BLUEBERRY FIELDS

by

Muhammad Saad

Submitted in Partial Fulfillment of The Requirements
for the Degree of Master of Science

at

Dalhousie University
Halifax, Nova Scotia
April 2021

DEDICATION

This MSc thesis dissertation is dedicated to my loving parents, Abdul Aleem and Lala Rukh Rana. Thank you for continually supporting me in my endeavors to better myself and the world around me.

Author

Muhammad Saad

TABLE OF CONTENTS

LIST OF TABLES

LIST OF FIGURES

ABSTRACT

Mechanical wild blueberry harvest efficiency depends heavily on operator skill. The harvesting picking reel requires accurate and precise positioning based on fruit zone, field topography and foreign obstacles. Spatially variable topography in wild blueberry fields poses a serious challenge for the operators to maintain the optimum head height for efficient harvester operation. In this research study, the potential of microwave radar technology was examined for detecting and measuring the ground surface height in wild blueberry fields by comparing the performance of three selected radars. Results indicated that the Terrahawk® radar outperformed other selected radars (0.21 cm $\leq$ SD $\leq$ 1.12 cm, 4.45 cm $\leq$ RMSE $\leq$ 5.62 cm) and successfully detected the ground surface non-destructively within wild blueberry fields in dynamic and standstill conditions ($R^2 > 0.92$). The developed ground surface detection system exhibited great potential in the automation of harvester picking reel by utilizing real-time ground surface detection in wild blueberry fields.

LIST OF ABBREVIATIONS USED

AGH	Actual Ground Surface Height
AiP	Antenna in Package
Ait	Aiton
ANOVA	Analysis of Variance
AYMS	Automated Yield Monitoring System
CAN	Controller Area Network
cm	Centimeter
CV	Coefficient of Variation
d	Index of Agreement
DBE	Doug Bragg Enterprises
dBi	Decibel Relative to Isotrope
DEM	Digital Elevation Model
DGPS	Differential Global Positioning Systems
DSP	Digital Signal Processing
EHF	Extremely High Frequency
ES	Early-summer
FC	Fruit Count
FFT	Fast Fourier Transform
FMCW	Frequency Modulated Continous Wave
FOI	Factor of Interest
FZH	Fruit Zone Height
g	Gram
GHz	Gigahertz
GIS	Geographical Information Systems
GPU	Graphics Processing Unit
GUI	Graphical User Interface
h^{-1}	Per Hour
ha	Hectare

HF	High Frequency
Hz	Hertz
IQR	Interquartile Range
km	Kilometer
LF	Low Frequency
LiDAR	Light Detection and Ranging
LS	Late-summer
LSD	Least Significant Difference
m	Meter
M/C	Metal/Control
M/G	Metal/Grass
M/H	Metal/Hay
MBE	Mean Bias Error
MCU	Microcontroller
MF	Medium Frequency
MLR	Multiple Linear Regression
mm	Millimeter
MMC	Multiple Means Comparison
MS	Mid-summer
ms	Millisecond
MSI	Micro-Star International
mV	Millivolts
n	Number of observations
N	Total number of samples
NS	Non-Significant
O-RMSE	Overall Root Mean Square Error
PCR	Pulse Coherent Radar
PGSH	Predicted Ground Surface Height
PMDC	Permanent Magnet Direct Current
R^2	Coefficient of Determination

RF	Radio Frequency
RMS	Root Mean Square
RMSE	Root Mean Square Error
RTK-GPS	Real-Time Kinematic Global Positioning System
S/C	Soil/Control
S/G	Soil/Grass
S/H	Soil/Hay
SAR	Synthetic Aperture Radar
SD	Standard Deviation
SDi	Stem Density
SFMV	Specialized Farm Motorized Vehicle
SH	Stem Height
SHF	Super High Frequency
SMMS	Slope Measurement and Mapping System
ST	Stem Thickness
TOF	Time of Flight
UHF	Ultra High Frequency
USB	Univeral Serial Bus
UWB	Ultrawide Band
VHF	Very High Frequency
VLF	Very Low Frequency
W/C	Wood/Control
W/G	Wood/Grass
W/H	Wood/Hay
WBPANS	Wild Blueberry Producers Association of Nova Scotia
τ	Treatment
°C	Degree Celsius
3D	3 Dimensional

ACKNOWLEDGEMENTS

First and foremost, I want to express my gratitude to Allah Almighty for providing me with the strength to complete this study, and I express my gratitude to Him for every good that comes into my life. I would like to thank my supervisors, Dr. Travis Esau, and Dr. Qamar Zaman, for their professional counsel, encouragement, and persistence during the course of my research project. Thank you for your thoughtful, positive, and constructive feedback. Your insightful and positive input has substantially strengthened my understanding of the wild blueberry industry, as well as my writing and analytical abilities. I would like to express sincere appreciation to my committee members, Dr. Arnold Schumann, and Dr. Aitazaz Farooque, for their ultimate support. I am thankful for their trust in me as well as their support, which never ceased to raise my spirits and assist me in remaining engaged and consistent throughout my studies.

I would like to acknowledge the endless support of Dr. Travis Esau and Dr. Aitazaz Farooque, who have been very approachable to give me guidance at each stage of my research and to answer any questions I had. I would also like to express my deepest appreciation to Dr. Qamar Zaman, who has given me the chance to collaborate with the Mechanized Systems and Precision Agriculture research team and has supported me with different facets of this project from start to finish. I would also like to acknowledge the helpful and kind support of Dr. Tessema Astatkie during the design of experiments and statistical analyses for my research project.

Carl Bragg, Stephen Bragg, Peter Swinkels, and Joe Slack deserve special thanks for their unwavering encouragement during my research. I would like to express my sincere gratitude to Doug Bragg Enterprise Limited and the National Science and Engineering

Research Council (NSERC) who have generously offered the financial assistance required to finish this project. I would also like to thank the wild blueberry growers and the Wild Blueberry Producers Association of Nova Scotia (WBPANS) for allowing me to use their fields for data collection.

Mechanized Systems and Precision Agriculture research teams' graduate students have contributed countless hours to assist me with data collection and provide intuitive input on my research. Craig MacEachern, Anup Kumar Das, Karen Esau, Ahmed Hanmbal Khan, Patrick Hennessy, and Mathieu Bilodeau deserve special thanks for their contributions to my project. Thank you to all of the summer students who have worked with the Mechanized Systems and Precision Agriculture research team over the last two years. Connor Mullins, Jack Lynds, Derrick Ouma, and Fady Ramsis, all put in a lot of effort to gather data during this research project. Thank you for your immense support.

My acknowledgments would be incomplete if I didn't thank the most substantial source of support, my family. I want to thank my caring parents, brothers, sisters, and other family members for their unwavering love and care during this journey. In the end, I am deeply obliged to Mr. and Mrs. Zaman for treating me with immense care and for helping me to acclimatize to Canada. All of this wouldn’t be possible without your kind support.

CHAPTER 1: INTRODUCTION

1.1 Literature Review

1.1.1 Wild Blueberry Cropping System

Northeastern North America is the world's largest producer of the wild blueberry (Vaccinium angustifolium Ait.) fruit, where marketed production was increased from 104,706 tons in 2015 to about 146,749 tons in 2016 (Statistics Canada, 2021). Wild blueberry production contributed about $600 million to the national economy in 2016 (Agriculture and Agri-Food Canada, 2016) and more than $100 million to the Nova Scotia economy in 2017 (WBPANS, 2018). Currently, the wild blueberry industry is facing challenges due to frost damage in the Maritime region (Khan, 2019), which led to comparatively low marketed fruit production in 2017 (101,943 tons), 2018 (90,420 tons), 2019 (96,948 tons), and 2020 (78,306 tons) respectively (Statistics Canada, 2021). Quebec, Nova Scotia, and New Brunswick are major contributors to wild blueberry production in Canada, providing 88% of the total wild blueberry production in 2016 (Yarborough, 2018). North-eastern North America contributed 90% to the production of worldwide wild blueberries in 2016 (Yarborough, 2018). The wild blueberry industry has grown rapidly in Canada from 7,700 ha of new acreage in 2009 (Yarborough, 2009), to 79,329 ha in 2016 (Statistics Canada, 2018).

Wild blueberry crop is one of the four major fruit crops native to north-eastern North America (Yarborough, 1997). Wild blueberry is a unique crop because it is not cultivated as other horticultural crops (Zaman et al., 2009). The plants commonly emerge from native stands followed by the removal of competing natural vegetation by the growers

(Eaton, 1988). Wild blueberry fields are developed by clearing woodlands and removing competing vegetation (Eaton, 1988). These fields are managed on a bi-year production cycle, with the perennial shoots pruned in alternative years to optimize floral bud initiation, fruit set, yield, and for ease of mechanical harvesting (Hall et al., 1979; Jordan & Eaton, 1995; Kinsman, 1993). Wild blueberry crop production is affected by management practices including pruning, weed, insect and disease control, irrigation, and fertilizer applications (Hall et al., 1979). Selective herbicides, fungicides, and fertilizers are applied for optimizing plant growth to encourage improved berry production (Esau et al., 2014). Newly developed blueberry fields can have large weed patches and bare spots (Zaman et al., 2009). Wild blueberries are low growing plants with the new shoots of maturing plants developing from dormant buds on underground stems called rhizomes, which originate from seedlings (Hall et al., 1979; Kinsman, 1993). The stem height of the wild blueberry plant typically ranges from 5 to 30 cm and the fruit size ranges from approximately 0.48 to 1.27 cm (Farooque et al., 2014). Wild blueberry crop is pruned either by mowing or burning in the early spring of the vegetative year or late in the fruit year after the harvest (Eaton, 1988). The environmental factors (Barker et al., 1964; Vander Kloet, 1978; Hepler & Yarborough, 1991), soil conditions (Farooque et al, 2012), and climatic factors (Hall et al., 1979) also play a major role in wild blueberry growth and development.

Wild blueberry crops can be harvested using manual hand rakes or mechanical harvester in August to mid-September when approximately 90 percent of berries are ripe (Kinsman, 1993; Ali, 2016; Farooque et al., 2014). Presently, more than 80% of the wild blueberry fields in Canada are harvested using commercial mechanical harvesters (Esau et

al., 2018), while the remaining fields are hand raked due to extremely rough terrains (Agriculture and Agri-Food Canada, 2017).

1.1.2 Mechanical Wild Blueberry Harvester

Wild blueberries have been hand raked using metal rakes over the past 100 years (Yarborough, 2001). Harvesting losses with hand raking practices varied from 15 to 40% with an overall average of 20% (Kinsman, 1993). Initial efforts to reduce production cost and reduce berry losses using mechanical harvesters began in the 1950s (Dale et al., 1994), but a functional harvester was not manufactured until the 1980s (Hall et al., 1983). Underlying factors for the development of mechanical harvester include the significant increase in blueberry yields in recent years (Esau et al., 2018), increase in labor wages (Government of Nova Scotia, 2019), short harvesting season, and shortage of labor (Yarborough, 2001). During the past 10 years, most wild blueberry farms in Atlantic Canada were mechanically harvested (Agriculture and Agri-Food Canada, 2017). Major challenges faced during the development of a mechanical harvester were uneven field topography, low plant height, presence of weeds and debris, and bare soil (Farooque, 2015). Although various prototypes of mechanical harvesters have been developed over the years (Rhodes, 1961; Richard, 1982; Farooque et al., 2014; Esau et al., 2018) but improving the field and harvest efficiency remains an on-going challenge.

The very first wild blueberry harvester was modified from a pre-existing mechanical cranberry picking machine and consisted of six combs that raked in the opposite direction of travel of the machine (Dale et al., 1994). The rigorous harvesting operations resulted in high fruit loss and soil digging problems with this harvester (Dale et

al., 1994). Gray (1970) modified this mechanical harvester by adding a hollow raking reel mechanism, which provided the basis of commercially used harvester today. It had a picking efficiency of 80% when it was developed but could only operate in 30-35% of the fields due to uneven field terrain (Soule, 1969). The picking efficiency of a harvester was defined as "a ratio of the weight of harvested berries to the weight of berries on the plants before harvesting" (Soule & Gray, 1972). Doug Bragg Enterprises (DBE) Limited, Collingwood, Nova Scotia, further improved this design by adding a hydraulic control system for the head height, head rotational speed, and changing the width of the picking head (Malay, 2000). Mechanical harvesters manufactured by DBE are towed alongside a tractor and utilize a single hydraulic cylinder to adjust the picking height of the rakes for optimal yield recovery (Esau et al., 2019). DBE is the largest manufacturer of wild blueberry harvesters for distribution in Atlantic Canada, and the US State of Maine (Esau et al., 2020). Farooque et al. (2014) reported that up to 1,500 mechanical harvesters with single or double head configurations are in use in these regions. A single tractor can tow up to three harvesters at once to further decrease harvesting time, but this can result in lower efficiencies as the operator has difficulties in monitoring the additional heads (Esau et al., 2019).

1.1.3 Spatial Variation in Wild Blueberry field and Precision Agriculture Technologies

Spatial variability in wild blueberry fields is a major concern for harvesting operations. Harvesting of spatially variable fields at standard ground speed and header revolutions without characterizing spatial variability in crop parameters, fruit yield, soil properties, and ground slope can result in an increased fruit loss during harvesting

(Farooque, 2015). Spatial variation in wild blueberry crop emphasizes the integration of precision agriculture (PA) technologies with a mechanical harvester to reduce fruit losses and enhance berry-picking adeptness (Farooque, 2015). The integration of innovative PA technologies comprised of sensors, controllers, hardware, software, differential global positioning systems (DGPS), and geographical information systems (GIS), with the traditional harvesting techniques can identify the factors affecting harvester's efficiency caused by the field spatial variability (Bausch & Delgado, 2003; Holland et al., 2006). An automated slope measurement and mapping system (SMMS) consisting of accelerometers, DGPS, custom-developed software, and a laptop computer were developed to map the topographic variation in real-time to facilitate the development of management zones for site-specific application of agrochemicals (Zaman et al., 2010a). An automated yield monitoring system (AYMS-II) consisting of two μ-eye color cameras, DGPS, custom software, and a laptop computer was developed and evaluated on specialized farm motorized vehicles (SFMV) to map the wild blueberry fruit yields (Chang et al., 2012). Farooque et al. (2013) developed and evaluated the performance of multiple ground-based sensors, including ultrasonic sensors, digital cameras, slope sensors, and real-time kinematic global positioning system (RTK-GPS), mounted on mechanical harvester to quantify and characterize the spatial variability within the wild blueberry cropping system. They estimated the wild blueberry fruit losses non-destructively in real-time. Spatial variation in wild blueberry fields and its impact on harvesting operation has been recognized and quantified by several researchers (Farooque et al., 2012, 2013, 2014, 2015, 2016a, 2016b, 2017; Malay, 2000; Zaman et al., 2009, 2010a, 2010b; Jameel et al, 2016; Chang et al., 2016, 2017). Spatial variation in topography not only creates a challenge for

the harvester operator to maintain the optimum head height but also leads to increased harvesting fruit losses (Farooque et al., 2016b, 2017). Ground surface variability within wild blueberry fields accentuates the need for an intelligent system, which can be integrated to automate the picker head height based on the real-time feedback from the ground surface during harvesting. Many researchers have utilized ultrasonic sensors in agriculture for measuring height in pastures (Fricke & Wachendorf, 2013; Fricke et al., 2011; Hutchings et al., 1990), canopy characterization in orchards (Escolà et al., 2011; Zaman & Salyani, 2004), wheat (Scotford & Miller, 2004), cotton (Sui & Thomasson, 2006), and maize (Aziz et al., 2004). The ultrasonic sensors are limited for their application due to low penetration capability, low resolution, and lack of scanning power (Colaço et al., 2018). Light detection and ranging (LiDAR) radar system has been used by several researchers in vegetation canopy characterization (Bietresato et al., 2016; Houldcroft et al., 2005; Naesset & Bjerknes, 2001). The ground slope variation, low height shrubs, and sparse vegetation cover significantly affect the accuracy of LiDAR systems (Spaete et al., 2011). The ultra-wideband (UWB) microwave radar technology operating in the radio frequency (RF) range has shown promising results in sensing the ground surface through vegetation cover in wild blueberry fields (Mohamed et al., 2018).

1.1.4 Microwave Technology and Applications in Agriculture

1.1.4.1 Introduction and Basic Principle

Electromagnetic waves are complex in nature as they can propagate through a vacuum without the need for a material medium, and they simultaneously behave like waves as well as particles (Dirac, 1927; Einstein, 1951). Electromagnetic waves are usually described in terms of their frequency, wavelength, and speed. They are classified over a

wide range of frequency spectrum, which is also called an electromagnetic spectrum that covers everything from ultra-long radio waves to high-energy gamma rays (Paul, 2006).

Table 1-1: Radio Frequency (RF) Waves Spectrum

Designation	Abbreviation	Frequencies	Wavelengths
Very Low Frequency	VLF	9 kHz – 30 kHz	33 km – 10 km
Low Frequency	LF	30 kHz – 300 kHz	10 km – 1 km
Medium Frequency	MF	300 kHz – 3 MHz	1 km – 100 m
High Frequency	HF	3 MHz – 30 MHz	100 m – 10 m
Very High Frequency	VHF	30 MHz – 300 MHz	10 m – 1 m
Ultra-High Frequency	UHF	300 MHz – 3 GHz	1 m – 100 mm
Super High Frequency	SHF	3 GHz – 30 GHz	100 mm – 10 mm
Extremely High Frequency	EHF	30 GHz – 300 GHz	10 mm – 1 mm

Electromagnetic waves can be harnessed to transmit information, acquire information from the medium, or transmit energy. Their applications include radar, radio astronomy, microwave thermography, and material permittivity measurement (Adamski & Kitlinski, 2001). The RF waves refer to a portion of the electromagnetic spectrum that can be generated with alternating current ranging from 20 kHz to 300 GHz (between the upper limit of audio frequencies and the lower limit of infrared frequencies) (Fleming, 1910). Frequencies above 1 GHz are conventionally called microwave frequencies (Kumar & Shukla, 2014). The RF spectrum is divided into several bands of different ranges (**Table 1-1**). Ultra-high frequency (UHF), super high frequency (SHF) and extremely high frequency (EHF) bands constitute the microwave spectrum (Brodie et al., 2016). Microwave frequencies occupy a portion of the RF spectrum and they can be utilized in communication, navigation, and defense industries. Radar utilizes time-of-flight (TOF) to determine the distance from a target. During its operation, the RF radar utilizes electromagnetic waves in the radio spectrum, which have much longer wavelengths than visible or infrared light, giving them unique propagating characteristics. This makes RF radars very beneficial, as radio waves can effectively penetrate through different media:

i.e., dust and smoke (Toomay & Hannen, 2004). The frequency modulation used by the radar can take many forms such as linear and sinusoidal modulations, both of which have been used in the past. Linear frequency modulation is the most versatile and suitable, when used with a fast Fourier transform (FFT) processor, for obtaining range information from targets over a wide range (Stove, 1992).

1.1.4.2 Applications of Microwave Technology in Precision Agriculture

Microwave energy with its illumination source can penetrate the plant canopy during day or night making it a promising remote sensing device for PA technologies (Brakke et al., 1981). Numerous studies have utilized active and passive microwave remote sensing techniques to obtain a spatial and temporal estimation of soil moisture over the large regions (Jackson et al., 1999; Ulaby et al., 1996; Du et al., 2000; Engman & Chauhan, 1995). Ground-penetrating radars operating in a radio frequency range offers a non-destructive and in-situ sensing tool, which has been widely used in Civil Engineering (Goodman, 1994; Maierhofer, 2003), archaeological research (McKeand, 2014; McKinley, 2007), geophysical investigations (Carrière et al., 2013; Davis & Annan, 1989) and tree root detection in agriculture (Hruska et al., 1999; Butnor et al., 2001; Borden et al., 2014). A microwave radar system was developed at the PA lab, Faculty of Agriculture, Dalhousie University, and its initial evaluation showed significant potential in employing radio frequency waves for detection of the ground surface through vegetation canopy in wild blueberry fields (Mohamed et al., 2018).

In agriculture, microwave techniques, methods, and instrumentation can be used to improve crop production, handling, and processing efficiency. Microwaves can propagate through free space, penetrate through dielectric materials, and offers non-destructive and

continuous monitoring, which makes them useful for industrial and agricultural applications (Kraszevvski & Nelson, 2003). Wood-based materials are relatively transparent at microwave frequencies, which makes early non-destructive detection of biological degradation possible (Daian et al., 2005). Active microwave radar systems operating at the frequency range from 1 to 25 GHz provide data for the classification of crops in conjunction with other observations. Active microwave radar system responses are selective for analyzing the vegetation canopy structure and the dielectric properties of the target; whereas visible and infrared systems responses primarily correspond to chlorophyll content, surface-moisture changes, and soil background color (Dobson & Ulaby, 1986; Ulaby & Jedlicka, 1984). Many researchers have employed microwave radar technology for remote sensing in agriculture. They have analyzed the backscattered data collected by microwave radar sensors, which suggested that the data at different frequency bands contain information on vegetation dynamics with potential implications for crop spectroscopy (Paget et al., 2016; Frolking et al., 2011; Friesen et al., 2012). Microwave radars' backscattered data from a vegetated surface comprises of three kind of backscatter information: i) direct data from the vegetation itself, ii) data from the soil surface that is attenuated by the canopy, and iii) data due to interactions between the vegetation and the underlying soil surface (Ulaby et al., 1981, 1996). Currently, most of the work in the field of crop spectroscopy relies on spaceborne synthetic aperture radar (SAR) data due to their finer spatial resolution (McNairn, & Brisco, 2004; Baghdadi et al., 2009; Skriver et al., 2011). The SAR imagery is widely used for the retrieval of biophysical parameters of different crops (Ballester-Berman et al., 2005). Ground-penetrating radars have been extensively used in agriculture to determine the soil micro variability (Collins & Doolittle,

1987), increase the quality and efficiency of soil surveys (Collins et al., 1986; Puckett et al., 1990), determine the thickness, and characterize the depth of organic soil materials (Shih and Doolittle, 1984), estimate the depth of argillic (Truman et al., 1988) and sporadic horizons (Doolittle, 1987), as well as to improve soil-landscape modeling (Doolittle et al., 1988).

1.2 Research Problem

Wild blueberry fields contain substantial spatial variability in terms of plant characteristics and field topography (Farooque et al., 2012). Spatial variations in agricultural fields affect crop production and fruit quality (Bramley, 2005), which can impact fruit losses during harvesting. Variation in soil texture and slope of the ground can create an imbalance of the harvester head during mechanical harvesting, thus affecting the picking performance of the harvester (Farooque, 2015). Mechanical harvesting of wild blueberries is mainly dependent on the operator's skills to maintain the optimum harvester head height, ground speed, and header revolution, keeping in view the variations in plant height to achieve high picking efficiency and to ensure maximum yield recovery (Chang et al., 2017; Farooque et al., 2017). Efficient mechanical harvesting of wild blueberries requires an experienced operator for maximizing berry recovery and profit margins (Farooque et al., 2014), however, this increase in berry picking efficiency is at an expense of elevated fatigue and operator stress. On the other hand, an unskilled operator can cause significant loss and lower farm profitability, as he/she is not able to maintain the head height keeping in view the spatial variations in plant height and ground topography. Spatial variations in plant height and un-even topography pose a serious challenge for the operator to maintain an optimal harvester picking head height. An accurate height in relation to the

variations in plant height is key to maximize harvestable fruit yield. (Chang et al., 2017; Farooque et al., 2014). These spatial variations in plant height and variable ground topography emphasize the need to develop an automated picker head height adjustment system to reduce operator stress and fruit losses during mechanical harvesting. Chang et al. (2016, 2017) developed and incorporated an advanced automated plant height measurement system to facilitate harvesting operation in variable plant height conditions. However, so far, very limited research has been done to automate the harvester head height based on ground surface variability. Plant height-based sensing systems using ultrasonic sensors are limited for their application in ground sensing due to low penetration capability, low resolution, and lack of scanning power (Colaço et al., 2018). The use of radiofrequency with microwave technologies offers a great potential to solve problems associated with agricultural production (Brodie et al., 2016). Preliminary research conducted at the PA Lab (Dalhousie University Agricultural Campus, Truro, NS, Canada) to evaluate the feasibility of microwave radar technology showed great potential for its application in ground surface detection in wild blueberry fields (Mohamed et al., 2018). Ground surface detection through non-destructive foliage penetration in lowbush blueberry fields can provide the basis for the automation of the picker head for the mechanical harvester. This research aims to develop a sensing system that can penetrate through the foliage in a non-destructive manner to detect the ground surface in real-time during mechanical harvesting. The developed system will eventually aid the automation of the picker head for the wild blueberry mechanical harvester.

1.2.1 Research Objectives

The goal of this research is to develop and evaluate a microwave radar system, which can penetrate through the vegetation canopy to detect variations in the ground surface to automate the harvester head. The specific objectives of this research are to:

1) Develop a custom microwave radar system and assess its application and feasibility for detecting the ground surface in wild blueberry fields.

Three different microwave radar systems will be developed using: 1) Walabot developer model (Walabot, Vayyar Imaging Ltd., #6023 Fairfield, USA) with operating frequency bandwidth of 3.3-10 GHz, 2) Acconeer XM112 (Acconeer AB, Scheelevägen, #223 63 Lund, Sweden) with an operating frequency of 60 GHz, and 3) Terrahawk® HT5230 (Headsight Inc., #45065 Bremen, Indiana, USA) with the operating frequency bandwidth of 1.5-6.5 GHz. The performance of the developed systems will be evaluated and compared in the Lab and field environments. The developed system with optimum performance results will be selected for further evaluations.

2) Analyze and compare the effect of field variations (i.e., stem density, stem height, fruit zone height, and fruit yield) on the performance of the developed ground surface detection system.

The effect of stem density, fruit zone, stem height, stem thickness, and fruit yield on the selected ground surface detection system will be statistically analyzed. The performance of the selected ground surface detection system out of all the three radar

sensors will be analyzed for its application in ground surface detection within the wild blueberry fields.

3) Evaluate the effect of ground speed on the performance of the developed ground surface detection system.

Performance of the selected system will be evaluated and compared at three traditional harvester ground speeds including 1.2, 1.6, and 2.0 km h^{-1} to determine the effect of machine operating parameter on the performance of developed system in detecting and measuring the ground surface in real-time.

This research study will explore the potential of microwave radars in detecting the ground surface in the wild blueberry fields. It will also delineate the optimum frequency band for detecting and measuring the real-time ground surface on-the-go. Future work will include the design and development of a closed-loop feedback system to integrate the developed system with wild blueberry harvester, which will serve as a base for automation of harvester head positioning.

CHAPTER 2: DEVELOPMENT OF GROUND SURFACE DETECTION SYSTEM USING MICROWAVE RADAR TECHNOLOGY FOR USE WITH MECHANICAL WILD BLUEBERRY HARVESTING

ABSTRACT

Mechanical harvesting of wild blueberries is highly dependent on operator skill to maintain optimum head height corresponding to the variable ground slope and fruit zone height to achieve optimum berry picking efficiency. Manual operation of the mechanical harvester including head height adjustment, ground speed control, and rotational speed control of the picking reel, not only affects the berry picking efficiency but also puts mental and physical stress on the operator. Microwave radar technology in the radio frequency range has been used in agriculture for various tasks but its potential in detecting ground surface in wild blueberry fields has never been analyzed. In this research study, three systems having distinct operation frequency ranges were developed using radar sensors, namely: i) Walabot Developer, 3.3-10 GHz, ii) Acconeer A111, 60 GHz, and iii) Terrahawk® HT5230, 1.5-6.5 GHz. Developed systems were analyzed and compared initially in indoor Lab conditions at Dalhousie University, Nova Scotia, Canada. Performance of the developed systems in detecting three selected surfaces (i.e., metal, wood, and soil) were compared at three distinct mounting heights (0.60, 0.80, and 1.00 m). Vegetation cover was simulated over the selected ground surfaces and the performance of the developed systems was analyzed using three different media to simulate real field conditions: a) Control (air as a medium), ii) Grass clippings, and iii) Hay. Precision, accuracy, and bias were calculated and compared using statistical parameters. Results indicated that the Terrahawk® radar sensor performed best as compared to the other selected radars with standard deviation ranging from $\pm$0.21 cm to $\pm$1.12 cm, Root Mean Square Error (RMSE) ranging from 4.45 cm to 5.62 cm, and Mean Bias Error (MBE) ranging from +4.33 cm to +5.57 cm under all simulated conditions. Overall, the Terrahawk® radar sensor offered high precision and accuracy with slight underestimation in the height measurement of detected ground surfaces. Results of this study show the potential for automation of the harvester picking reel using the Terrahawk® radar sensor for real-time foliage penetration and ground surface detection in wild blueberry fields.

2.1 Introduction

Wild blueberry (*Vaccinium angustifolium Ait.*) crops with a total cultivated area of 161,399 acres contributed to the marketed production of 78,584 tons and the national economy by farm gate value of $112.17 million in 2020 (Statistics Canada, 2021), thus marking itself as one of the most important agricultural commodities in Canada. The wild blueberry crop is native to Northeastern North America with their fields originated and spread from naturally pre-existing blueberry rhizomes in uncultivated farmlands (Eaton, 1988; Jamieson, 2008). Wild blueberry fields are unique to this topographic region of the world as it has never been cultivated on a larger scale (Barker et al., 1964). Wild blueberry fields undergo a bi-yearly management cycle with rigorous vegetative growth during sprout year followed by fruit growth during the crop year (Esau et al., 2018; Farooque et al., 2016a; Eaton & Nams, 2006). Fields under management are typically pruned after harvesting during the crop year either by mowing or burning (Yarborough, 2004), which improves the plant growth and fruit yield (Barker et al., 1964). Wild blueberry fields are usually harvested during August in crop year either by hand raking or mechanically using harvesters (Kinsman, 1993).

Over the years, the mechanical harvester has been proven the most cost-effective way to reduce the production cost within wild blueberry fields (Yarborough, 2004). High agricultural labor wages (Government of Nova Scotia, 2019) along with the declining trend of labor availability during the past few years (Borjas, 2003) and short harvesting period (Ali et al., 2018) instigated the transition from traditional hand raking harvesting techniques to mechanized harvesting of wild blueberries. The pursuit to develop a mechanical harvester for wild blueberry fields began in the 1950s which led to the

manufacturing of the very first mechanical harvester in 1956 (Dale et al., 1994). This harvester was modified from a cranberry picking machine and consisted of six raking combs picking in opposite direction with respect to the direction of travel, but due to high fruit losses, further modifications were required (Rhodes, 1961). The design of the wild blueberry mechanical harvester was modified by incorporating more sophisticated features in the subsequent years such as the introduction of variable rotational speed of picking heads, picking combs rotation direction parallel to the direction of travel, and hydraulic modulation of the picking head height. (Gray, 1970; Malay, 2000; Soule, 1969; Esau et al., 2020). Doug Bragg Enterprises (DBE) in Collingwood, Nova Scotia, has played a significant role in the efficiency improvement of the wild blueberry harvester design and currently, they are the largest producer of wild blueberry mechanical harvesters (Esau et al., 2020).

Several mechanical harvester designs have been developed over the past but increasing the harvest efficiency still remains a challenge for researchers and industry (Farooque, 2015; Dale et al., 1994). Improved field management practices have resulted in a significant increase in fruit yield but have also created major challenges affecting harvest efficiency such as healthy and tall plants, tall weeds, and high plant density (Farooque et al., 2014). Wild blueberry fields possess substantial spatial variability in terms of plant characteristics, fruit characteristics, and ground slope (Farooque et al., 2012; Zaman et al., 2010a).

Ground slope variation in wild blueberry fields can create an imbalance of the harvester head, which can affect its picking efficiency in addition to the increased possibility of picking teeth getting damaged by digging into uneven soil. Uneven field

topography deems it necessary to maintain the picking height of the harvester head at the correct level to optimize harvester picking efficiency, which in turn requires almost constant operator input causing operator stress and fatigue (Farooque et al., 2014).

Precision agriculture has greatly benefitted from sensors utilizing microwave spectroscopic techniques specifically in crop monitoring (Nelson, 2005; Brodie et al., 2016; Kraszewski & Nelson, 1995; Brakke et al., 1981). Several researchers have utilized microwave radars for non-destructive ground surface detection through vegetation (Noyman & Shmulevich, 1996; Woods et al., 1999; Bush & Ulaby, 1978; Yuzugullu et al., 2015; Laymon et al., 2001), but the potential of microwave altimeters has not been explored in wild blueberry fields for their application in ground-level sensing and feedback. This research study focuses on the comparison and selection of optimum frequency range for non-destructive ground surface detection through vegetation covers, for real-time feasibility analysis in wild blueberry fields.

2.2 Material and Methods

2.2.1 Research Site

The designed experiments for comparison and selection of optimum microwave frequency range were carried out in the Mechanized Systems and Precision Agriculture (PA) Lab, Dalhousie University Agriculture Campus (Dalhousie Agriculture Campus, Truro, NS, Canada).

2.2.2 Selected Radars

Three microwave radars, operating in different frequency bands, were analyzed for their accuracy, precision, and error using statistical measures: i) Walabot radar (3.3-10 GHz); ii) Terrahawk® radar (1.5-6.5 GHz); and iii) Acconeer radar (60 GHz).

2.2.2.1 Walabot Radar

Walabot Developer is a three-dimensional radio-frequency (RF) based sensor with a development board having a footprint of 0.072 m x 0.140 m x 0.001 m (**Figure 2-1**). It was developed by Vayyar Imaging Ltd., (Walabot, Vayyar Imaging Ltd., #6023 Fairfield, USA) particularly for its application as an in-wall stud finder (Walabot, 2020). Other applications include in-wall 3D imaging, tracking objects, fall detection, and breath monitoring (Wang et al., 2019). It senses the environment by transmitting, receiving, and recording signals from an array of linearly polarized broadband antennas. The Walabot is an ultrawideband, multi-input multi-output (MIMO), frequency modulated continuous wave (FMCW) radar, equipped with 18 antennas, 14 receivers, and 4 transmitters to transmit amplitude modulated signals. The FMCW radar differs from Pulse Coherent Radar (PCR) as the electromagnetic signal is continuously transmitted and the frequency of this signal changes over time, generally in a sweep across a defined bandwidth. Analysis of sequences of images allow detecting changes in the environment. The Walabot can be programmed for its application using Linux, Windows, or Android platforms (Walabot, 2019). The scanning area it projects on the ground can be defined by programmable parameters including polar angle (theta) and azimuthal angle (phi) (**Figure 2-2**; **Table 2-1**). The Walabot is capable of short-range imaging into dielectric environments, such as drywall and concrete (K. Meng & Y. Meng, 2019; Cunha & Youcef-Toumi, 2018).

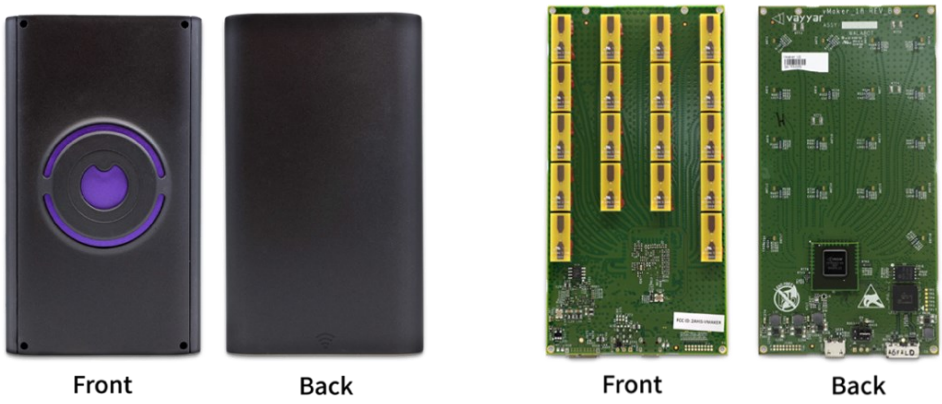

(a) **(b)**

Figure 2-1: The Walabot radar sensor footprint with plastic casing (a) and the development board itself (b).

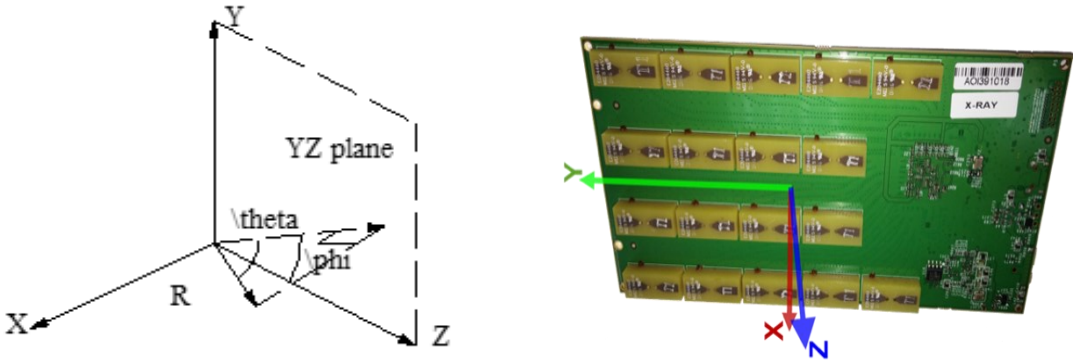

(a) **(b)**

Figure 2-2: Projected field of view for the Walabot radar sensor along with polar angles definition (a) and three dimensional axis clarification (b).

Table 2-1: The Walabot scanning area configuration parameters.

Scanning arena	Values (cm)	Vertical projected cone	Values (degrees)	Horizontal projected cone	Values (degrees)
Radar start distance	10.0	Min theta	-10.0	Min phi	-20.0
Radar end distance	100.0	Max theta	10.0	Max phi	20.0
Resolution	0.5	Theta resolution	1.0	Phi resolution	1.0

A customized script was written in python language using functions included in the pre-defined library (Walabot, 2020) with a custom-defined field of view (FOV) (**Table 2-1**). Sensor target class was utilized to obtain the output height of the detected ground

surface with the sensitivity threshold set to 15. The algorithm governed by the radar was modified to detect the ground surface as a single target instead of multiple target detection. The defined sensitivity threshold helped to mitigate very weak reflected signals. The Walabot radar was calibrated using a pre-defined calibration function at maximum mounting height of 1.10 m and air as a medium of propagation for a sent signal. The detected ground surface as an output of the radar sensor was displayed using Python 3.9.1 for data acquisition (**Figure 2-3**).

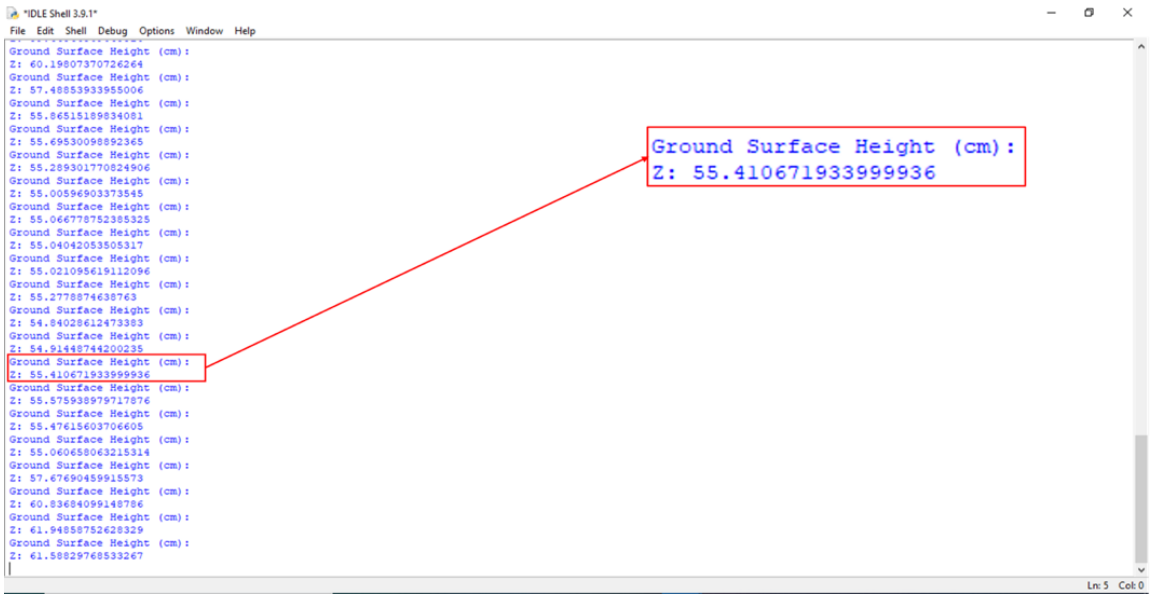

Figure 2-3: Output of the the Walabot radar displaying the ground surface height (cm) on the z-axis.

2.2.2.2 Acconeer Radar

Acconeer XM112 (Acconeer AB, Scheelevägen, #223 63 Lund, Sweden) is a reference module with an optimized form-factor (0.024 m x 0.016 m x 0.001 m), which offers high precision measurements with 1 mm accuracy. The XM112 comes with an Atmel ATSAME70Q20A microcontroller (MCU) and A111 sensor equipped with single pair of transmitter and receiver (**Figure 2-4**).The Acconeer A111 radar sensor is based on a sliding correlator principle to estimate the energy at different time-of-flight (TOF) of the

transmitted wave when reflected on different objects (Montgomery et al., 2019). The Acconeer mm-wave radar operates as a pulsed short-range radar sensor that measures distances to all objects within its field of view. The A111 radar sensor can detect multiple objects at close range with single measurements as well as continuous sweeps (Acconeer, 2019).

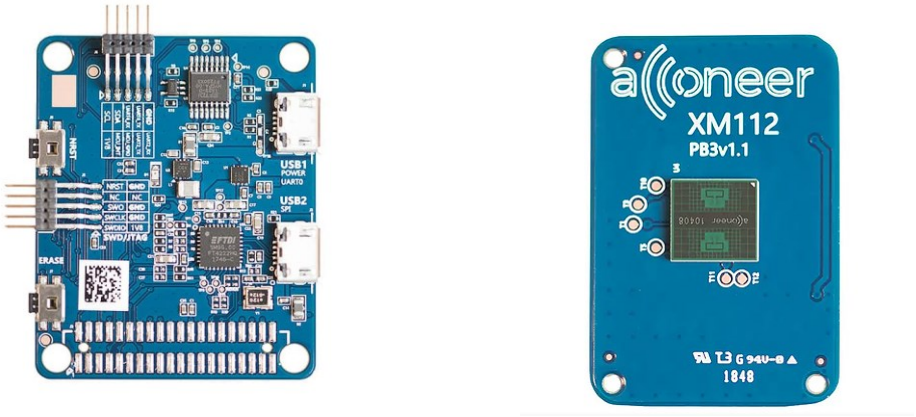

(a) **(b)**

Figure 2-4: XM112 devolopment board with bulit in microprocessor (a) and A111 radar sensor module (b).

A custom script was written in python language to configure the radar sensor and output was displayed using Python 3.9.1 (**Figure 2-5**). The range of the radar sensor was scaled to be 10-110 cm with a data acquisition sweep rate of 30 Hz and amplitude gain of 0.1. The algorithm of the radar sensor was modified to measure the ground surface height. To visualize the output, a graphical pane was also designed with ground surface height in meters on the x-axis and amplitude with 0.1 gain displayed on the y-axis (**Figure 2-5a**).

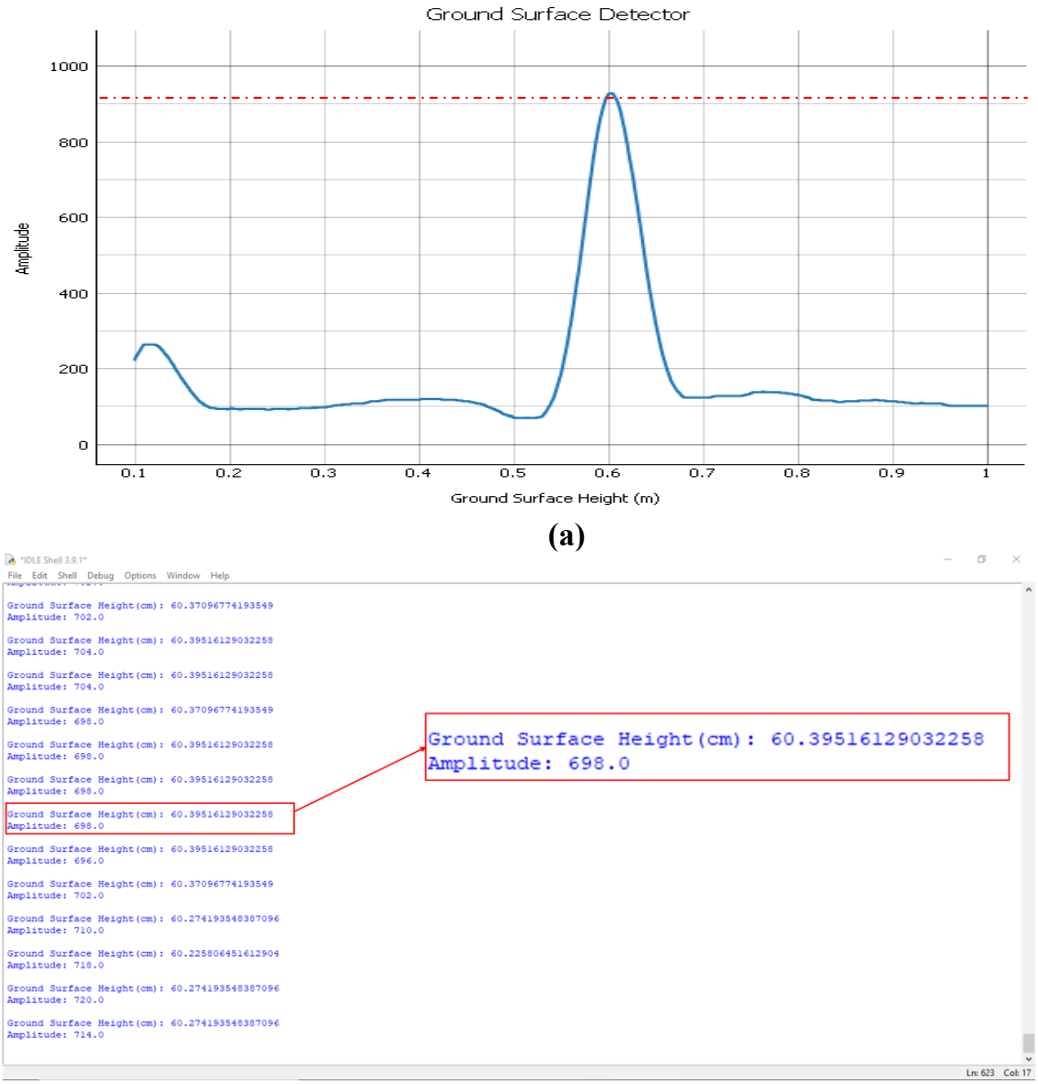

Figure 2-5: Output of the Acconeer radar with graphical (a) and numerical (b) feedback displayed on the programmed window panes. In graphical feedback (a), the highest amplitude

2.2.2.3 Terrahawk® Radar

Terrahawk® HT5230 (Headsight Inc., #45065 Bremen, Indiana, USA) is a ground detecting radar sensor developed by Headsight (Headsight Inc., 2019), to measure the real-time distance of ground surface in grain and corn crops relative to the operating combine harvester head position (**Figure 2-6**). The Terrahawk® projects 90 degrees FOV on the ground for data acquisition with an adjustable resolution between 4 mm and 8 mm with a

default resolution of 4 mm. Reflected signals can be processed either using a built-in microprocessor along with Controlled Area Network (CAN) communication or using an external (third party) microprocessor when USB 2.0 (serial) communication is utilized. The Terrahawk® radar sensor has a built-in microprocessor for signal processing which can only be utilized if CAN communication is active. The Terrahawk® radar comes with the rugged outdoor environment compatible designed casing having a total footprint of 0.211 m x 0.104 m x 0.079 m (**Figure 2-6**).

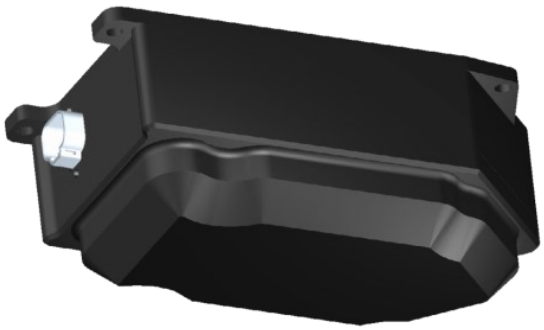

Figure 2-6: Rugged hard plastic casing enclosing the Terrahawk® radar sensor module with output ports (CAN, USB 2.0).

Data acquisition, numerical/graphical outputs visualization, and parameters definition were carried out using a graphical user interface (GUI), provided by Headsight Inc. (Headsight Inc., #45065 Bremen, Indiana, USA). The trials for this research study were carried out in a continuous reading mode with a default resolution of 4 mm, sensitivity threshold (RMS threshold multiplier) value of 6, radar start distance of 0.00 m, and DSP start distance of 0.20 m.

2.2.2.4 Specification Comparison of the Selected Radars

The Terrahawk® and the Walabot radars utilize the UWB and FMCW technology with their operating frequency lying between L, S, C, and X bands of nominal frequency range (**Table 2-2**). The Acconeer radar was based on PCR technology with transmitting

waves having fixed frequency. The general operating parameters of selected radar sensors are listed below for comparison purposes (**Table 2-2**)

Table 2-2: General specifications of selected radar sensors.

Operating Parameters	Walabot Radar	Acconeer Radar	Terrahawk® Radar
Bandwidth (GHz)	3.3 – 10.0	60	1.5 – 6.5
Radar Type	UWB/FMCW	PCR	UWB/FMCW
FOV	Programmable	Fixed	Fixed
Resolution (mm)	Varies with FOV	1	4, 8

UWB – Ultrawide band; FMCW – Frequency modulated continuous wave; PCR – Pulse coherent radar; FOV – Field of view

2.2.3 Mounting Assembly

A custom-built modular mounting assembly was utilized to mount radar sensors at three selected heights: 0.60 m, 0.80m, and 1.00 m (**Figure 2-7**). The mounting plate was modified to allow horizontal tilt adjustment which helped to mount the sensor at 0º with respect to the ground surface plane, allowing the transmitted signals to have a 90º angle of incidence at the top surface of selected ground surfaces.

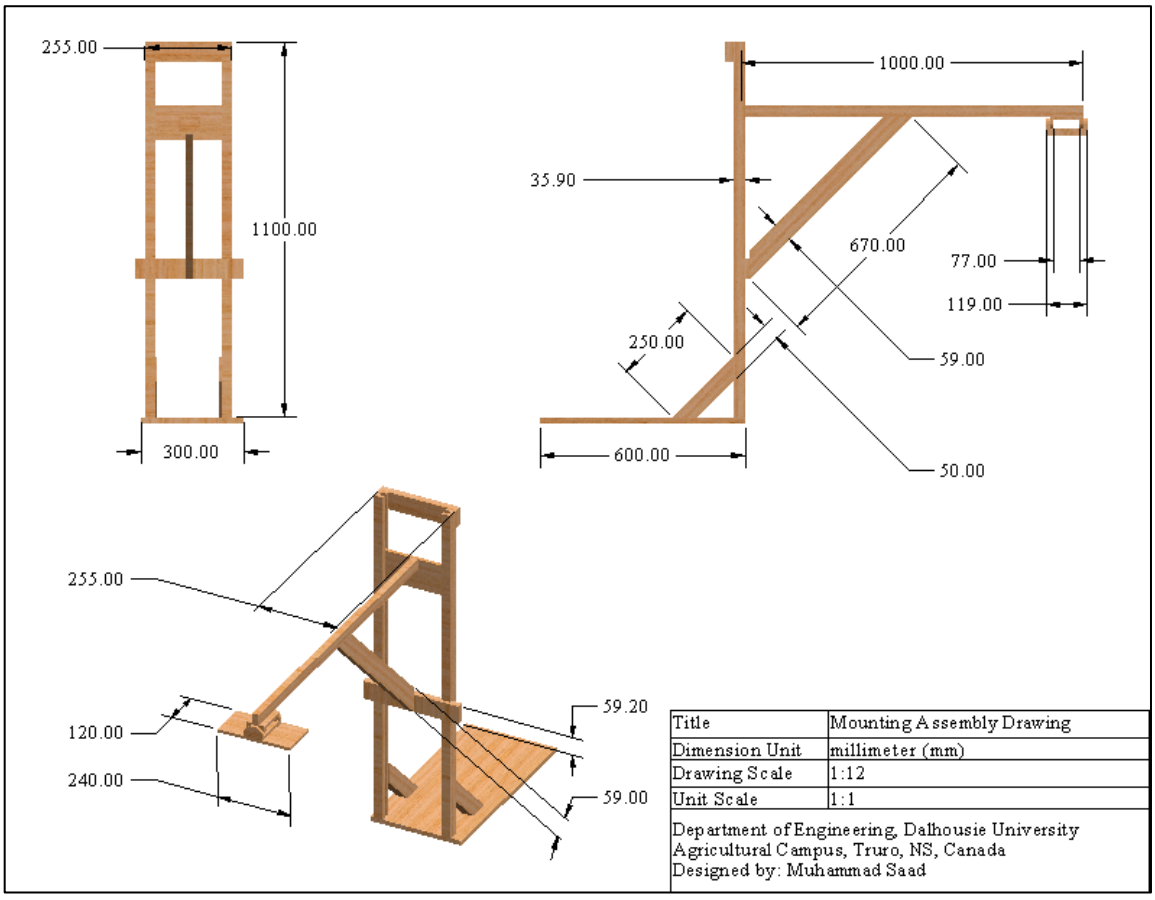

Figure 2-7: SolidWorks drawing of radar mounting assembly for data collection in standstill conditions.

2.2.4 Experimental Design

Experimental setup for Lab trials to analyze the optimum frequency for through-vegetation ground surface detection comprised three selected surfaces acting as true ground surfaces including: i) Wood (0.02 m thick); ii) Aluminium metal surface (0.0006 m thick);

and iii) Soil surface (0.10 m thick). A total of 18 sampling units of each ground surface were utilized to cover maximum variability which also allowed six replications for the performance evaluation of all three radar sensors. Performance of the radar sensors was compared for detection of ground surfaces in a controlled environment (with no vegetation cover) and using a vegetation cover. The factor including the vegetation cover type in Lab trials was further segregated to three distinct levels/media: a) Control (with air); b) Grass clippings; and c) Alfalfa hay. The bulk densities of vegetation cover created over the selected ground surfaces using hay and grass clippings were approximately 48.62 kg m^{-3} (actual sample vertical height ≈ 7-10 cm) and 63.38 kg m^{-3} (actual sample vertical height ≈ 3-5 cm), respectively.

Each radar sensor at a specific mounting height level from the selected ground surface was subjected to three different trials including the trials with no vegetation cover (control), trials with hay as vegetation cover, and trials with grass clippings as a vegetation cover (**Figure 2-8**). The combination of selected vegetation cover type and ground surfaces constitutes a single treatment at a particular mounting height which was subjected to selected radar sensors separately. Samples were numbered and randomly assigned to the iterations for each radar sensor.

Selected radar sensors were analyzed to detect the ground surface at three distinct mounting heights: 0.60, 0.80, and 1.00 m. The upper bound (1.00 m) of the selected mounting heights was chosen in order to cover the whole width of the harvester head (0.91 m) during each scan and the lowest bound (0.60 m) provided the lowest point at which maximum clearance is achieved without destroying the stems and fruit in the fields.

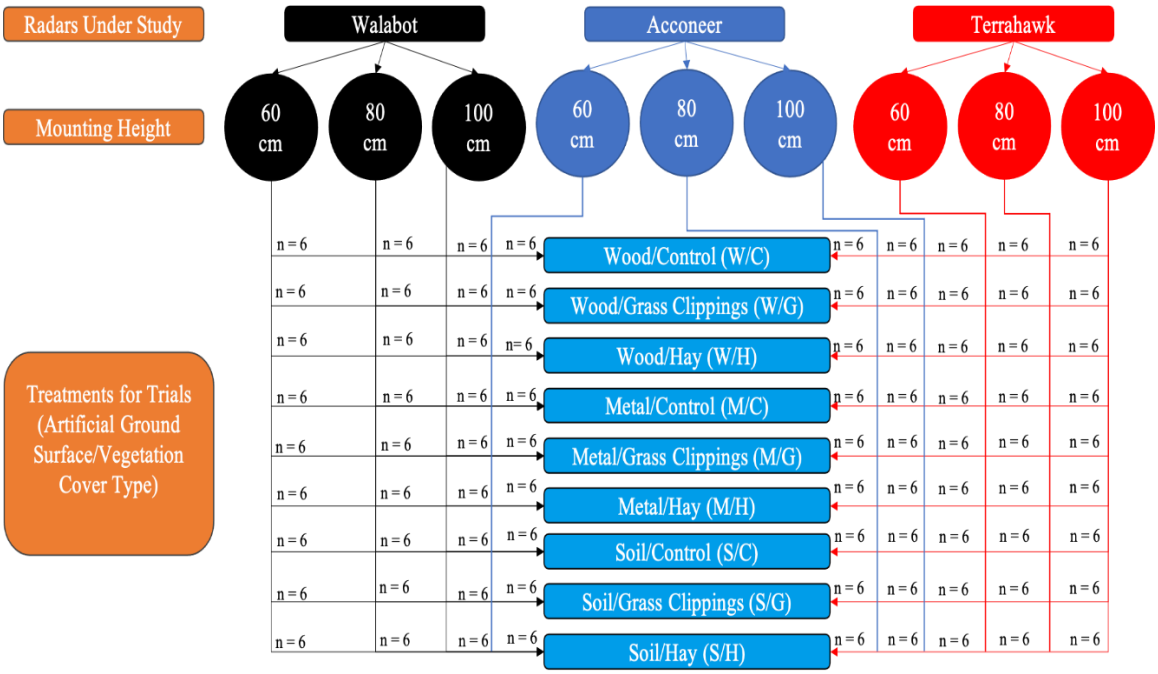

Figure 2-8: Graphical summary of the experimental trial setup with treatments and the factors included of the research study. Replications associated with each trial are represented by n=6.

2.2.5 Data Collection

The data collection process for Lab evaluations comprised a total of 81 trials including 27 trials for each radar sensor ((3 radars) x (3 levels of mounting) x (3 ground surfaces) x (3 vegetation cover conditions). Selected ground surfaces (i.e., wood, metal, and soil) were included in separate trials for each radar sensor (**Figure 2-8**). A total of 486 iterations (N) were conducted cumulatively for all the trials including 6 replications (n) for a single trial (81 trials x 6 replications each = N). Selected radars took 12 seconds time period for each sample data collection and readings were recorded at the end of the defined period. Radar sensors were mounted at the centre of each sampling unit using the developed mounting assembly (**Figure 2-9**, **Figure 2-10**, **Figure 2-11**). The mounting height was calibrated before each trial by adjusting the modular mounting arm on the assembly to

attain the required distance from the bottom of the radar casing to the top of the selected ground surface and the metric tape was utilized to ensure the proper height level.

(a) (b)

Figure 2-9: The Terrahawk® radar setup with bare soil/control (S/C) treatment (a) and Soil/Hay (S/H) treatment (b).

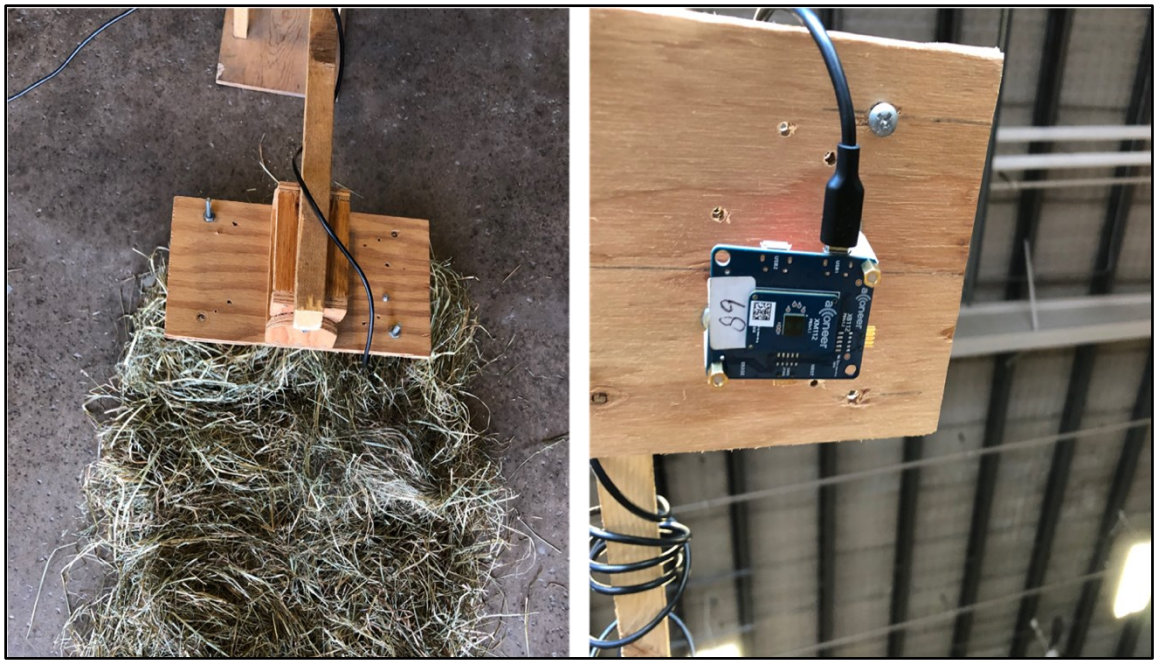

(a) (b)

Figure 2-10: The Acconeer radar with mounting socket (b) on mounting plate and trial with Metal/Hay clipping (M/H) treatment (a).

(a) (b)

Figure 2-11: The Walabot radar trial with Wood/Grass clipping (W/G) treatment (a) and mounting socket (b) on mounting plate.

2.2.6 Statistical Analysis

Various statistical parameters were computed to analyze the performance of the selected radar sensors using Minitab 19 (Minitab Inc., Pennsylvania, USA). The performance of each system was analyzed by calculating precision, accuracy, and bias. For the selected radar sensors above-mentioned statistical measures were calculated separately for each simulated condition in the Lab environments (i.e., separately for selected height levels and treatment conditions). The precision of a measurement device is usually explained by the spread of the data or statistical variability in the recorded data (Walther & Moore, 2005). In this research study, precision was examined by calculating the standard deviation (SD) of the recorded data for each radar sensor (Eq. 1).

$$SD = \sqrt{\frac{\sum_{i=1}^{n}(y_i - \bar{y})^2}{n}} \quad \text{Eq. 1}$$

Interquartile range (IQR) is another parameter to examine the variability which gives the data spread range in which 50% of the total data points lie. The spread of the data in this research study was examined by calculating IQR in each trial (Eq. 2)

$$IQR = Q_3 - Q_1 \quad \text{Eq. 2}$$

Root mean square error (RMSE) is another extensively employed statistical measure in the research studies to analyze the performance of a system (Astatkie, 2006; Walther & Moore, 2005). The accuracy of the selected radar sensors was examined by calculating RMSE (Eq. 3).

$$RMSE = \sqrt{\frac{\sum_{i=1}^{n}(y_i - x)^2}{n}} \quad \text{Eq. 3}$$

Mean bias error (MBE) represents the bias in the performance of the predictive systems (Walther & Moore, 2005). To analyze the over or underestimation of the ground surface height for selected radar sensors, the mean bias error (MBE) was calculated (Eq. 4).

$$MBE = \frac{\sum_{i=1}^{n}(x - y_i)}{n} \quad \text{Eq. 4}$$

In above-mentioned equations (Eq. 1-3), y_i represents the simulated values (predicted by radar), $\bar{y}$ represents the mean of the simulated values, x represents the observed values (ground truth values), n represents the sample size, SD represents the sample standard deviation, Q_1 represents the first quartile (where 25% of the data lies), and Q_3 represents the third quartile (where 75% of the data lies).

2.2.6.1 Criteria of Performance Comparison

Statistical measures used to compare the performance of three radar sensors in this research study were computed separately for each radar sensor and compared with each

other. Low values of SD represented less variation hence more precision of the radar sensor used in each trial. Each radar sensor was involved in 27 trials which resulted in a range of SD values. The variation of the SD values was also analyzed by comparing the range resulting from the total number of trials for each radar sensor. A shorter variation range indicated more precision and *vice versa*.

For the numerical reference, the SD values resulting from each trial involving a particular radar sensor were grouped into three categories: i) High precision (SD < 1.27 cm); Moderate precision (1.27 cm < SD < 5.08 cm); and Low precision (SD > 5.08 cm). Precision categories were developed based on the study done by Esau et al. (2020), where they developed a closed-loop control system that drives the actuator in eight steps with a 2.54 cm increment. The total vertical height of the actuator (20.32 cm) was translated to 10.16 cm vertical travel distance between teeth of the picking reel and the ground. The high precision group categorizes the radar sensor system with the mean ground height measurement discrepancy under a half an inch mark (< 1.27 cm).

Radar systems were also compared using the IQR where trials with lower values of IQR indicated a more stable system. Negative bias (overestimation) was considered unacceptable as it could lead to harvester head damages if integrated with the harvester head height controller. Positive bias values (underestimation) and RMSE values were considered acceptable only if these values resulted in a constant or linear trend which could be accounted for by calibration techniques.

2.3 Results and Discussion

2.3.1 Precision

The precision of the selected radars was evaluated by calculating SD and IQR (**Table 2-3**).

Table 2-3: Mean of the detected ground surface height with SD and IQR of the selected radar sensors output under selected treatments and mounting height levels.

MH (cm)	τ	Walabot		Acconeer		Terrahawk®	
		IQR (cm)	Mean ± SD (cm)	IRQ	Mean ± SD (cm)	IQR (cm)	Mean ± SD (cm)
60	W/C	2.38	62.54 ± 2.29	1.78	60.80 ± 1.09	0.90	55.10 ± 0.47
	M/C	3.15	65.30 ± 2.54	0.35	60.33 ± 0.19	1.00	55.05 ± 0.71
	S/C	7.05	58.30 ± 3.37	0.50	60.15 ± 0.29	1.30	55.13 ± 0.67
	W/G	8.59	58.78 ± 5.07	2.33	56.33 ± 1.31	0.53	55.15 ± 0.32
	M/G	14.14	60.31± 7.37	4.05	56.58 ± 2.90	1.40	54.83 ± 0.77
	S/G	4.32	59.20 ± 3.06	5.18	53.70 ± 2.59	1.15	55.07 ± 0.60
	W/H	3.31	56.45 ± 1.72	1.83	54.03 ± 0.92	0.60	55.07 ± 0.41
	M/H	14.27	60.78 ± 8.77	2.53	53.08 ± 1.68	0.70	54.92 ± 0.70
	S/H	10.43	55.67 ± 5.56	5.05	54.87 ± 3.27	2.28	54.55 ± 1.12
80	W/C	3.87	84.42 ± 3.51	1.03	81.10 ± 0.78	0.93	75.55 ± 0.68
	M/C	1.13	84.37 ± 1.35	0.43	80.38 ± 0.29	1.38	74.95 ± 1.02
	S/C	12.85	78.58 ± 7.36	0.50	80.32 ± 0.30	1.35	75.27 ± 0.65
	W/G	13.80	83.47 ± 6.69	1.33	76.70 ± 1.27	0.38	75.67 ± 0.23
	M/G	12.36	76.44 ± 6.62	1.95	77.43 ± 1.57	1.85	74.67 ± 1.03
	S/G	7.55	77.60 ± 5.27	1.30	75.53 ± 0.65	1.75	74.83 ± 0.95
	W/H	8.70	80.51 ± 4.35	4.10	82.93 ± 2.11	0.70	75.38 ± 0.41
	M/H	17.10	81.95 ± 15.62	1.25	73.75 ± 0.80	0.83	75.25 ± 0.38
	S/H	6.30	76.02 ± 4.94	1.35	74.20 ± 0.88	1.73	74.43 ± 0.89
100	W/C	2.70	93.68 ± 3.72	0.95	101.28 ± 0.46	0.58	95.15 ± 0.33
	M/C	1.90	103.52 ± 1.16	0.53	100.60 ± 0.27	1.85	94.52 ± 0.92
	S/C	3.35	99.02 ± 1.79	0.35	100.20 ± 0.35	1.30	94.98 ± 0.86
	W/G	10.28	101.20 ± 4.88	2.13	96.32 ± 1.36	0.55	95.33 ± 0.37
	M/G	12.38	101.52 ± 7.59	3.63	96.18 ± 1.99	1.08	94.68 ± 0.65
	S/G	6.08	97.73 ± 4.21	6.32	93.73 ± 2.98	1.35	94.80 ± 0.73
	W/H	6.90	96.88 ± 3.75	2.95	91.78 ± 1.58	0.30	95.17 ± 0.21
	M/H	9.50	102.60 ± 6.85	1.03	94.48 ± 0.54	1.20	94.85 ± 0.68
	S/H	17.35	100.30 ± 8.95	1.78	92.07 ± 1.17	1.33	94.85 ± 0.67

W/C – Wood/Control, W/G – Wood/Grass Clippings, W/H – Wood/Hay; M/C – Metal/Control, M/G – Metal/Grass Clippings, M/H – Metal/Hay; S/C – Soil/Control, S/G – Soil/Grass Clippings, S/H – Soil/Hay; IQR – Interquartile range; SD – Standard deviation; τ – Treatments; MH – Mounting height

2.3.1.1 Performance of the Walabot Radar

Trials including grass clippings as vegetation cover between the Walabot radar and selected ground surfaces resulted in lower variation of SD values (±3.06 - ±7.59 cm) relative to other treatments SD values, with mean offset ranging from -3.47 to 3.56 cm. Trials including the control (air as a medium) treatment resulted in relatively higher variation of SD values varying from ±1.16 to ±7.36 cm with the mean offset ranging from -5.30 to 6.32 cm. Similarly, the trials including hay as vegetation cover resulted in the highest range of SD values relative to other treatments SD values, varying between ±1.72 and ±15.62 cm with mean offset range of -1.95 to 4.33 cm. The Walabot radar resulted in 4% of SD in the high precision group, 55% in the moderate precision group, and 41% in the low precision group. The Walabot resulted in IQR ranging from 1.90 to 17.35 cm which indicated an extremely large variation in a range where 50% of the data spread out. The trend in the mean detected height under control condition suggested that the output of the Walabot radar was overestimated when it tried to detect the true ground surface height of metal and wooden surfaces by maximum factor of 5.30 cm while the mean detected height was underestimated by the maximum factor of 1.70 cm when soil surfaces were included in the trials. The Walabot radar exhibited irregular and inconsistent behavior in mean detected heights and SD values during the corresponding trials (**Figure 2-12**). While detecting the metal surface with hay as a vegetation cover, the output of the radar resulted an overlap in the mean intervals (mean ± SD) for 0.80 m and 1.00 m mounting height trials (**Figure 2-12**). Mean interval overlap was also observed in the same trial for 0.60 m and 0.80 m mounting height (Figure 2-12). The observed overlap of mean intervals suggested

extremely poor precision of the Walabot radar in trials for hay as a vegetation cover (**Figure 2-12**).

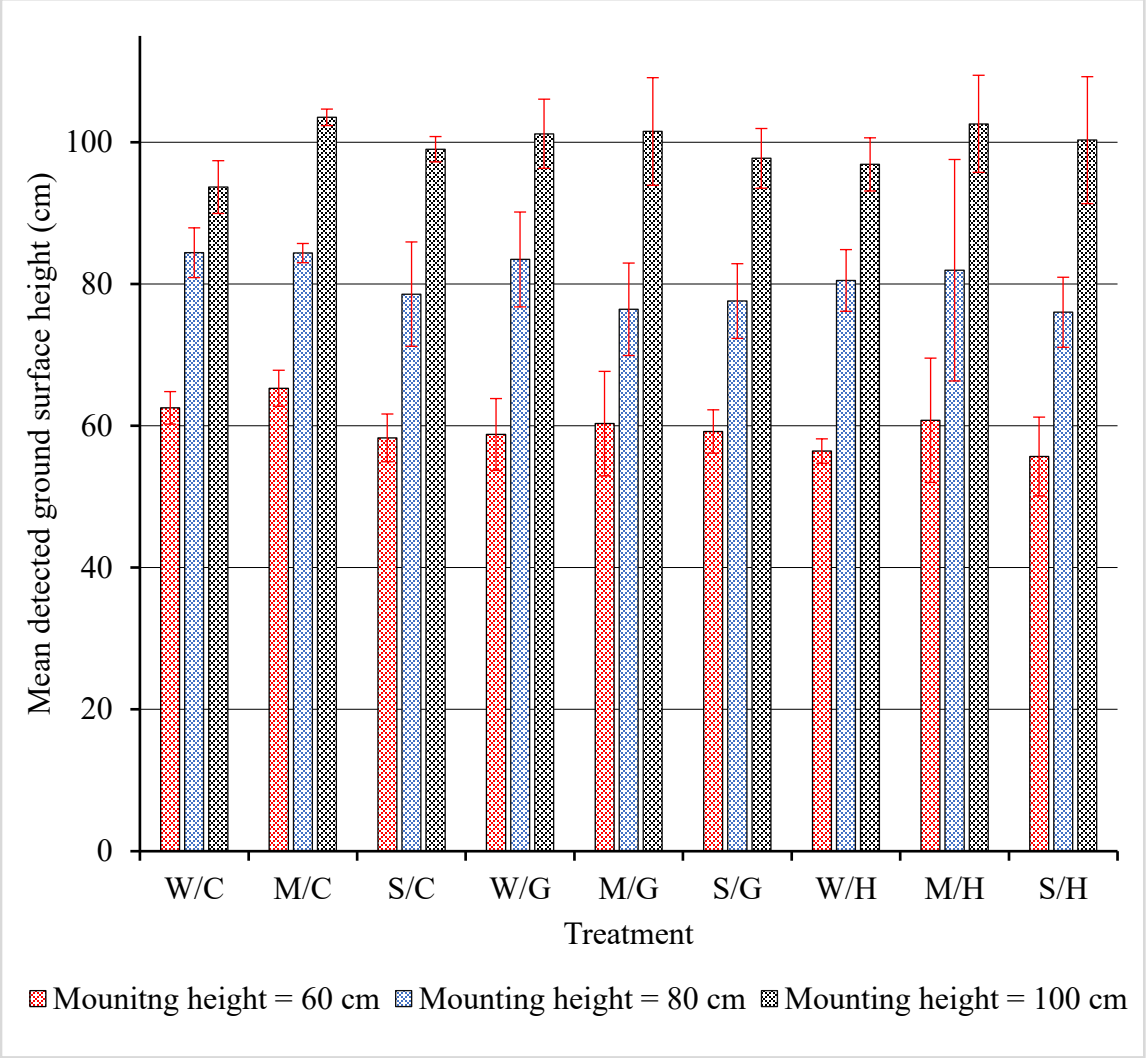

Figure 2-12: Bar graph of the mean detected ground surface heights by the Walabot radar under selected treatments (i.e., selected ground surface/vegetation cover type) and mounting heights.

2.3.1.2 Precision of the Acconeer Radar

The Acconeer radar showed more consistent behavior as compared to the Walabot radar under the same trial conditions (**Figure 2-13**). Trials with the control condition (air as a medium) resulted in a relatively low variation in SD values as compared to other treatments, varying from $\pm$0.29 to $\pm$1.09 cm with the mean offset ranging from -1.28 to -

0.15 cm. Trials with grass clippings as a vegetation cover indicated relatively high variation in SD values ranging from $\pm$0.65 to $\pm$2.98 cm with the mean offset ranging from 2.57 to 6.27 cm. Trials with hay as a vegetation cover resulted in the relatively highest variation in SD values varying between $\pm$0.80 and $\pm$3.27 cm with mean offset ranging from -2.93 to 8.22 cm. The high precision group included 59% and the moderate precision group included 41% of total SD values resulting from all the trials. Trials with the Acconeer radar did not result in any SD values belonging to the low precision group which indicated more consistency and precision in the Acconeer radar's performance as compared to the Walabot radar. The Acconeer radar resulted in IQR varying between 0.35 and 6.32 cm which indicated low variation in a range where 50% of the data spread lies, as compared to the Walabot radar. Mean detected heights were slightly overestimated for selected ground surfaces under the control conditions of vegetation cover which indicated that the Acconeer radar showed slight overestimation ($\leq$ -1.27 cm) while detecting the true ground surface height. However, an anomaly was observed in the trial including wood and hay at 0.80 m mounting height where it resulted in a mean detected height of 82.93 cm. This anomaly could be considered as an outlier based on the fact that the mean offset (-2.93 cm) was greater than the maximum value of absolute mean offset observed in control conditions. Close examination of the detected mean heights trend (**Figure 2-13**) suggested that the Acconeer radar tried to read the canopy height with slight penetration as the mean offset of detected heights lied between 2.57 and 6.27 cm when grass clippings were used as vegetation cover. The upper and lower bound of the mean offset nearly coincided with the density of the grass clipping samples (3-5 cm). Since the upper bound of the mean offset resulted by the radar under control conditions was overestimated by the maximum value

of 1.27 cm (6.27 – 1.27 = 5 cm (maximum height of grass clipping cover)), the maximum mean offset bound in detected height might be representing the canopy height. A similar trend was observed when hay was used as vegetation cover (**Figure 2-13**). Considering the anomalous behavior of the radar as an outlier (82.93 cm), the mean offset varied between 5.33 cm to 8.22 cm which nearly coincides with the density range of hay samples (7-10 cm).

The penetrative capability of the Acconeer radar was found to be more effective when hay was used as vegetation cover as compared to grass clippings. Although further studies are required to support the observation where the Acconeer radar tends to read the canopy heights.

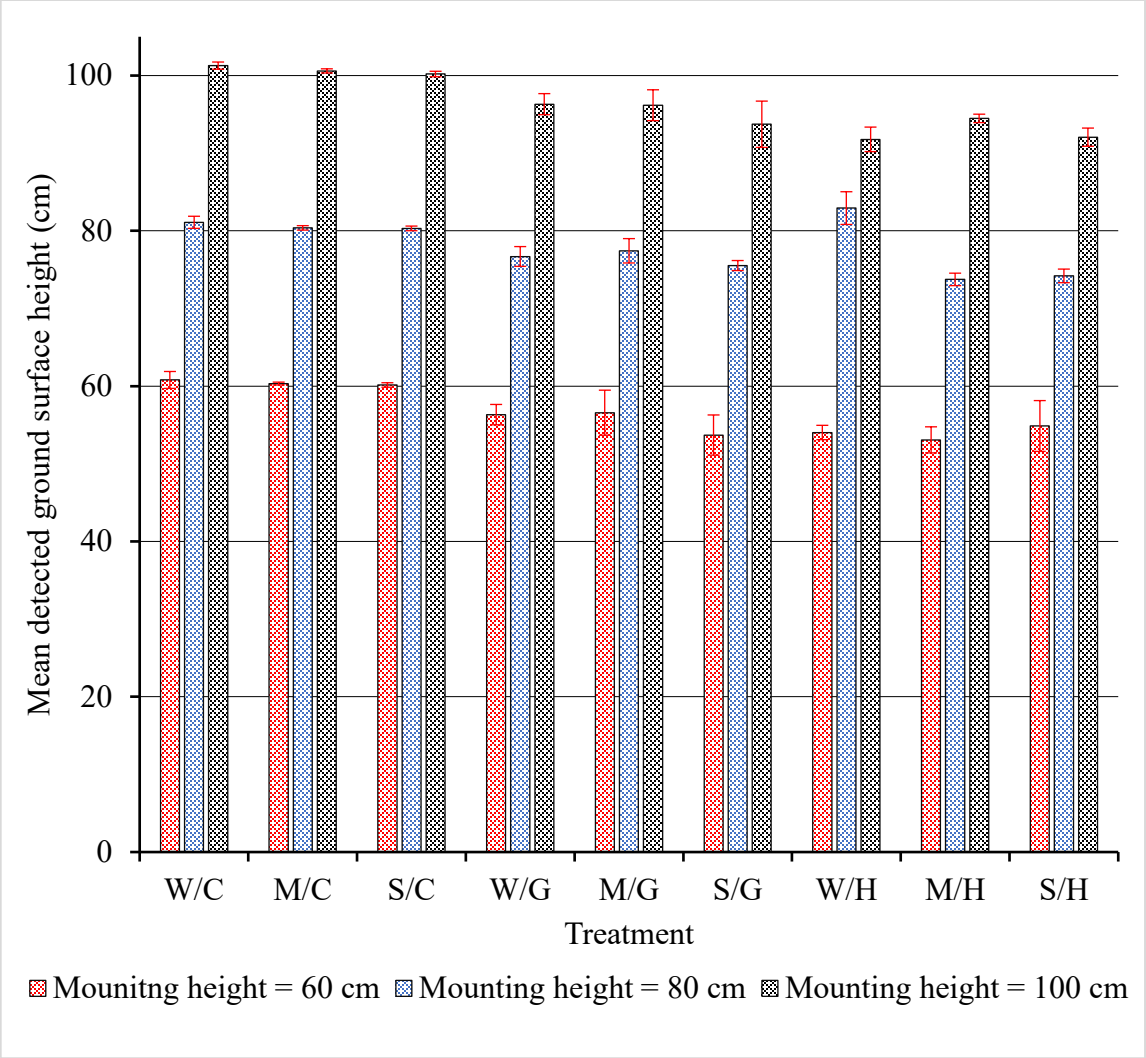

Figure 2-13: Bar graph of the mean detected ground surface heights by the Acconeer radar under selected treatments (selected ground surface/vegetation cover type) and mounting heights.

2.3.1.3 Precision of the Terrahawk® Radar

The Terrahawk® radar showed nearly constant and consistent behavior as compared to the other radar sensors under similar trial conditions (**Figure 2-14**). Variation in SD values was lower in the Terrahawk® radar's output as compared to other selected radars, where SD values for the Terrahawk® radar varied collectively between 0.23 to 1.12 cm overall trial conditions with mean offset ranging between 4.45 to 5.57 cm. Trials including control condition indicated that the Terrahawk® radar underestimated the mean detected

heights by a maximum factor of 5.48 cm. Considering this maximum observed underestimation of 5.48 cm as reference point for mean offset, the Terrahawk® detected the true ground surface height in 96% of the total trials (26/27 trials) which indicated that it successfully penetrated the introduced vegetation cover. Trial including soil and hay at 0.80 m mounting height resulted in a slightly larger underestimation (5.57 cm) in mean detected height as compared to the upper bound of the reference point (5.48 cm), hence considered as a failed trial. All the resulted SD values lied in the high precision group (SD < 1.27 cm). The Terrahawk® radar resulted in IQR ranging between 0.30 to 2.28 cm, which was the lowest as compared to other selected radars, hence indicating highest precision.

Overall, the range of SD values (1.12-0.23 = 0.89 cm) for the Terrahawk® radar was found to be lower as compared to other radars. Similar behaviour was observed in the spread of mean offset values (5.57-4.45 = 1.12 cm). The results suggested most consistent behaviour of the Terrahawk® radar, hence making this the most precise radar for through vegetation ground surface detection. The Terrahawk® radar was also found to be least prone to be affected by vegetation cover as it detected the true ground surface height in 96% of trials.

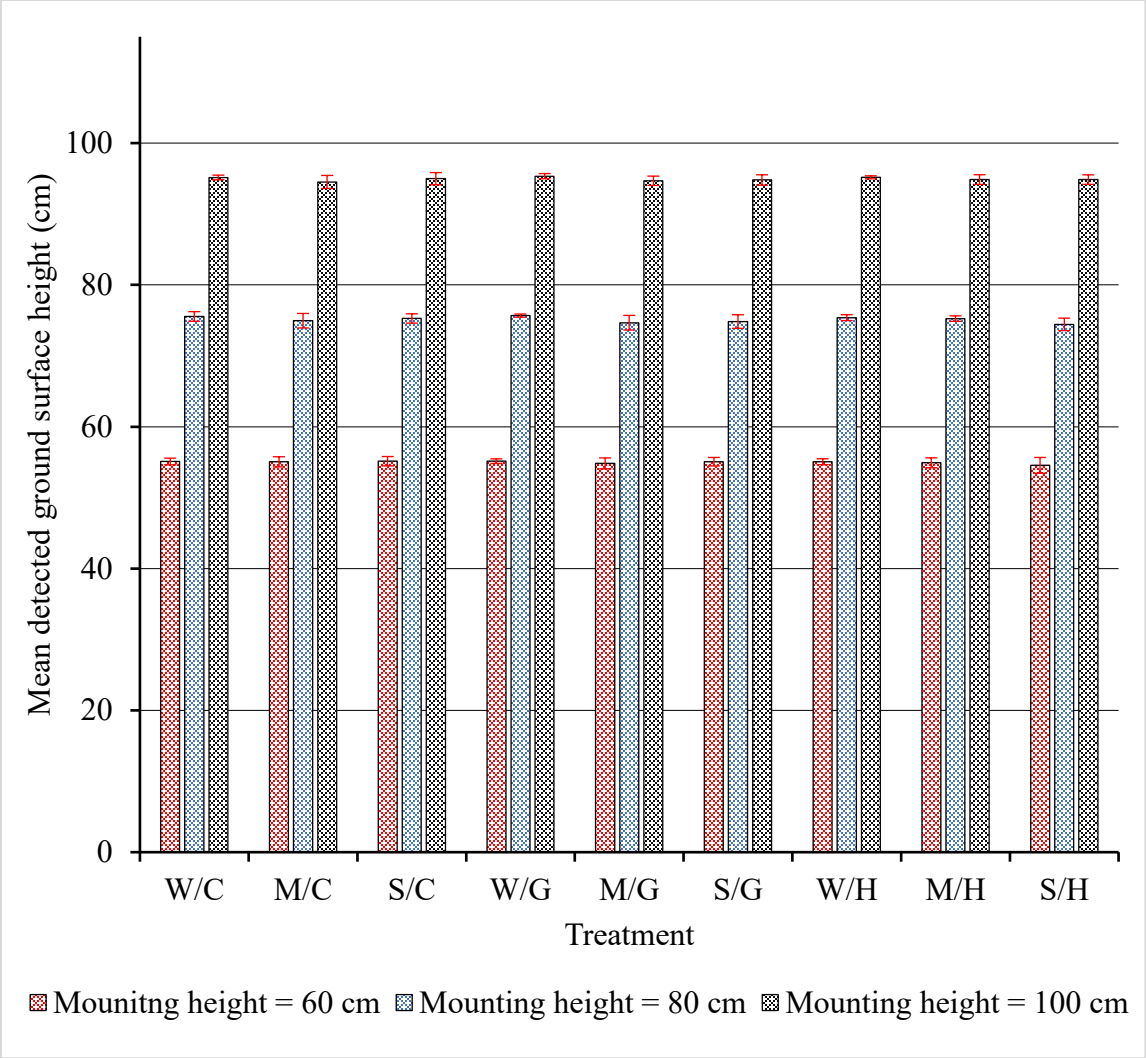

Figure 2-14: Bar graph of the mean detected ground surface heights by the Terrahawk® radar under selected treatments (selected ground surface/vegetation cover type) and mounting heights.

2.3.2 Accuracy

The accuracy of the radar sensors was compared by calculating corresponding RMSE values (**Table 2-4**) for selected radar sensors under subjected treatment conditions and mounting height levels.

Table 2-4: RMSE in detected ground surface heights by the selected radar sensors under selected treatments and mounting height levels.

Mounting Height (cm)	Treatment	RMSE (cm)		
		Acconeer	Walabot	Terrahawk®
60	W/C	1.28	3.29	4.92
	M/C	0.37	5.78	4.99
	S/C	0.30	3.52	4.90
	W/G	3.86	4.79	4.86
	M/G	4.32	6.74	5.21
	S/G	6.73	2.91	4.96
	W/H	6.03	3.89	4.95
	M/H	7.08	8.04	5.12
	S/H	5.94	6.67	5.54
80	W/C	1.31	5.46	4.49
	M/C	0.46	4.54	5.14
	S/C	0.42	6.87	4.77
	W/G	3.50	7.02	4.73
	M/G	2.94	6.93	5.42
	S/G	4.51	5.38	5.24
	W/H	3.51	4.00	4.63
	M/H	6.29	14.39	4.76
	S/H	5.85	6.02	5.62
100	W/C	1.35	7.17	4.86
	M/C	0.65	3.67	5.55
	S/C	0.38	1.91	5.08
	W/G	3.89	4.61	4.68
	M/G	4.23	7.10	5.35
	S/G	6.83	4.46	5.24
	W/H	8.34	4.63	4.84
	M/H	5.54	6.77	4.45
	S/H	8.00	8.18	5.19

W/C – Wood/Control, W/G – Wood/Grass Clippings, W/H – Wood/Hay; M/C – Metal/Control, M/G – Metal/Grass Clippings, M/H – Metal/Hay; S/C – Soil/Control, S/G – Soil/Grass Clippings, S/H – Soil/Hay; RMSE – Root Mean Square Error

2.3.2.1 Accuracy of the Acconeer Radar

The Acconeer radar showed RMSE value varying between 0.30 and 8.34 cm. Although the output of the Acconeer radar showed irregularities with the treatments including metal/grass clippings, wood/hay, soil/hay at 0.80 m mounting height, wood/hay, soil/hay at 0.60 m mounting height, and metal/hay at 1.00 m mounting height. Under the control condition of vegetation cover, the RMSE value resulted at all the mounting heights were found to be extremely low relative to other treatment conditions.

2.3.2.2 Accuracy of the Walabot Radar

The Walabot radar showed RMSE values ranging between 2.91 and 14.39 cm, with inconsistent behaviour at all three mounting height levels. Results indicated more variation in RMSE values as compared to the Acconeer radar, which indicated less accuracy of the system. Moreover, the inconsistent behaviour RMSE values indicated unpredictable pattern over all treatment conditions, which suggested that the Walabot radar was more prone to the nuisance factors involved in designed experiments.

2.3.2.3 Accuracy of the Terrahawk® Radar

The Terrahawk® radar exhibited the most consistent behavior in resultant RMSE values for all treatment conditions and mounting height levels as compared to other selected radars. Resulted RMSE values varied between 4.45 and 5.62 cm. The lowest bound of RMSE values range resulted by the Terrahawk® radar were higher as compared to lowest bound resulted by the Walabot and the Acconeer radar sensor. However, the consistent behavior made it more acceptable as the RMSE trend suggested by the Terrahawk® radar followed an approximately constant pattern which could be accounted for by linear calibration models as an offset. Furthermore, the RMSE values showed a

slight variation, and this variation was independent of the treatment conditions and mounting height level.

Overall, the Walabot radar exhibited the least accurate behavior with the highest upper bound of the RMSE range (14.39 cm) and more spread in the RMSE range (2.91-14.39 cm). The Acconeer radar performed better than the Walabot radar but was unsuccessful to completely penetrate the vegetation cover density. The Terrahawk® radar exhibited the most accurate performance with the least spread in RMSE values (4.45-5.62 cm) and approximately constant behavior.

2.3.3 Bias

Bias in the performance of radar sensors was evaluated and compared by calculating MBE under subjected treatment conditions and mounting height levels (**Table 2-5**).

Table 2-5: MBE in detected ground surface heights by the selected radar sensors under selected treatments and mounting height levels.

Mounting Height (cm)	Treatment	MBE (cm)		
		Acconeer	Walabot	Terrahawk®
60	W/C	-0.80	-2.54	4.90
	M/C	-0.33	-5.30	4.95
	S/C	-0.15	1.70	4.87
	W/G	3.67	1.22	4.85
	M/G	3.42	-0.31	5.17
	S/G	6.30	0.80	4.93
	W/H	5.97	3.56	4.93
	M/H	6.92	-0.78	5.08
	S/H	5.13	4.33	5.45
80	W/C	-1.10	-4.42	4.45
	M/C	-0.38	-4.37	5.05
	S/C	-0.32	1.42	4.73
	W/G	3.30	-3.47	4.33
	M/G	2.57	3.56	5.33
	S/G	4.47	2.40	5.17
	W/H	-2.93	-0.51	4.62
	M/H	6.25	-1.95	4.75
	S/H	5.80	3.98	5.57
100	W/C	-1.28	6.32	4.85
	M/C	-0.60	-3.52	5.48
	S/C	-0.20	0.98	5.02
	W/G	3.68	-1.20	4.67
	M/G	3.82	-1.52	5.32
	S/G	6.27	2.27	5.20
	W/H	8.22	3.12	4.83
	M/H	5.52	-2.60	5.15
	S/H	7.93	-0.30	5.15

W/C – Wood/Control, W/G – Wood/Grass Clippings, W/H – Wood/Hay; M/C – Metal/Control, M/G – Metal/Grass Clippings, M/H – Metal/Hay; S/C – Soil/Control, S/G – Soil/Grass Clippings, S/H – Soil/Hay; MBE – Mean Bias Error

2.3.3.1 Bias in the Acconeer Radar Performance

Acconeer radar showed a slight negative bias under control condition at all three mounting height levels with MBE values varying between -0.15 and 1.28 cm. Positive bias was indicated by the Acconeer radar under treatments including vegetation cover with a single anomalous reading resulted from a trial including wood/hay at 0.80 m mounting height. Apart from this anomaly, Acconeer radar showed a positive bias and resulted MBE values varied between 2.57 and 8.22 cm.

2.3.3.2 Bias in the Walabot Radar Performance

The Walabot radar trial resulted in irregular behavior with the same treatment conditions indicating randomly positive and negative bias with a change in the mounting height level. The soil surface was mostly underestimated except for a trial including hay at 1.00 m mounting height. Metal surface was mostly overestimated except for the trail including grass at 0.80 m mounting height. The wood surface showed the most inconsistent behavior with randomly switching between positive and negative bias values even under the same mounting height level. Overall, the Walabot radar resulted in MBE values varied between -5.30 and 6.32 cm.

2.3.3.3 Bias in the Terrahawk® Radar Performance

The Terrahawk® radar showed the most consistent behavior with 100% positive bias performance and resulted in the lowest variation in MBE values varying from 4.33 to 5.57 cm. The Terrahawk® radar indicated approximately constant straight horizontal line behavior irrespective of selected mounting height level and treatment conditions which suggested a relatively highly stabilized response as compared to other selected radar

sensors. Nearly constant MBE values suggested that this offset might be the operating offset of the radar sensor introduced while hardware design/manufacturing or by algorithm it was operating on, rather than being introduced by experimental conditions. This observation leads to the possibility that the operating offset of the Terrahawk® radar sensor could be mitigated by proper calibration of the sensor in field or Lab conditions which would help to increase the accuracy and performance of the radar sensor.

2.4 Conclusion

A novel ground surface detection system was developed using non-destructive, non-contact, and penetrative techniques employing microwave radar. Three selected frequency domains were analyzed for their application through vegetation ground surface detection. Results indicated that the lower frequency band performed better in penetrating the vegetation than selected higher frequency bands. The Terrahawk® radar resulted in the most precise performance with output lying in the high precision group (SD < 1.27 cm) for all treatment conditions and mounting height level. Accuracy analysis indicated the least variation in RMSE (4.45-5.62 cm) related to the Terrahawk® radar's performance as compared to other selected radars. The Terrahawk® radar showed a positive bias trend with the least variation in MBE (4.33-5.57 cm) under all treatment conditions and mounting height level. Overall, the Terrahawk® radar sensor offered high precision and accuracy with slight underestimation in the height measurement of detected ground surfaces. Results of this study show the great potential for automation of the harvester picking reel using the Terrahawk® radar sensor for real-time foliage penetration and ground surface detection in wild blueberry fields.

CHAPTER 3: FEASIBILITY ANALYSIS OF LOW-FREQUENCY ULTRAWIDE BAND MICROWAVE RADAR FOR REAL-TIME GROUND SURFACE DETECTION WITHIN WILD BLUEBERRY FIELDS

ABSTRACT

Harvest efficiency for wild blueberry mechanical harvesters depends on the operator's skill and full automation of picking heads rely on the accurate and precise determination of berry picking height. Spatial variation related to the ground slope in wild blueberry fields creates a serious challenge for the operators to maintain the optimum head height. A non-destructive foliage penetration ground detection technique is required to automate the harvester head height for optimum berry picking operation and to reduce operator stress. Microwave radars have been vastly utilized in agriculture for their application in penetrative spectroscopy, but research is still needed to determine the potential to detect the ground surface in wild blueberry fields in real-time while harvesting. In this research study, an ultrawideband (UWB) microwave radar with a built-in microprocessor connected to a ruggedized laptop operating custom-built software was evaluated in real-time and its feasibility for non-destructive ground surface detection in wild blueberry fields was analyzed. The performance of the selected radar was evaluated at three distinct mounting heights (0.60, 0.80, and 1.00 m). The developed system was calibrated with manually measured height using linear regression for selected surfaces ($R^2 = 0.99$). A factorial design was conducted to analyze the significance of mounting height (p-value < 0.001), dry vegetation cover (p-value > 0.05), and wet vegetation cover (p-value > 0.05) on the performance of the radar. The developed system was then analyzed for its performance in selected wild blueberry fields and comprehensive surveys were conducted for data collection at three stages during the summer. Linear regression models were developed to analyze the significance of stem and fruit parameters on the performance of the developed system. The output of the selected radar was strongly correlated with actual ground height (R^2 = 0.92-0.99) while resulting in a non-significant correlation with stem and fruit parameters. Overall, the developed system measured the ground surface with a high degree of accuracy and showed great potential in real-time ground surface detection in wild blueberry fields.

3.1 Introduction

Wild blueberry (*Vaccinium angustifolium Ait.)* is an important horticultural and commercial commodity in Canada with a farm gate value of more than $112 million in the year 2019 and 2020 (Statistics Canada, 2021). Wild blueberry is unique as it's native to northeastern North America and has never been cultivated on commercial scale (Zaman et al., 2009). The production cycle of wild blueberry fields is managed biannually with vegetative growth in the first year and fruit production followed by pruning of perennial shoots in the second year after harvest (Eaton, 1994). Being an ecologically dominant and economically significant crop, it has been a constant struggle within the industry to reduce the cost of production and improve yields with an efficient way of harvesting (Farooque, 2015).

High wages, quality and shortage of labor (Yarborough, 2017) along with the brief harvesting period (Farooque et al., 2014) and significant harvesting losses (Kinsman, 1993) outline a few factors contributed towards the shift from traditional practices to mechanized wild blueberry harvesting. Initial efforts to reduce production cost and berry losses using mechanical harvesters began in the 1950s (Dale et al., 1994), but a functional harvester was not manufactured until the 1980s (Hall et al., 1983). Major challenges faced during the development of a mechanical harvester were variable field topography, high degree of ground slope variation, low stem height, and natural existence of weeds, debris, and bare soil patches (Farooque, 2015). The very first mechanical harvester was originally modified from a cranberry picker in 1956 and consisted of six raking combs rotating opposite to the direction being traveled. However, the rigorous harvesting operations resulted in high fruit losses and soil digging problems (Dale et al., 1994). Later, it was modified by adding a

hollow reel mechanism (Gary, 1970), which provided the basis for the commercial harvester of today. Different prototypes were developed over the years and analyzed for their real-time performance in the fields (Soule, 1969; Gray, 1970; Richard, 1982), but none of them were commercially adopted due to inefficient harvesting and difficulties caused by uneven topography (Farooque et al., 2014). Doug Brag Enterprises (DBE) Limited of Collingwood, Nova Scotia redesigned the wild blueberry mechanical harvester by adding technical features including a hydraulic control system for head height adjustment and variable picking head rotational speed (Malay, 2000). DBE is the largest manufacturing company of wild blueberry harvesters in North America with over 1500 machines currently operational in this region and has been a key player with several wild blueberry harvester advancements to enhance real-time performance (Esau et al., 2020; Farooque et al., 2014).

Mechanical harvesting of wild blueberries has been considered as one of the most reliable techniques for reducing labor costs (Yarborough et al., 2017). However, efficient mechanical harvesting operation requires an experienced operator to maximize berry recovery and profit margins, which comes at an expense of elevated operator stress and fatigue (Farooque et al., 2014). Wild blueberry fields contain substantial ground slope variation within the fields and between the fields (Zaman et al., 2010a; Esau et al., 2021), which requires constant adjustment in head height positioning during mechanical harvesting operations (Esau et al., 2020). Uneven topography in wild blueberry fields, if not accounted for during real-time mechanized harvesting, can act as one of the major factors influencing harvest efficiency (Gary, 1970; Soule, 1969; Rhoades, 1961; Farooque et al., 2020) and can also cause damage to the picking head. Continuous maneuvering by

the operator to adjust the head height with respect to the topography of the field is a strenuous job, nonetheless, it is possible to some degree for the single and double head configurations (Esau et al., 2020; Chang et al., 2017). As the industry intends to improve the harvesting experience by adding more heads to their machines and to reduce operator's stress by automating the harvester head operation, an automated system is required which can detect the ground surface in real-time and back feed the controller for head height adjustments on the go (Esau et al., 2020).

Many researchers have contributed to delineating the factors affecting wild blueberry harvest efficiency and analyze the potential of different precision agricultural techniques to provide an optimal solution (Chang et al., 2017; Esau et al., 2021, 2020; Farooque et al., 2013, 2014, 2016a, 2016b, 2017, 2020; Jameel et al., 2016; Zaman et al., 2009, 2010a, 2010b). However, very limited attention has been paid to mitigate the challenges caused by uneven topography within wild blueberry fields. Chang et al. (2017) developed an automated plant height measurement system using an ultrasonic sensor which can serve as an indirect way to estimate the flat ground surface by subtracting the plant height from the mounting height of the sensor. However, large degree of slope variation (Esau et al., 2021; Zaman et al., 2010a) along with spatially variable stem and fruit density (Farooque, 2015) within wild blueberry fields would make this technique less effective for true ground sensing.

Microwave technology can penetrate the plant canopy regardless of the time of day making it a promising remote sensing device for precision agriculture technologies (Brakke et al., 1981). Ground-penetrating radars operating in a radio frequency range offers a non-destructive and in-situ sensing tool, which has been widely used in civil engineering

(Goodman, 1994; Maierhofer, 2003), archaeological research (McKeand, 2014; McKinley, 2007), geophysical investigations (Carrière et al., 2013; Davis & Annan, 1989) and agricultural studies (Butnor et al., 2001; Borden et al., 2014). Hruska et al. (1999) utilized ground-penetrating radar for mapping tree roots where they were successful to separately detect the roots with 3-4 cm in diameter. Sinusoidal modulated low-frequency microwave radar systems, also known as FMCW radars with their ability to penetrate through vegetation and insensitivity to water, dust, and gasses at lower frequencies can offer precise distance measurements (Noyman & Shmulevich, 1996; Kraszewski & Nelson, 1995). Noyman & Shmulevich (1996) employed X-band (8-12 GHz) microwaves to successfully detect flat ground surface with 5 mm accuracy through *Panicum miliaceum, Senecio Vernalis,* and *Ceratonia*. Woods et al. (1999) found that optimal frequency to measure ground surface distance in sugar cane crop lies between 2.6-4 GHz while S-band (2.6-3.95 GHz) showed the greatest potential in sensing ground level as compared to C-band (3.3-4.9 GHz) and X-band (8.2-12.4 GHz). Microwave radars have been vastly utilized in agriculture for their application in penetrative spectroscopy, but research is still needed to determine the potential to detect the ground surface in wild blueberry fields in real-time while harvesting. This research study focuses on the feasibility of low frequency (1.5-6.5 GHz) UWB FMCW microwave radar sensor to penetrate in a non-destructive manner through the wild blueberry crop for ground surface sensing, which can feedback the controller for automated harvester head height adjustment in real-time.

3.2 Material and Methods

3.2.1 Hardware Components

3.2.1.1 Radar Sensor

The radar sensor used in this study was a Terrahawk® (Model: HT5230) with a footprint of 0.211 m x 0.104 m x 0.0794 m, developed by Headsight Inc. (Headsight Inc., Bremen, Indiana, USA) for height control applications in grain and cornfields. The Terrahawk® radar sensor is a low-frequency UWB microwave radar sensor with transmission frequency ranging from 1.510 to 6.425 GHz centered at 3.9675 GHz, which overlaps the L, S, and C frequency bands defined by IEEE (Bruder, 2013). Antennas used in the Terrahawk® radar sensor are modified bowtie antennas (BT6100) with a gain of 4-6 dBi developed by Flat Earth Inc. (Flat Earth Inc., Bozeman, Montana, USA). It has a pulse repetition frequency of 41.66 Hz (24 ms). The Terrahawk® offers 90° field of view (FOV) for data acquisition with an adjustable resolution of 4 mm and 8 mm. It can communicate with the host using either Universal Serial Bus (USB) or Communication Area Network (CAN) interfaces. The Terrahawk® radar sensor has a built-in microprocessor for signal processing which can only be utilized if CAN communication is active. In contrast, if the USB interface is employed for debugging and communication, it disables the built-in microprocessor and uses the host microprocessor for signal processing. In the developed system for ground sensing in wild blueberry fields, the latter way of communication was employed to visualize the reflected signals using a host laptop.

3.2.1.2 Processing Unit

Signal processing and data acquisition were carried out using an MSI WS65 9TM-1410CA workstation laptop (Micro-Star International Co., Ltd., Taipei, Taiwan) as a host.

It was powered by Intel Core i9-9880H/2.3-4.8 GHz chipset (Intel Co., California, USA) with a dedicated Nvidia Quadro RTX 5000/16GB GDDR5 (Nvidia Co., California, USA) graphic processing unit. Communication between the radar sensor and the host processor was established using a USB 2.0 port. Parameters of the radar sensor including resolution, sensitivity threshold, radar start distance, and distance of the radar projected beam accumulated for digital signal processing by the algorithm were defined during data collection using custom-built software developed by Headsight Inc.

3.2.2 Mounting Assembly

A modular wooden mounting stand was built for performance evaluation of radar data, both in the Lab and in field (**Figure 3-1**). The mounting assembly consisted of three parts: a sensor mounting plate, an adjustable mounting arm, and a supporting stand. The supporting stand had a total height of 1.10 m from the ground, and it was designed to provide height adjustment for the sliding modular mounting arm with an adjustable resolution of 0.02 m, starting from 0.58 m from the ground (**Figure 3-1**). The 0.08 m thickness of the radar sensor's footprint when mounting at the lowest position provided the sensor with a clearance of approximately 0.50 m off the ground.

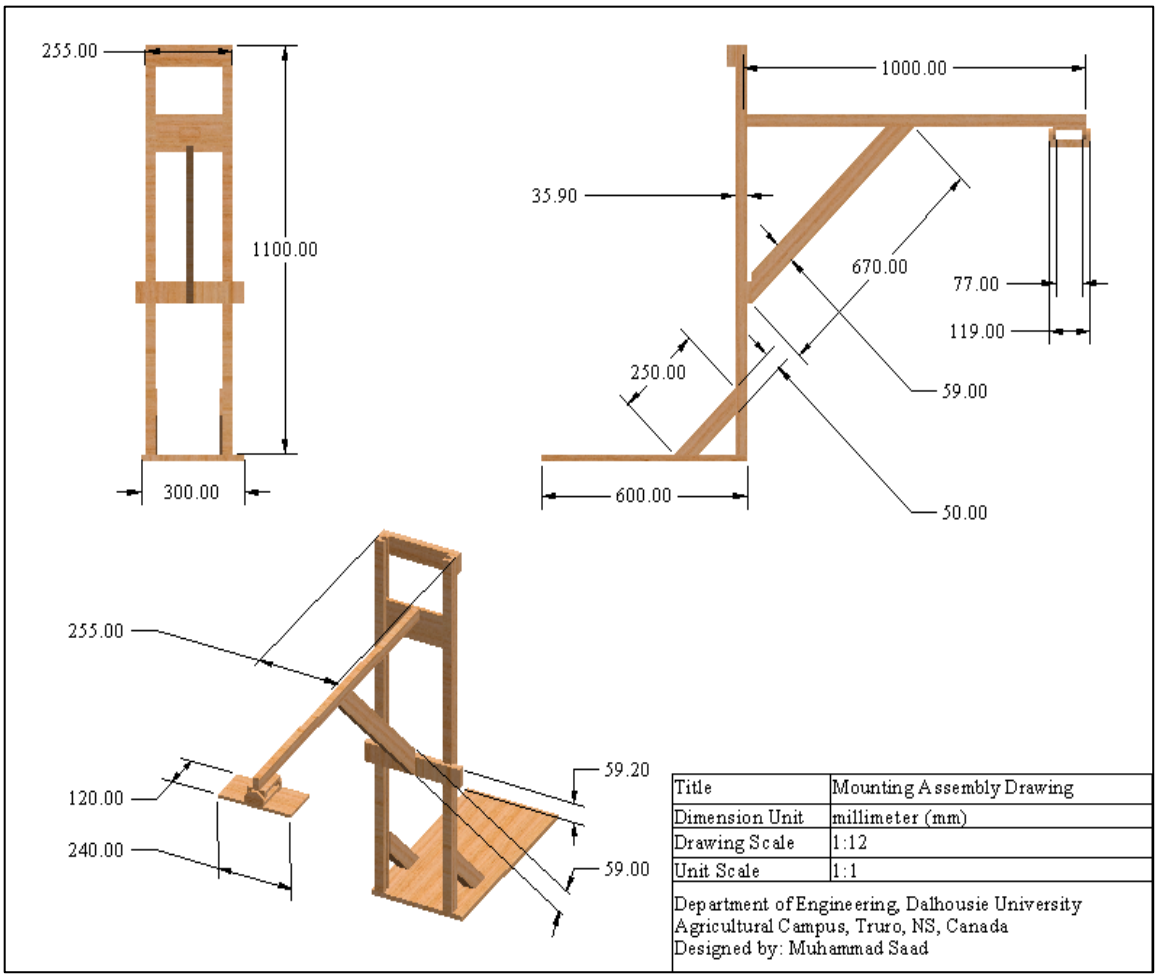

Figure 3-1: Custom-built assembly for mounting the radar sensor during standstill data collection in Lab and field environments.

3.2.3 Data Acquisition Software

The *TerrahawkBuddyLite* (Version: 1.20) executable program was used for data visualization, acquisition, and signal processing on the host workstation. It is a custom-built software developed by Headsight Inc., which provides a simplified graphical user interface (GUI) for visualizing the output data and defining different input parameters for the Terrahawk® radar operation. The trials for this research study were carried out keeping the radar stationary at selected mounting heights with default resolution (4 mm), RMS threshold value of 4, radar start distance of 0.00 m, and DSP start distance of 0.20 m.

3.2.4 Lab Evaluations

3.2.4.1 Lab Evaluation Site

Preliminary evaluations were carried out in the Mechanized Systems and Precision Agriculture (PA) Lab, Dalhousie Agricultural Campus, Truro, NS, Canada. Traditional statistical experiments were designed to analyze the feasibility of the Terrahawk® radar sensor to detect the ground surface through created vegetation cover. Three surfaces were selected as ground surfaces to evaluate the performance of radar: a) wooden surface; b) metal surface; and c) soil surface. Calibration of the sensor was performed by developing six separate regression models corresponding to each selected ground surface and mounting height separately. The vegetation cover was created using grass clippings and hay. The effect of the dry and moist vegetation on the performance of the radar at three different mounting heights was analyzed separately using a 3x3 factorial design.

3.2.4.2 Experimental Setup

The experimental setup for Lab trials comprised aluminium sheets, wooden boards, soil, grass clippings, and hay. Aluminium sheets (breadth = 0.0006 m), wooden boards (breadth = 0.02 m), and soil samples (breadth = 0.10 m) were used as a ground surface. The width of each experimental unit was kept constant (0.91 m) to match the width of the traditional wild blueberry harvester head manufactured by DBE. To emulate the vegetation canopy in wild blueberry fields, grass clippings and hay were used separately to create two different types of vegetation cover over the randomly selected ground surfaces. The radar sensor was evaluated at three selected mounting heights: a) 0.60 m; b) 0.80 m; and c) 1.00 m. The mounting height was measured from the bottom of the radar's casing to the top of the selected surface. Different mounting heights were selected to evaluate the performance

of the radar sensor at each height. The upper bound (1.00 m) of the selected mounting heights were chosen to cover the whole width of the harvester head (0.91 m) during each scan. The selection of the lowest bound (0.60 m) provided the lowest point at which the radar sensor could be mounted without getting in contact with stems in the wild blueberry fields.

Table 3-1: Lab trials setup with two types of experiments related to each selected ground surface and corresponding factors of interest.

Type of Trials	**Set 1 FOI (Wooden Surface)**	**Set 2 FOI (Metal Surface)**	**Set 3 FOI (Soil Surface)**
Trial-1	Mounting Height	Mounting Height	Mounting Height
	Dry vegetation cover	Dry vegetation cover	Dry vegetation cover
Trial-2	Mounting Height	Mounting Height	Mounting Height
	Wet vegetation cover	Wet vegetation cover	Wet vegetation cover

To cover maximum experimental variability within a Lab environment, a 3x3x2 (levels of height x levels of vegetation cover x replications) experimental design was established with a total of 18 samples of each ground surfaces (i.e., metal sheets, wooden boards, and soil samples) (**Table 3-1**; **Figure 3-2**). During Lab trials, each sample was numbered and assigned randomly to different treatment levels. Lab trials were divided into three distinct sets of experiments with two replications each (**Figure 3-2**, **Figure 3-3**).

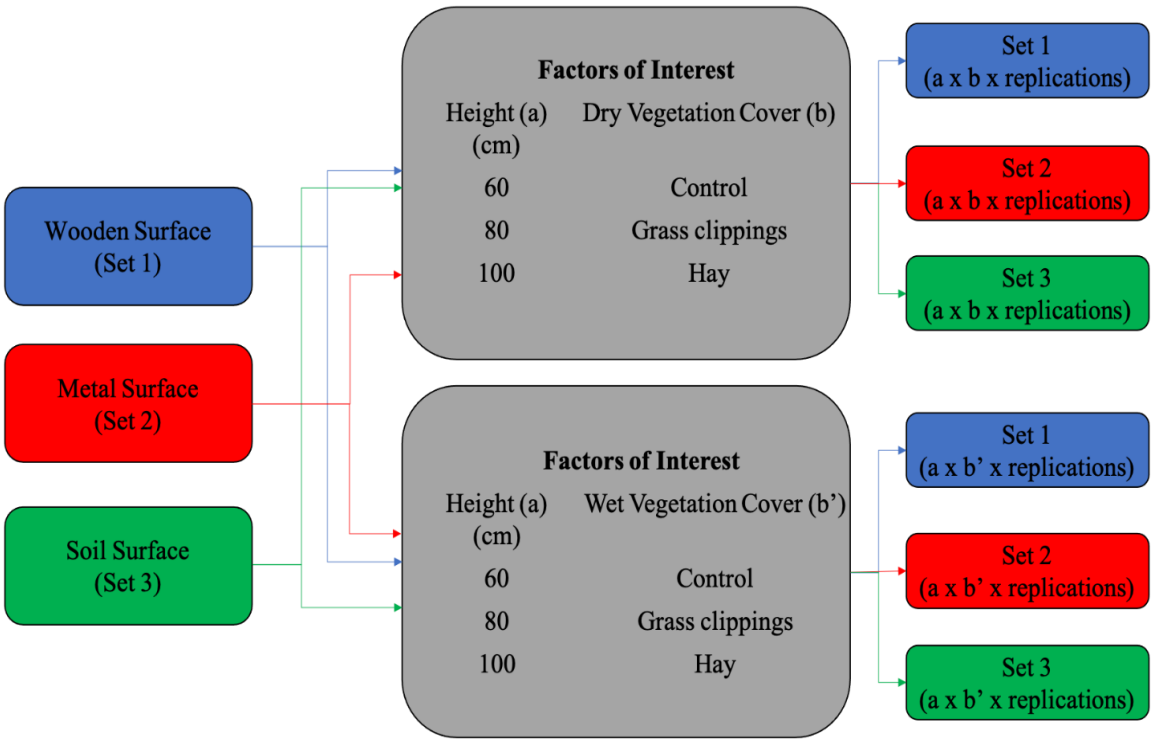

Figure 3-2: Experimental setup chart for Lab evaluations. The selected experimental units in each set were involved in two types of 3x3x2 factorial design experiments: i) experiments with the dry vegetation cover (b) and ii) experiments with wet vegetation cover (b').

Grass clippings and hay were distributed uniformly over the randomly selected ground surfaces (**Figure 3-3**). Density was measured in terms of the bulk density of the vegetation cover which was kept approximately at 48.62 kg m^{-3} (sample vertical height = 7-10 cm) for hay and 63.38 kg m^{-3} (sample vertical height = 3-5 cm) for grass clippings. Each trial was carried out in a controlled environment which eliminated the possibility of interference from any material other than designated experimental units. During the second set of trials, moisture was created over the vegetation cover using a handheld water sprayer and uniform distribution of the droplets was ensured by keeping the hand sprayer at 1 m height for all the randomly selected samples. Moisture content was measured using ProCheck (Decagon Devices, Inc., Washington, USA) handheld reader and was maintained at approximately 0.90 kg m^{-2} for all the selected samples. During each set of trials, the total

scan period lasted twelve seconds for continuous radar operation with three separate readings recorded after four seconds each using the *TerrahawkBuddyLite* GUI, and the final output was generated using the average of recorded readings.

Figure 3-3: Experimental sets: Set 1) wooden boards as ground surface; Set 2) metal sheets as ground surface; Set 3) soil samples as the ground surface.

3.2.5 Field Evaluations

3.2.5.1 Data Collection Site

Two wild blueberry fields were selected in central Nova Scotia for data collection. These fields include the Field A (45°25'28.9"N, 63°28'56.2"W) and Field B (45°25'37.6"N 63°28'55.2"W). These fields had been under commercial management and received biennial pruning by mowing along with the application of conventional fertilizers and weed management practices over the past few years. Selected wild blueberry fields were in fruit year during the trial year 2020.

3.2.5.2 Experimental Design

An inverted W-pattern technique (**Figure 3-4**) was followed to ensure an unbiased and randomized selection of the plot locations within selected wild blueberry fields (McCully et al., 1991; Thomas, 1985; Tamado & Milberg, 2000). A total of 36 points were flagged, with each leg of inverted W-pattern including 9 points separated by 20 paces. The starting point was determined by walking 100 paces along the edge of each field followed by 100 paces into the field at 90 degrees angle (Thomas, 1985). A 0.81 m^2 wooden frame quadrat was placed at selected points in each field to define the area of interest for collecting radar sensor data and acquiring ground-truthing data. Ground truthing data including stem density, stem height, fruit-zone height, ground surface height, stem thickness, and fruit count, were recorded manually using a 0.0225 m^2 quadrat at three random locations within each 0.81 m^2 plot and average values were extrapolated to give overall estimated values for each area of interest. Stem density (SDi) refers to the average stem count while stem height represents the average height of the stems within a 0.81 m^2 plot. Stem thickness (ST) was measured 0.05 m off the ground using a digital vernier caliper which represents the average thickness of stems in selected 0.81 m^2 plots. Blueberry fruits were counted manually on the stems and their average count in 0.81 m^2 plot is referred to as fruit count (FC). Three fruit zone heights were recorded within 0.81 m^2 plot and estimated fruit zone height was determined by averaging fruit zone height (FZH) corresponding to smaller areas of interest (0.0225 m^2). The output of the radar was recorded by placing the sensor at three locations separated by 0.30 m each along the straight line joining the centers of the parallel sides of the 0.81 m^2 plot and the mean value of three readings were calculated to give a better estimation of ground surface data related to each

plot. The radar sensor's data for selected mounting heights and ground-truthing data were recorded for all 36 plots in each field, which helped in developing different statistical models for performance analysis of the radar sensor at selected mounting heights.

Digital Elevation Models (DEMs) indicating the digital elevation profile of selected fields were developed using ArcMap 10.5 (Esri Inc., California, USA). Elevation data for the selected fields were obtained from a database maintained by the government of Nova Scotia, namely GeoNOVA (GeoNOVA, 2019) (**Figure 3-5**).

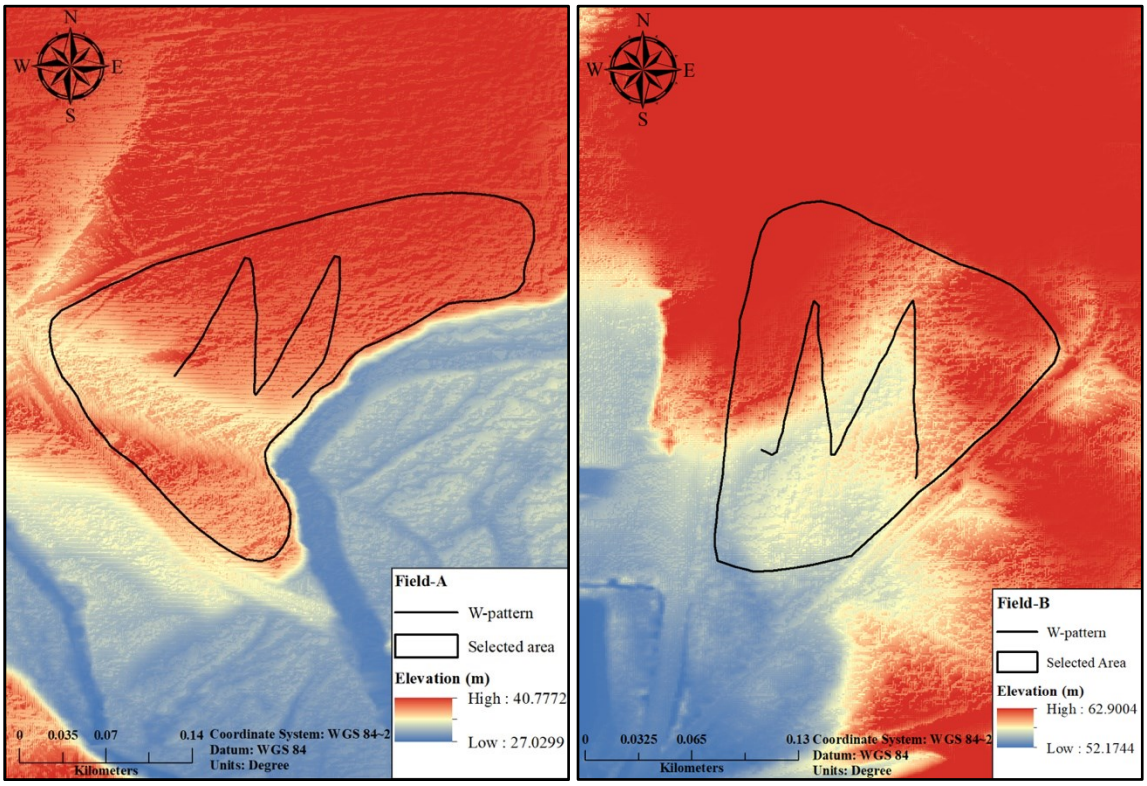

Figure 3-4: Data collection sites: Field-A (left) with the selected area of 3.91 hectares and Field-B (right) with the selected area of 2.14 hectares and inverted W pattern. The elevation profile of the selected fields has been shown by the gradient color bar.

Field data collection was repeated three times before harvesting: a) early-summer (May-June); b) mid-summer (June-July); and c) late-summer (August), and analyses were performed for each time frame separately (**Figure 3-5**). Besides covering maximum

variability to get more accurate findings, three sets of data also allowed to compare the performance of ground surface detection system during different growth stages of stem and berries within the fruit year.

Figure 3-5: Growth stages in Field A: i) early-summer (left most); ii) mid-summer (middle); and late-summer (right most).

3.2.6 Sensor Output Calibration

Before the data analysis, the radar sensor output was calibrated to compensate existing offset in the output readings. For calibration purposes, the total of 162 radar outputs were sampled and recorded with according to height (i.e., 0.60 m, 0.80 m, and 1.00 m) and ground surface (i.e., wooden board, metal sheets, and soil samples). Similarly, 18 sampling locations were determined randomly during the early summer in each selected research field and a total of 108 output readings were recorded according to each selected height. The data for calibration was collected using selected ground surfaces without involving any vegetation cover in the Lab environment and with the least vegetation in selected fields (i.e., early-summer season) to avoid the possible effect of vegetation cover on radar calibration.

3.2.7 Statistical Analysis

Statistical analyses in this research study were performed using Minitab 19 (Minitab Inc., Pennsylvania, USA). Multiple linear calibration models using the best fitted plot regression analyses were developed separately for calibration of data collected by the radar in the Lab and field environments. Multiple 3x3 factorial designs with two replications were used to evaluate the Lab experimental data with two main factors of interest including height and vegetation cover each having three levels of a factor. The above-mentioned factorial design allowed comparison of radar performance in detecting selected ground surfaces. It also helped determining the significance of different vegetation cover type (i.e., control treatment with air as a medium, grass clippings, and hay). A similar experimental design was also used to examine the significance of moisture content on the performance of the radar sensor.

For data collected in each field, Multiple Linear Regression (MLR) models were created using stepwise regression to examine the significance of plant characteristics (i.e., SDi, ST, FZH, ST, and FC) on the output of the radar sensor at selected mounting heights. Standard stepwise regression in Minitab 19 adds and removes predictors as needed for each step unless all the variables not in the model have p-values that are greater than the specified alpha-to-enter value and all variables in the model have p-values that are less than or equal to the specified alpha-to-remove value. All the statistical analyses included in this research study were performed at a 95% level of confidence interval except for the stepwise MLR which utilized an alpha of 0.15 for both alpha-to-enter and alpha-to-remove values. Index of agreement (d) and root mean square error (RMSE) was used to determine the accuracy of developed models in selected fields using the following equations:

$$d = 1 - \frac{\sum_{t=1}^{n}(O_t - P_t)^2}{\sum_{t=1}^{n}(|P_t - \bar{O}|)^2 (|O_t - \bar{O}|)^2} \quad \text{(Eq. 1)}$$

$$RMSE = \sqrt{\frac{\sum_{t=1}^{n}(O_t - P_t)^2}{n}} \quad \text{(Eq. 2)}$$

where O_t represents the observed ground distance values (manually measured), P_t represents the predicted ground distance value using predictive models developed by regression analyses, and $\bar{O}$ represents the mean observed value of manually measured ground distances. Index of agreement (*d*) lies between 0 and 1 and it is a relative measure of performance of the model with higher values representing the better performance and *vice versa* (Astatkie, 2006).

The data collected for calibration purposes (calibration data) were correlated with ground truth data using regression analyses. To examine the offset in radar output, a total of 300 data points (162 in Lab and 108 in selected fields) corresponding to radar output were recorded, and corresponding offset values were calculated (Eq. 3).

$$Offset = y - y^* \quad \text{(Eq. 3)}$$

where y represents the actual ground surface height measured manually and y^* represents the ground surface height measured by radar.

3.3 Results and Discussion

3.3.1 Calibration of Radar Sensor

The offset values were graphed separately for the Lab (**Figure 3-6**) and field environments (**Figure 3-7**) along with their RMSE values. The analysis resulted in RMSE values of 0.0484 m and 0.0483 m for respectively lab and field environments. The selected

plots in both fields respectively with an overall RMSE (O-RMSE) of 0.0483 m for combined data (i.e., data collected in Lab and field collectively).

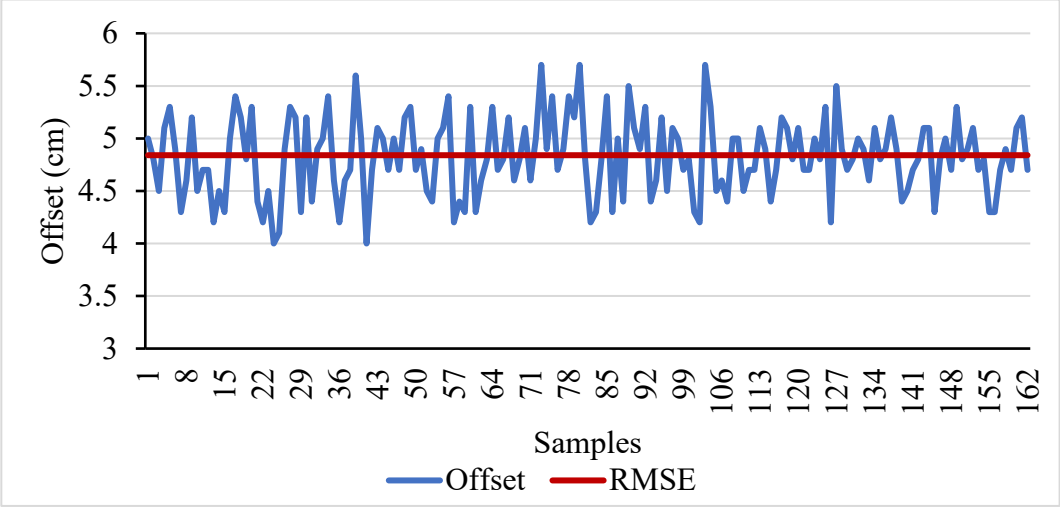

Figure 3-6: Offset values of radar output corresponding to samples collected in Lab environment were plotted using blue trend line while RMSE (0.0484 m) is indicated by a red straight line.

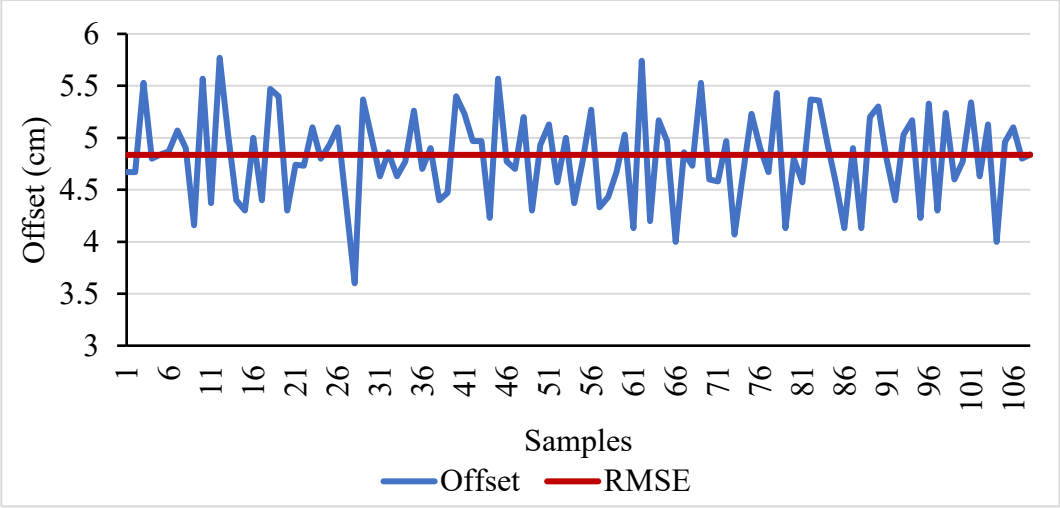

Figure 3-7: Offset values of radar output corresponding to randomly selected locations in selected fields were plotted using a blue trend line while RMSE (0.0483 m) is indicated by a red straight line.

To compensate the offset in radar output, linear calibration models were developed by plotting the radar output corresponding to the predicted ground surface height in the

Lab and selected fields against the actual ground distance (Farooque et al., 2014). These models were utilized to predict the ground surface heights in subsequent analyses.

Regression analyses of the data collected for calibration purposes in the Lab environment revealed that radar output had a strong correlation with ground surface height, irrespective of the surface type used as the ground surface. Separate linear calibration models were developed corresponding to selected ground surfaces: i) wooden surface (R^2 = 99.94%, p-value < 0.001) (**Figure 3-8**); ii) metal surface (R^2 = 99.93%, p-value < 0.001) (**Figure 3-9**); and iii) soil surface: (R^2 = 99.97%, p-value < 0.001) (**Figure 3-10**). Linear calibration models were also developed for Field-B (**Figure 3-11**) and Field-A (**Figure 3-12**) which resulted in a highly significant correlation between ground truth readings and radar output (Field-B: R^2 = 99.94%, p-value < 0.001; Field-A: R^2 = 99.94%, p-value < 0.001).

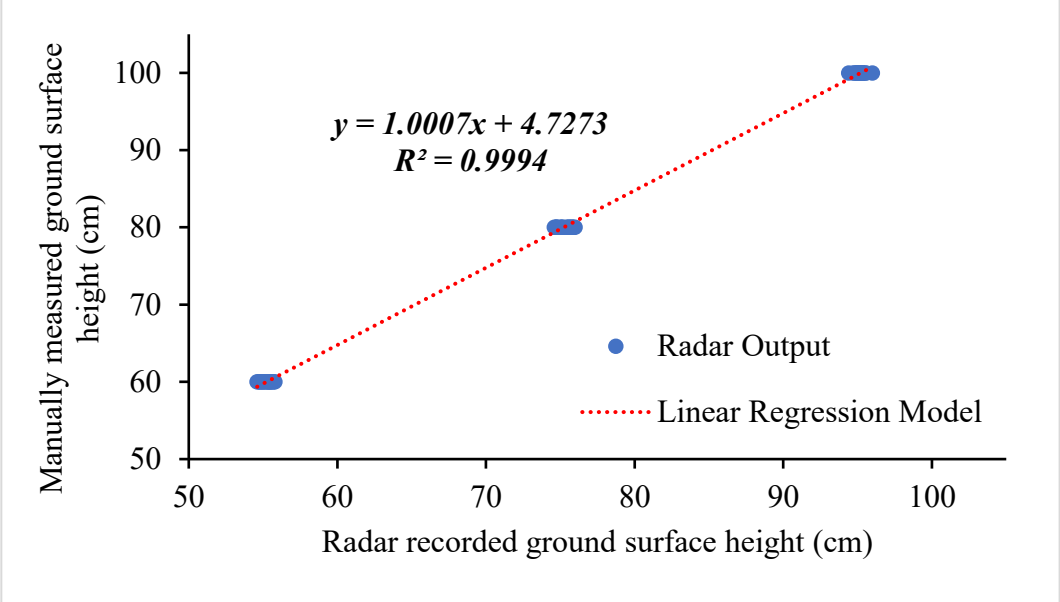

Figure 3-8: Relationship between the radar recorded output and actual ground distance measured manually corresponding to the wooden surface as a selected ground surface.

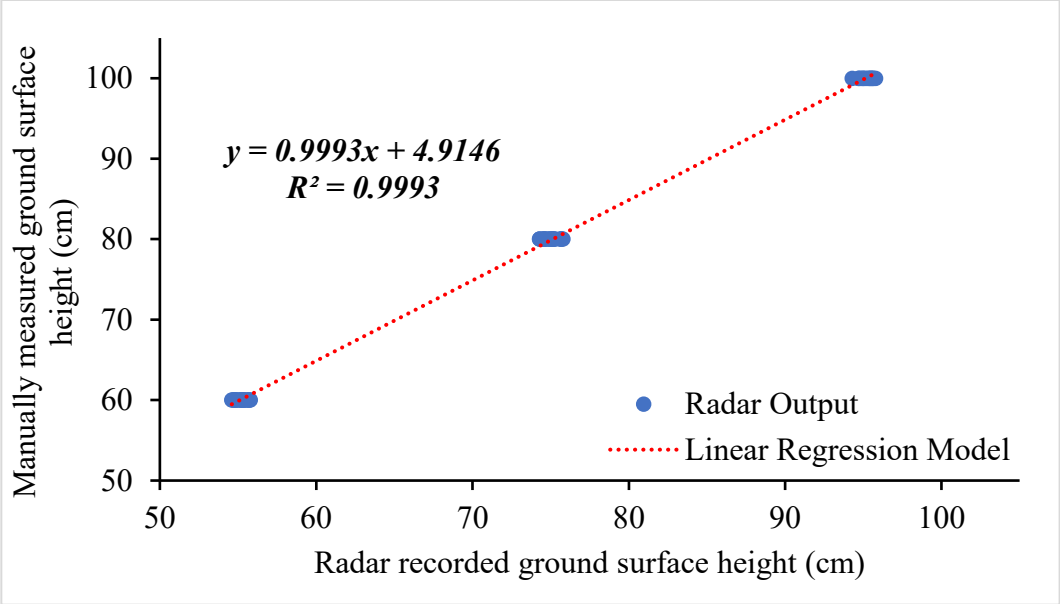

Figure 3-9: Relationship between the radar recorded output and actual ground distance measured manually corresponding to the metal surface as a selected ground surface.

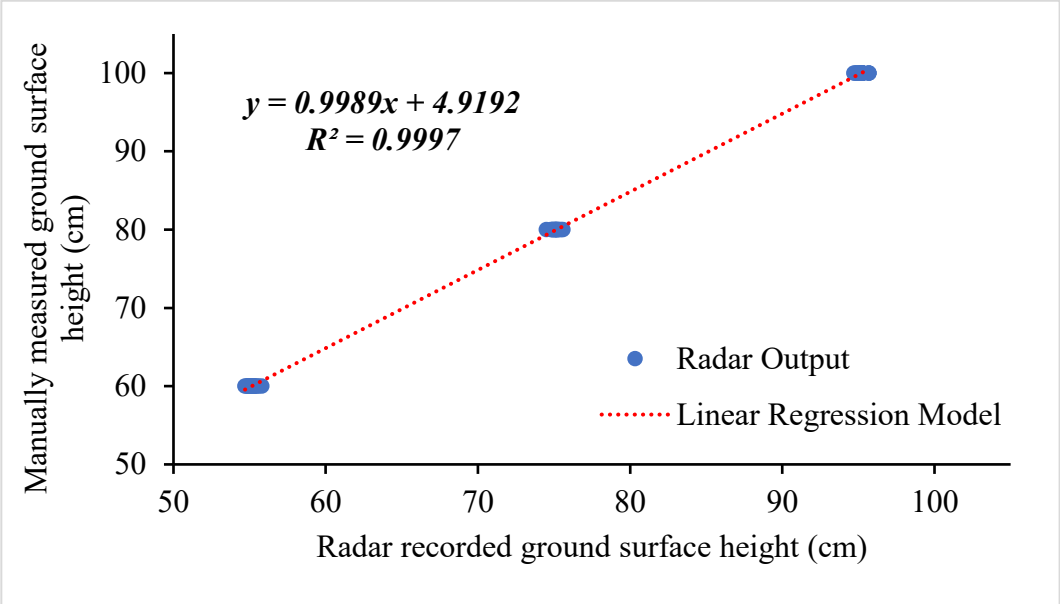

Figure 3-10: Relationship between the radar recorded output and actual ground distance measured manually corresponding to the soil surface as a selected ground surface.

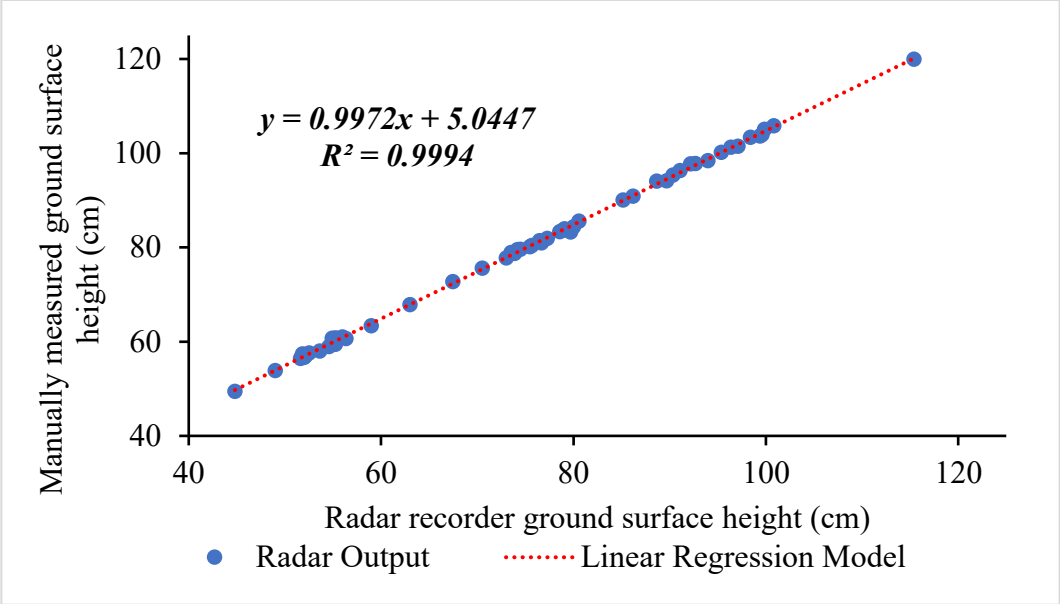

Figure 3-11: Relationship between the radar output and actual ground distance measured manually (Field-B).

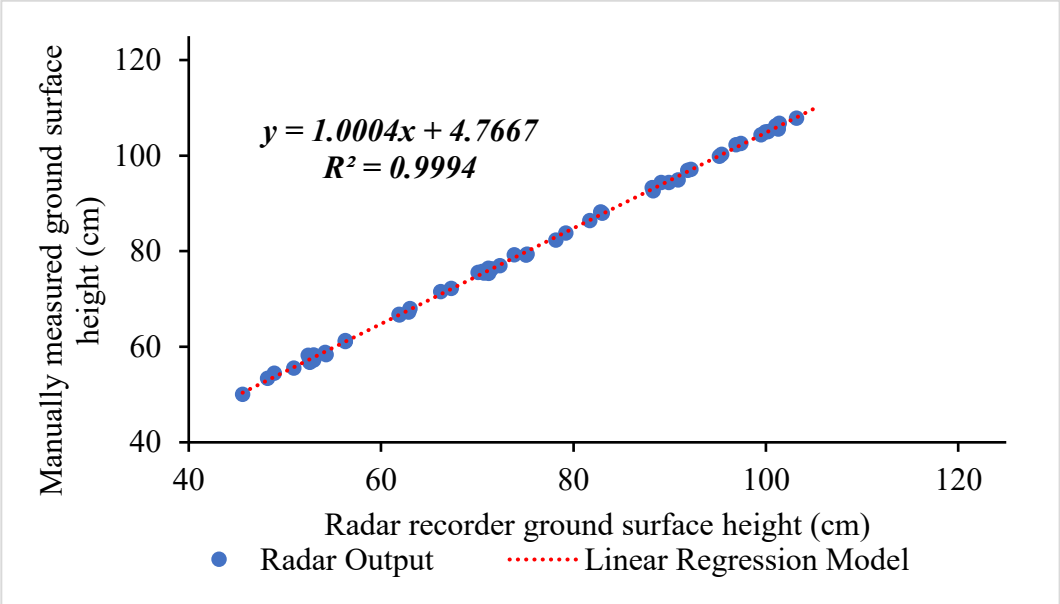

Figure 3-12: Relationship between the radar output and actual ground distance measured manually (Field-A).

For validation of developed calibrated models, the ground distance was predicted using calibrated model equations for selected ground surfaces and RMSE was calculated (**Figure 3-13**, **Figure 3-14**).

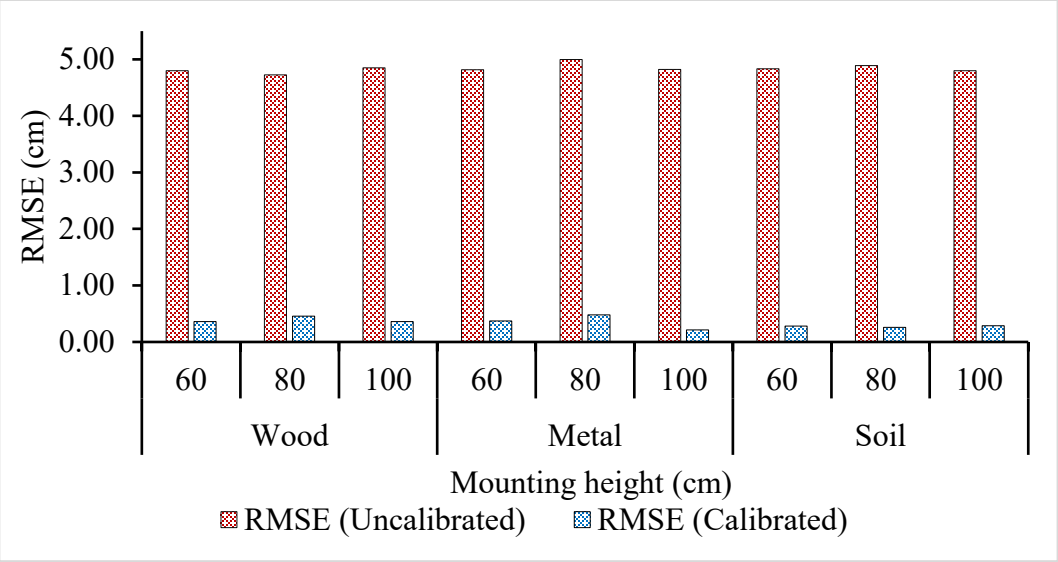

Figure 3-13: Comparison of RMSE in radar output for uncalibrated and calibrated models developed using calibration data collected in the lab.

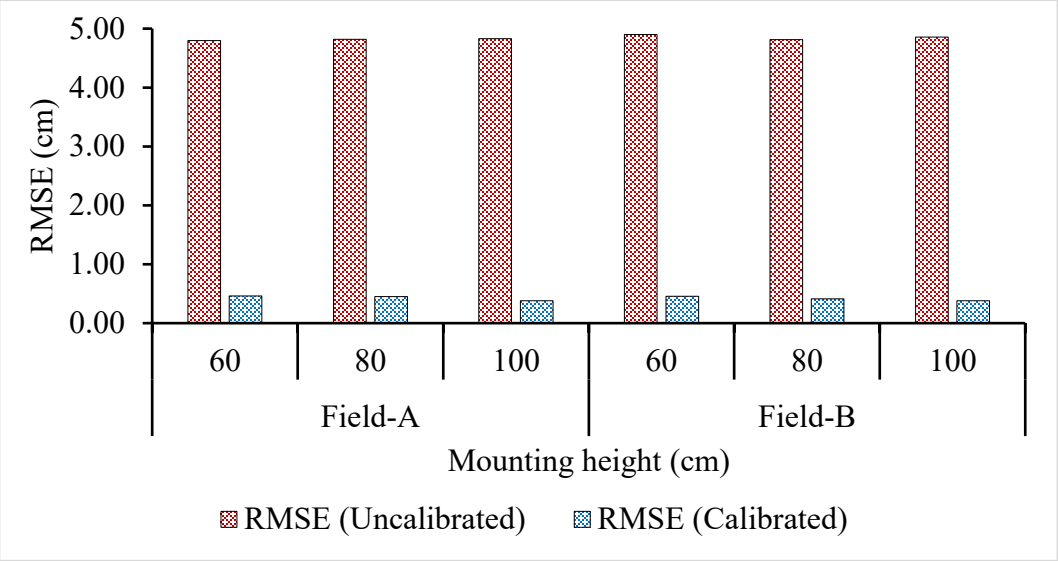

Figure 3-14: Comparison of RMSE in radar output for uncalibrated and calibrated models developed using calibration data collected in both fields.

The average percentage reduction in RMSE was calculated by averaging the percentage reduction in RMSE values for three mounting height levels (i.e., 0.60, 0.80, 1.00 m) corresponding to the ground surfaces (Eq. 4).

$$Percentage\ reduction\ in\ RMSE\ = 100 - (\frac{RMSE\ (calibrated\ model)}{RMSE\ (uncalibrated\ model)}\ X\ 100) \quad \text{(Eq. 4)}$$

Calibrated models helped to reduce the RMSE by the average of 91% for wooden surfaces, 92% for metal surfaces, and 94% for soil surfaces. For the data collected in fields, the developed calibration models reduced the RMSE by an average of 91% in both fields. Percentage reductions in RMSE values indicated that the linear calibration model successfully calibrated the radar output to detect the true ground surface height.

3.3.2 Lab Data Analysis

To compare the performance of radar sensor at different heights and to analyze the penetrative capability of the sensor through created vegetation covers in the Lab environment, multiple 3x3 factorial designs were used for each selected ground surface. Regression analyses were performed to correlate the calibrated radar output to ground truthed data. A total of six analyses of variance (ANOVA) were performed: three including dry vegetation cover (Trial-1) and three including wet vegetation cover (Trial-2.) (**Table 3-2**). These separate ANOVA analyses helped to examine the effect of dry and wet vegetation covers on the performance of radar sensor.

Table 3-2: Significance level and the p-values calculated from Analysis of Variance (ANOVA) using two 3x3 factorial designs: Trial-1) Height (0.60, 0.80, 1.00 m) x Vegetation Cover-Dry (Control, Grass Clippings, Hay); and Trial-2) Height (0.60, 0.80, 1.00 m) x Vegetation Cover-Wet (Control, Grass Clippings, Hay).

Source	Wooden Surface	Metal Surface	Soil Surface
Height[1]	* ($p < 0.001$)	* ($p < 0.001$)	* ($p < 0.001$)
Height[2]	* ($p < 0.001$)	* ($p < 0.001$)	* ($p < 0.001$)
Vegetation Cover[1]	NS ($p = 0.438$)	NS ($p = 0.515$)	NS ($p = 0.814$)
Vegetation Cover[2]	NS ($p = 0.881$)	NS ($p = 0.991$)	NS ($p = 0.876$)
Height x Vegetation Cover[1]	NS ($p = 0.726$)	NS ($p = 0.994$)	NS ($p = 0.534$)
Height x Vegetation Cover[2]	NS ($p = 0.111$)	NS ($p = 0.206$)	NS ($p = 0.135$)

* represents the significant factor of interest at a 95% confidence level; NS represents the Non-Significant factor of interest at a 95% confidence level; [1]Trial-1; [2]Trial-2; p – p-value resulted by statistical analyses

Analysis of variance (ANOVA) for the selected trials indicated that the only significant factor of interest was the height which was expected as radar was mounted at

three discrete mounting heights (**Table 3-2**). Vegetation cover showed a non-significant effect which implied that radar waves penetrated through all the selected mediums (i.e., air as a medium, grass clippings, and hay) in a similar manner without being significantly affected by their presence. It also implied that radar waves were not significantly altered by the presence of moisture content over the vegetation cover. Interaction of height and vegetation cover also resulted in a non-significant result which indicated that there is no significant effect on the performance of radar by the interaction of two main factors of interest.

Table 3-3: Results of simple linear regression analyses between calibrated radar predicted output and manually measured ground surface height for selected trials.

Source	Trial-1		Trial-2	
	R-sq (%)	p-value	R-sq (%)	p-value
Wooden Surface	99.96	<0.001	99.98	<0.001
Metal Surface	99.97	<0.001	99.65	<0.001
Soil Surface	99.87	<0.001	99.94	<0.001

Simple linear regression models were developed to correlate the predicted ground surface height for selected surfaces with manually measured height (**Table 3-3**). Results indicated that output of the calibrated model of the radar was correlated significantly with manually measured ground height for both trials.

The significant factor of interest in each ANOVA analysis was further analyzed using Tukey's MMC to examine the radar output for overlapping erroneous readings at three different mounting heights. Letter grouping generated by Tukey's MMC indicated that there was no overlapping response by radar at three different mounting heights (**Figure 3-15**).

The trials with the wooden surface showed a slight bias which can be observed in Tukey's MMC results (**Figure 3-15**), where the calibrated model for the respective ground

surface resulted in an overestimation of ground surface height. This overestimation in the radar output might have occurred due to the reason that higher wavelength waves corresponding to the lower frequencies within the UWB of the radar sensor tend to penetrate the wooden surface (Liu et al., 2014). Since the application of the radar sensor for each trial was for a limited time interval, the overestimation trend was not consistent except for the mounting height of 0.80 and 1.00 m in Set 1 trials.

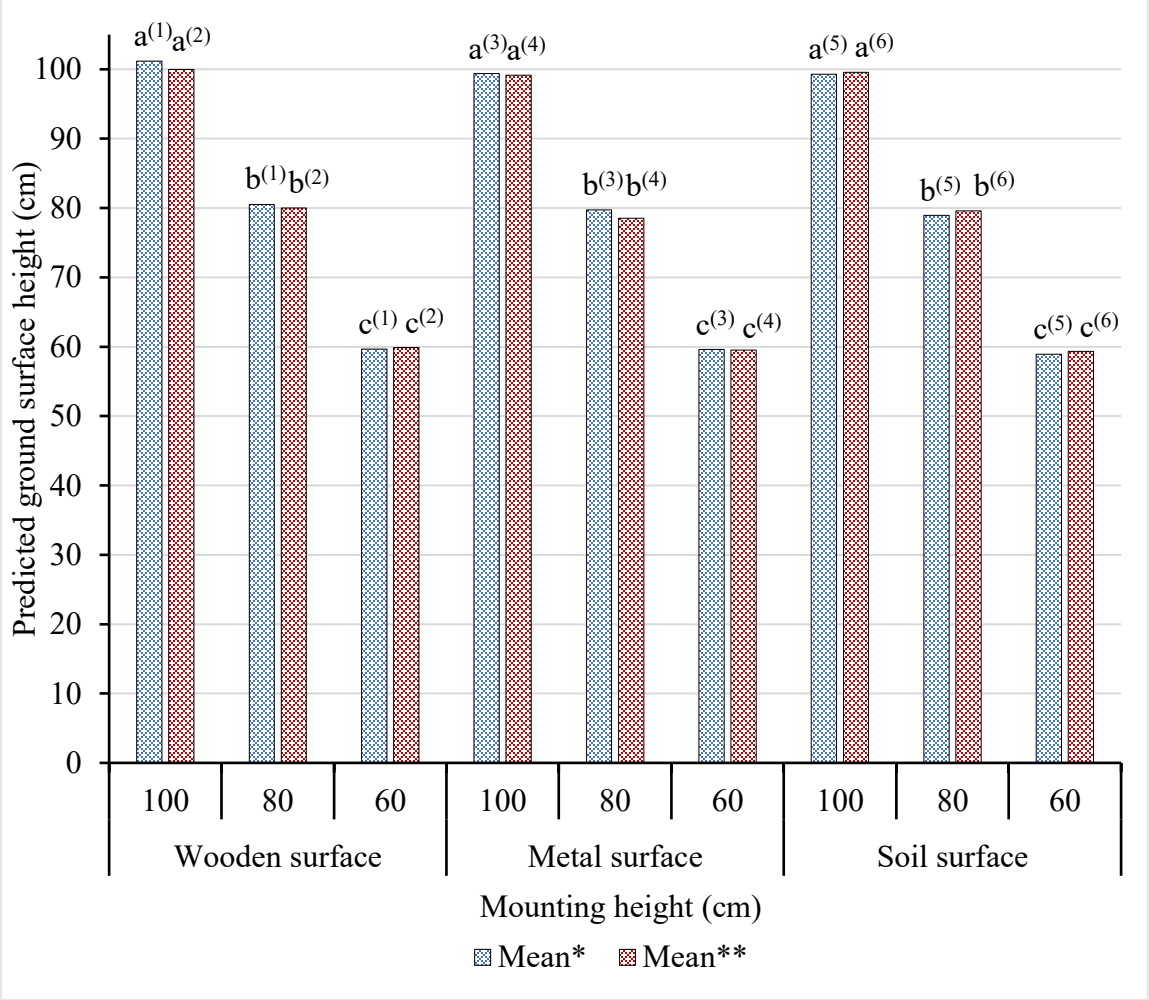

Figure 3-15: Letter grouping resulted from Tukey's MMC analyses. Mean* represents the mean ground surface height detected by radar when dry vegetation cover was included as a factor of interest. Mean** represents the mean ground surface height detected by radar when wet vegetation cover was included as a factor of interest in experimental design. Means that do not share a letter differ significantly from each other. Letters sharing the superscripts represent the result of the same MMC.

3.3.3 Field Data Analysis

Spatial variation for different parameters included in the study were examined by coefficient of variance (CV) following the criteria set by Wildling (1985), which states that selected parameters are considered least variable if CV < 15%, moderately variable if 15% < CV < 35%, and extremely variable if CV > 35%. Summary statistics suggested that in both fields, SDi, ST, and SH were moderately variable parameters during early and mid-summer (May - July) data analyses (**Table 3-4**, **Table 3-5**).

Table 3-4: Summary statistics of stem density, stem height, and stem thickness for Field-A.

Variable	N	Mean	SD	CV (%)	Minimum	Maximum	Skewness
Early-Summer (May – June)							
SDi (m^{-2})	36	955.8	283.30	29.64	528	1540	0.40
SH (cm)	36	21.15	5.41	25.57	12.50	36.20	0.78
ST (mm)	36	1.89	0.34	18.08	1.24	2.57	-0.05
Mid-Summer (July)							
SDi (m^{-2})	36	979	288.1	29.43	440	1540	0.04
SH (cm)	36	21.01	5.64	26.84	9.74	35.68	0.46
ST (mm)	36	1.88	0.33	17.80	1.30	2.66	0.76

SDi – Stem density; SH – Stem height; ST – Stem thickness

Table 3-5: Summary statistics of stem density, stem height, and stem thickness for Field-B.

Variable	N	Mean	SD	CV (%)	Minimum	Maximum	Skewness
Early-Summer (May – June)							
SDi (m^{-2})	36	932.60	247.70	26.57	484	1452	0.24
SH (cm)	36	20.81	5.12	24.85	13.40	31.83	0.45
ST (mm)	36	1.84	0.28	15.20	1.23	2.40	-0.54
Mid-Summer (July)							
SDi (m^{-2})	36	988.80	222.20	22.48	572	1540	0.50
SH (cm)	36	22.11	7.46	33.77	8.65	38.78	0.09
ST (mm)	36	1.88	0.39	20.79	1.39	2.77	0.66

SDi – Stem density; SH – Stem height; ST – Stem thickness

Results of this study were similar to the previous research done in quantifying plant characteristics within wild blueberry fields (Jameel et al., 2016; Farooque, 2015). Regression analyses were performed to examine the relationship between radar output and selected factors (i.e., SDi, ST, SH, FC, FZH). For the early-summer and mid-summer field data collection, since the berries did not reach the fully grown stage, only SH, ST, and SDi were correlated with the radar performance. In the late-summer season (August), the data for FZH and FC were collected before harvesting and included in the regression analyses for corresponding plots.

Stepwise regression was performed to select the best fit subset while developing the MLR models to examine the effect of selected factors (i.e., ST, SH, and SDi) on the output of the radar sensor during early and mid-summer data collection, at each mounting height separately. Further, manually measured ground surface height was also included in MLR models as a continuous predictor. Separate MLR models were developed for each mounting height while using the calibrated output of the radar as a response variable.

Table 3-6: Best-fit subset selected by the standard stepwise regression at alpha = 0.15

Season	Variates	Best-Fit Variate	R^2 - adj
Early-summer	*AGH, SDi, ST, SH	AGH	> 90%
Mid-summer	*AGH, SDi, ST, SH	AGH	> 90%
Late-summer	*AGH, SDi, ST, SH, FC, FZH	AGH	> 90%

*AGH – Actual ground surface height measured manually; SDi – Stem density; SH – Stem height; ST – Stem thickness

Stepwise regression analysis for selected mounting heights (i.e., 0.60, 0.80, and 1.00 m) indicated that radar output strongly correlated to a factor of interest representing the manually measured ground surface heights (**Table 3-6**), while the other factors were eliminated from the developed models. The correlation between radar predicted ground surface height and actual ground surface during early-summer in Field-A (**Figure 3-16b**,

Figure 3-17b, **Figure 3-18b**) and in Field-B (**Figure 3-16a**, **Figure 3-17a**, **Figure 3-18a**) were found to be highly significant. Strong correlations were also found between radar predicted and actual ground surface height during mid-summer in Field-A (**Figure 3-19b, Figure 3-20b, Figure 3-21b**)and in Field-B (**Figure 3-19a, Figure 3-20a, Figure 3-21a**).

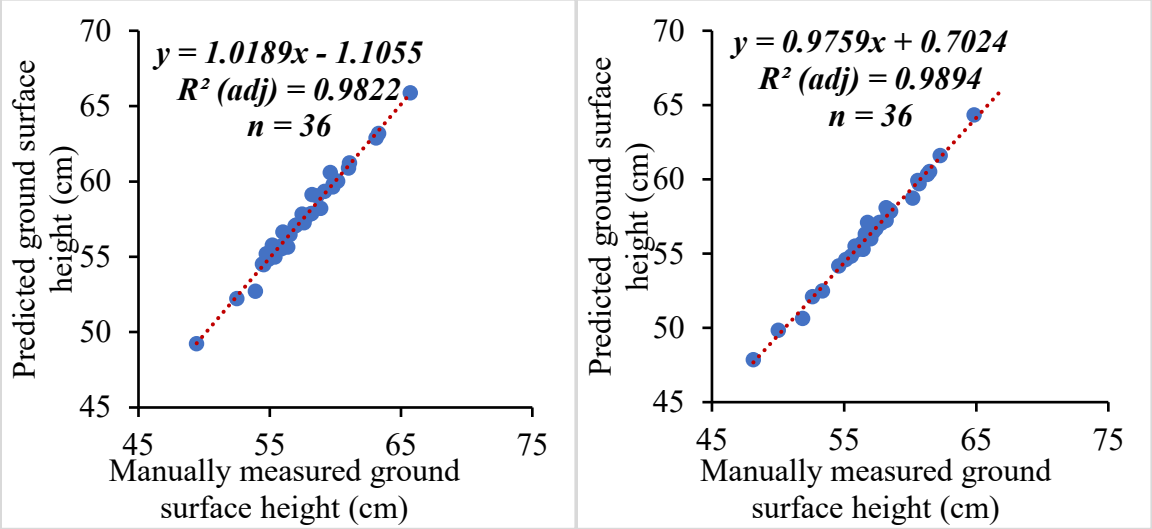

(a) (b)

Figure 3-16: Relationship between the predictive values and actual ground distance measured manually at 0.60 m mounting height during early-summer in both fields: (a) Field-B; (b) Field-A.

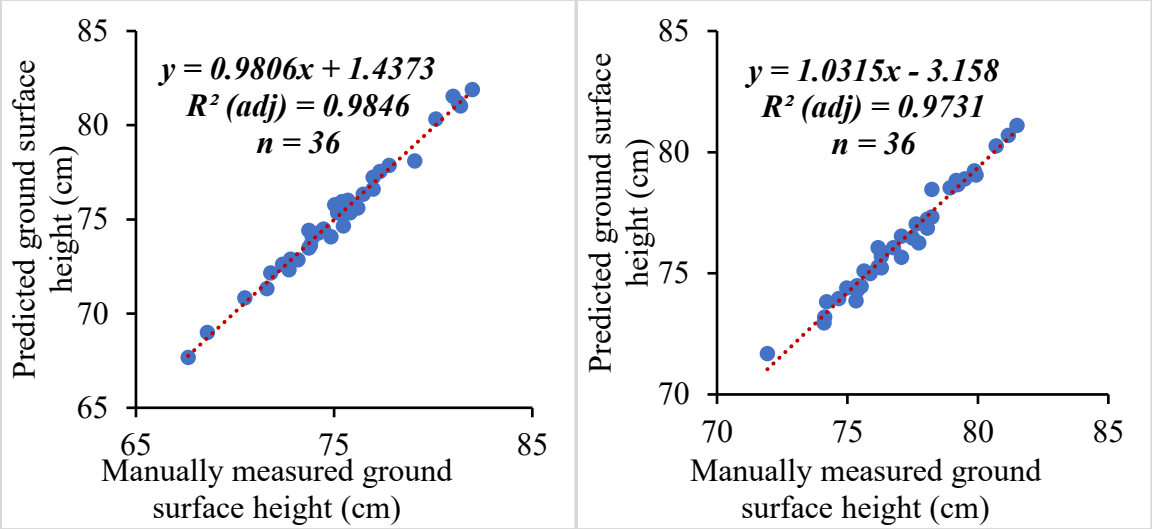

(a) (b)

Figure 3-17: Relationship between the predictive values and actual ground distance measured manually at 0.80 m mounting height during early-summer in both fields: (a) Field-B; (b) Field-A.

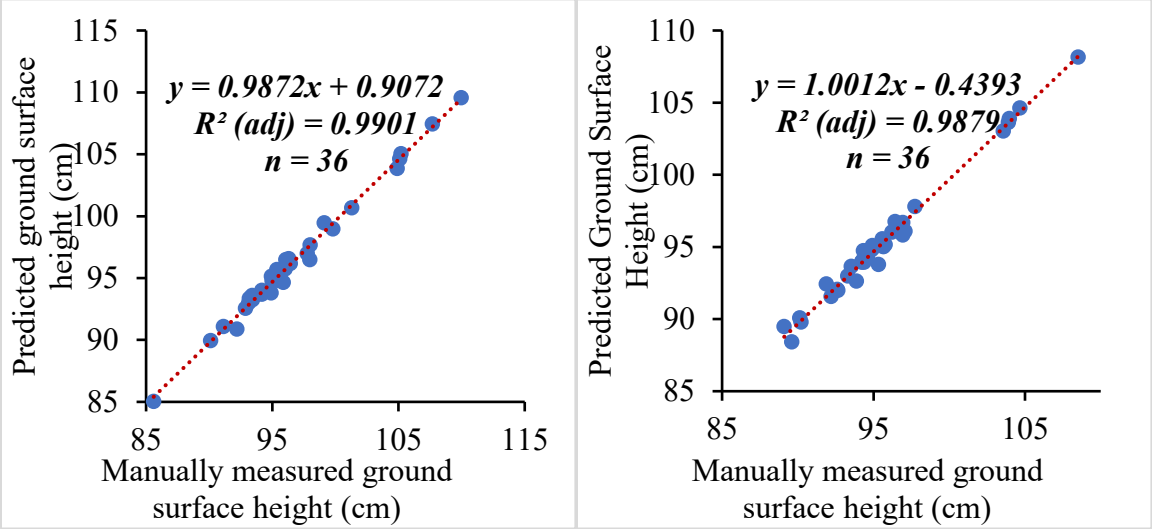

(a) (b)

Figure 3-18: Relationship between the predictive values and actual ground distance measured manually at 1.00 m mounting height during early-summer in both fields: (a) Field-B; (b) Field-A.

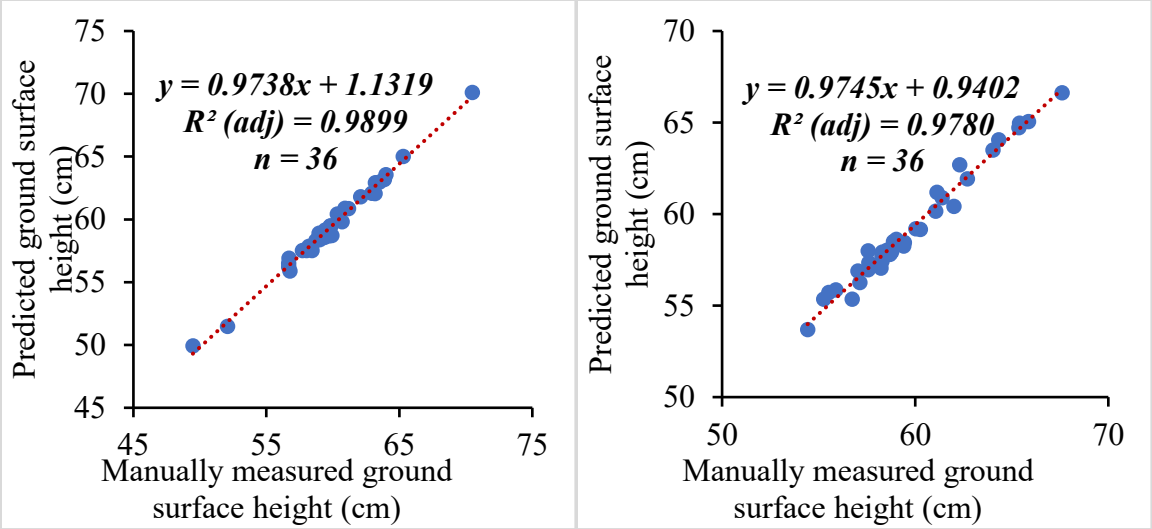

(a) (b)

Figure 3-19: Relationship between the predictive values and actual ground distance measured manually at 0.60 m mounting height during mid-summer in both fields: (a) Field-B; (b) Field-A.

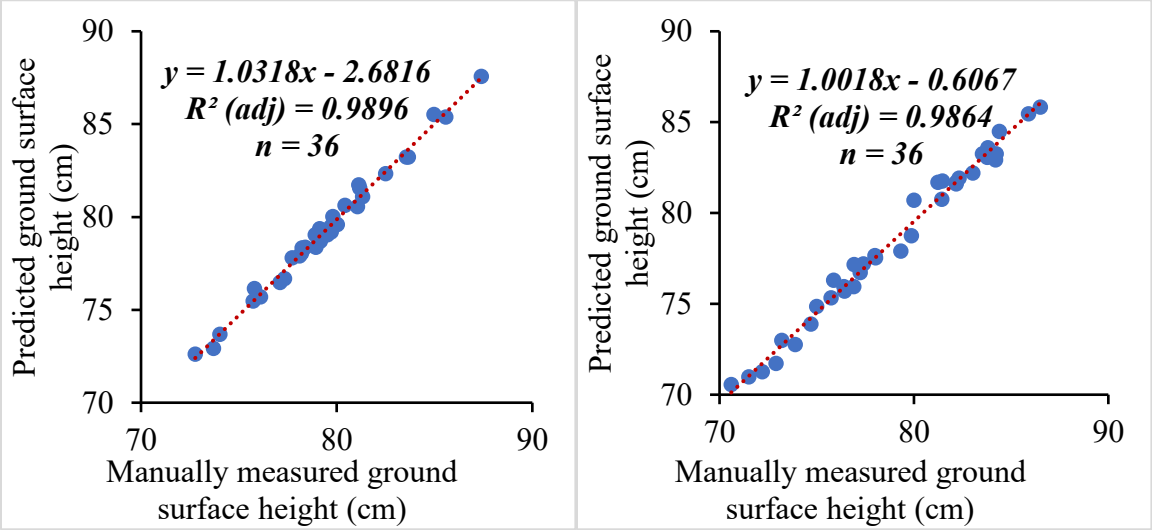

(a) (b)

Figure 3-20: Relationship between the predictive values and actual ground distance measured manually at 0.80 m mounting height during mid-summer in both fields: (a) Field-B; (b) Field-A.

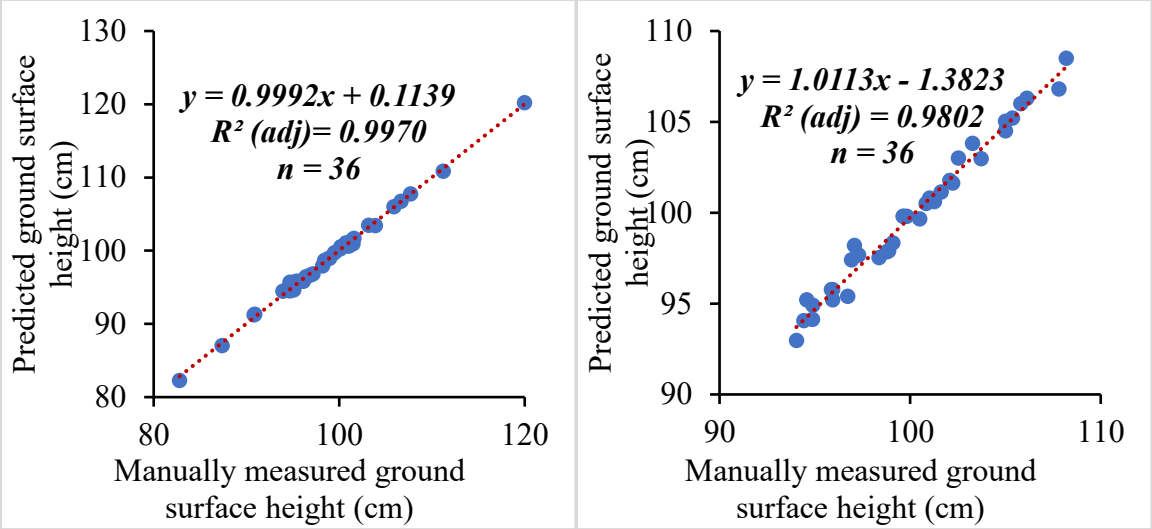

Figure 3-21: Relationship between the predictive values and actual ground distance measured manually at 1.00 m mounting height during mid-summer in both fields: (a) Field-B; (b) Field A.

Results from developed stepwise MLR models suggested that radar output does not depend significantly upon the factors including ST, SH, and SDi during early-summer and mid-summer season of plant growth, which implies that radar waves can penetrate through vegetation cover without being significantly affected by it. Since manually measured height strongly correlated with radar output, it suggested that the radar under study can be used to detect the ground surface height non-destructively within wild blueberry fields during early-summer (May) and mid-summer (June-July).

Late-summer data were collected one week before mechanical harvesting of the selected fields. In addition to stem parameters (i.e., ST, SH, and SDi), fruit parameters (i.e., FC and FZH) were also recorded and added as individual parameters in the models to examine the effect of fruit parameters on the performance of radar sensor.

Table 3-7: Summary statistics of stem density, stem height, and stem thickness for Field-B.

Variable	N	Mean	SD	CV (%)	Minimum	Maximum	Skewness
Field-A							
SDi (m^{-2})	36	1081.7	302.2	27.94	572	1672	0.14
SH (cm)	36	23.45	4.75	20.28	15.83	37.77	0.82
ST (mm)	36	1.92	0.33	17.53	1.37	2.78	0.54
FC (m^{-2})	36	3454	1254	36.32	1144	5500	-0.31
FZH (cm)	36	17.92	3.96	22.1	9.83	27.7	0.39
Field-B							
SDi (m^{-2})	36	1108.6	274.8	24.79	484	1628	-0.47
SH (cm)	36	22.66	6.21	27.41	10.33	35.7	0.06
ST (mm)	36	1.92	0.33	17.29	1.37	2.81	0.60
FC (m^{-2})	36	3653	1280	35.03	1188	5500	-0.30
FZH (cm)	36	14.69	3.33	22.68	8.83	21.77	0.39

SDi – Stem Density, SH – Stem Height, ST – Stem Thickness; FC – Fruit count, FZH – Fruit zone height

In summary statistics, the fruit parameter named FC which could be referred to as an indirect measure of fruit yield was found to be highly variable in both fields (**Table 3-7**). Jameel et al. (2016) reported high variability of fruit yield in one of the selected fields while Farooque et al. (2014) found fruit yield to be highly variable in three out of four selected fields. The parameter accounting for FZH came out to be moderately variable in both selected fields, which was also validated by Farooque et al. (2016), where he found the FZH to be moderately variable in all the selected fields. Stepwise linear regression resulted in a strong correlation between radar predicted ground and manually measured ground distance in Field A (**Figure 3-22a, Figure 3-23a, Figure 3-24a**) and Field-B (**Figure 3-22b, Figure 3-23b, Figure 3-24b**).

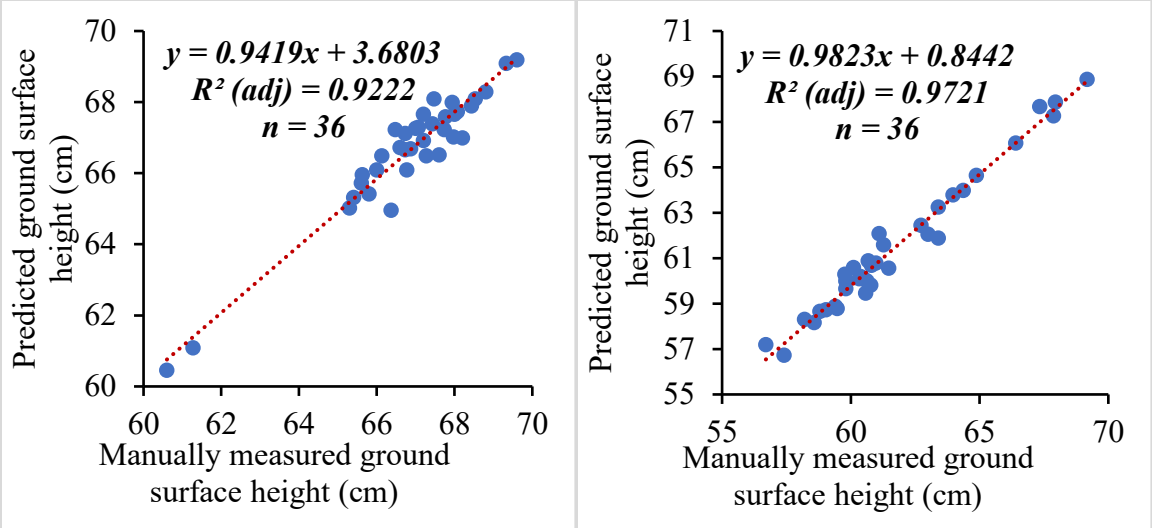

(a) (b)

Figure 3-22: Relationship between the predictive values and actual ground distance measured manually at 0.60 m mounting height during late-summer in both fields: (a) Field-A; (b) Field B.

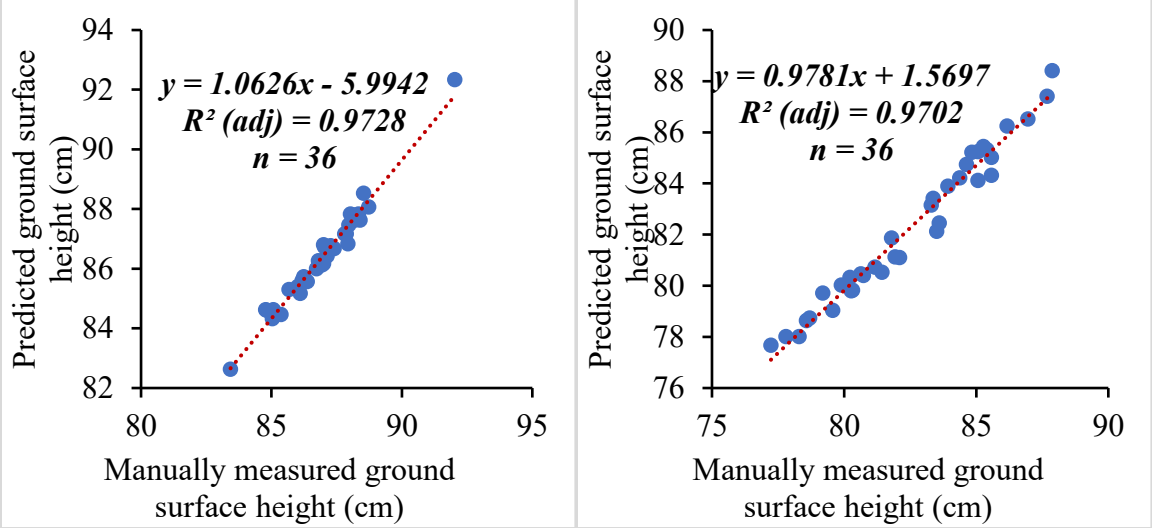

(a) (b)

Figure 3-23: Relationship between the predictive values and actual ground distance measured manually at 0.80 m mounting height during late-summer in both fields: (a) Field-A; (b) Field B.

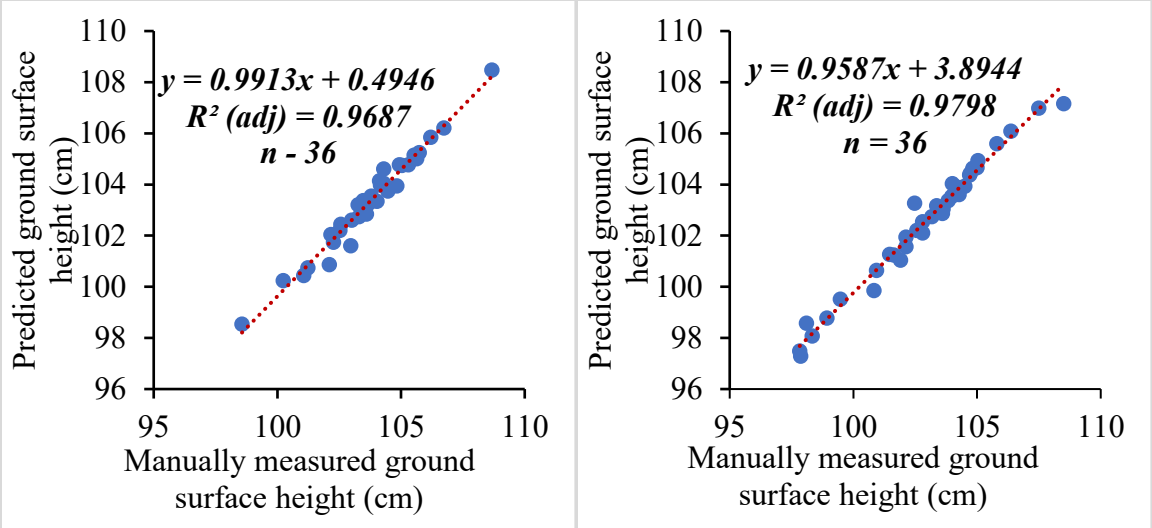

(a) (b)

Figure 3-24: Relationship between the predictive values and actual ground distance measured manually at 1.00 m mounting height during late-summer in both fields: (a) Field-A; (b) Field B.

The results deducted from stepwise MLR analyses suggested that selected radar sensor performance remained unaffected by stem and fruit characteristics which suggests that it can be used to detect the ground surface during late-summer within wild blueberry fields.

Table 3-8: Index of agreement (*d*) calculated for calibrated and uncalibrated models in both fields.

Season	MH (m)	*d* of Calibrated Model (Field-A)	*d* of Calibrated Model (Field-B)	*d* of Uncalibrated model (Field-A)	*d* of Uncalibrated model (Field-B)
Early-summer (May 1st – June 15th)	0.60	0.9864	0.9954	0.2766	0.6533
	0.80	0.9669	0.9962	0.4842	0.6701
	1.00	0.9956	0.9964	0.7443	0.7895
Mid-summer (June 16th – July 31st)	0.60	0.9860	0.9936	0.6057	0.6660
	0.80	0.9938	0.9965	0.7467	0.6476
	1.00	0.9917	0.9986	0.7038	0.8699
Late-summer (August 1st – 15th)	0.60	0.9770	0.9915	0.4505	0.6098
	0.80	0.9625	0.9922	0.3653	0.6229
	1.00	0.9807	0.9899	0.4470	0.5719

MH – Mounting Height; *d* – Index of agreement

Index of agreement calculated for both field's data indicated that calibrated models performed with high accuracy as compared to uncalibrated models (**Table 3-8**; **Figure**

3-25). Furthermore, results also suggested that calibrated models can predict the ground surface height with very high accuracy (d > 0.95) throughout the growing season within wild blueberry fields.

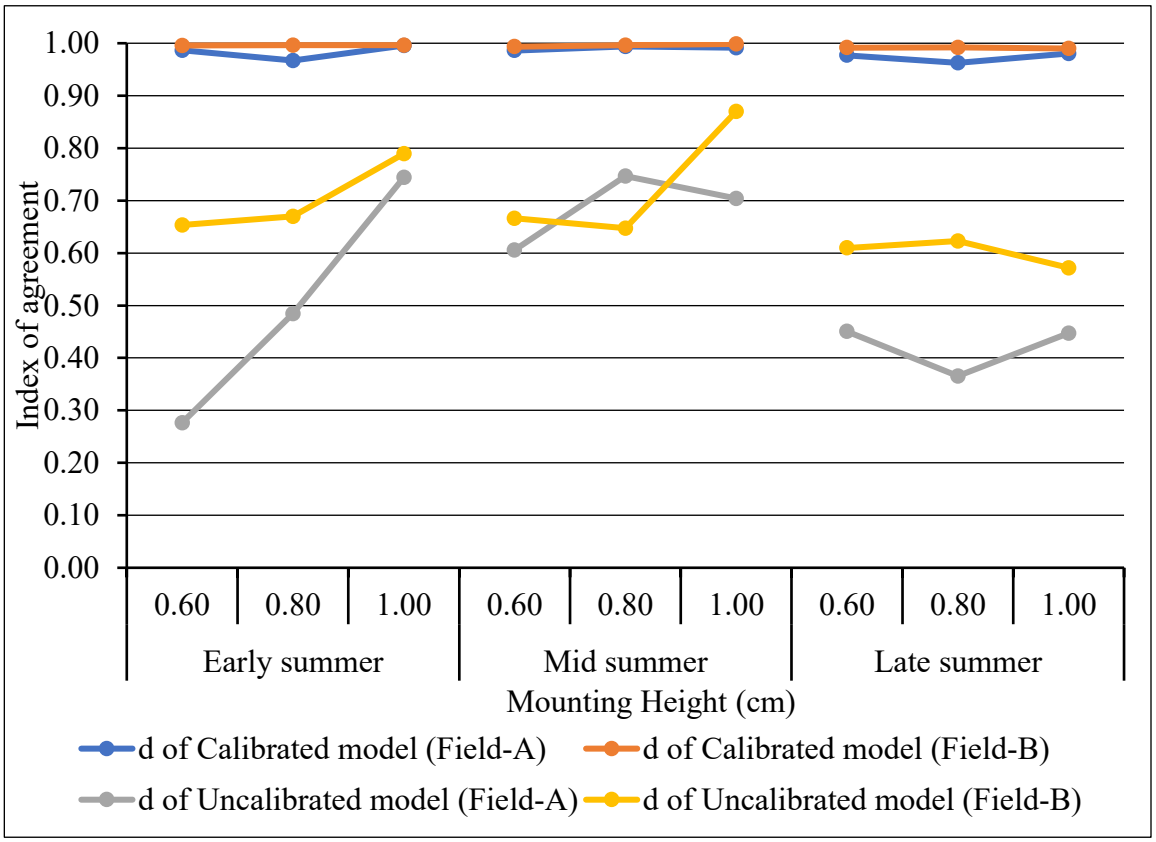

Figure 3-25: Performance comparison of calibrated and uncalibrated models for estimating the true ground surface height in both fields using the index of agreement (*d*).

3.4 Limitations of the Research Study

Several factors contributed to define few limitations in data collection for feasibility analysis of selected microwave radar sensors in wild blueberry fields. Wild blueberry fields exhibit a high degree of spatial variation, especially in ground slope which varies between 0.7-31 degrees (Zaman et al., 2010a; Esau et al., 2021). Variation in slope created challenges while collecting the actual ground height of the selected plots in both fields. The same plots were utilized for data collection during three defined seasons, but slope

variation made it nearly impossible to recreate the same ground truth readings of ground surface height. Due to this limitation, there were slight differences in the manually measured ground surface height data collected for all three seasons which can be visualized in a 1:1 trend line (**Figure 3-26**).

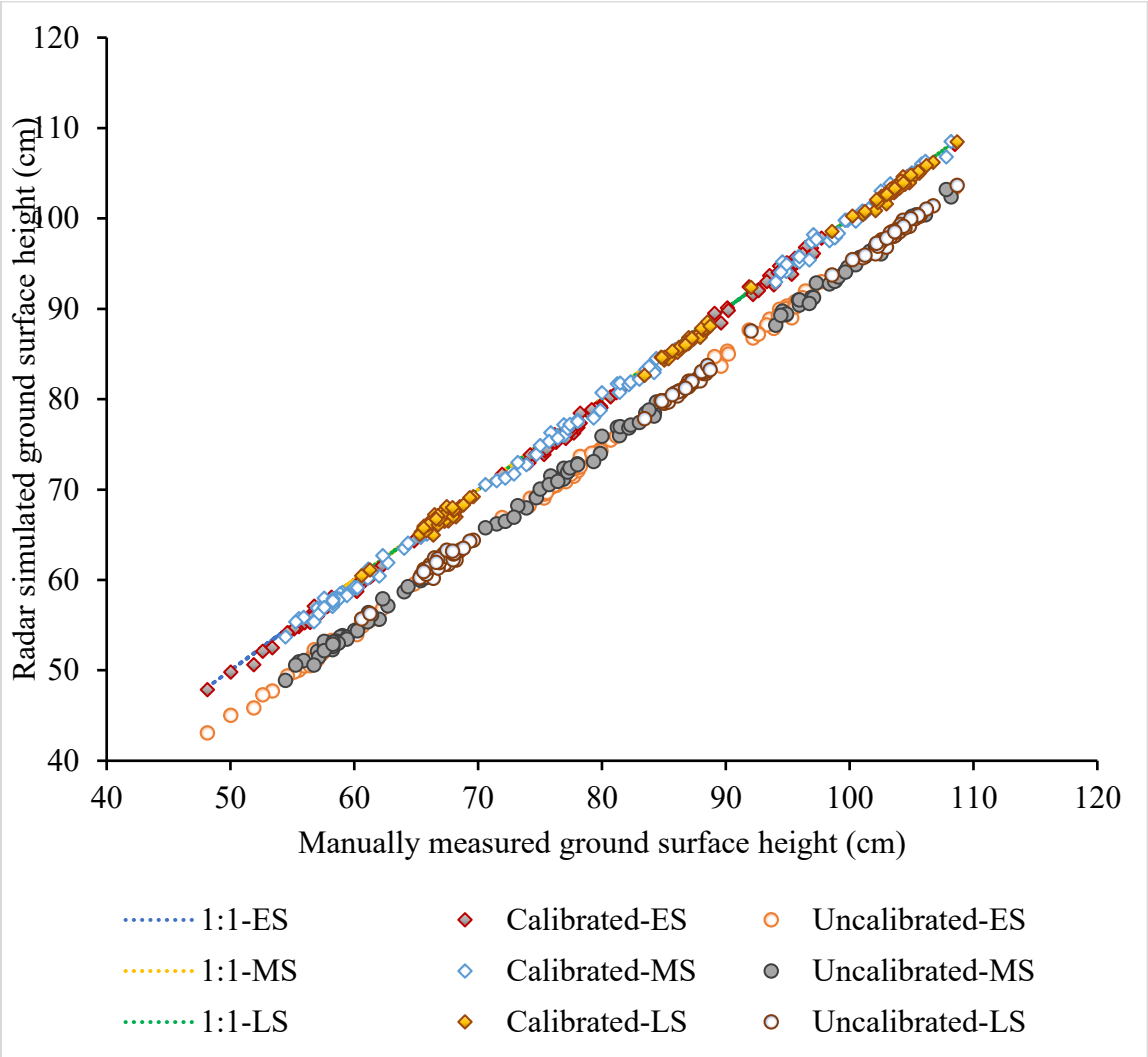

(a)

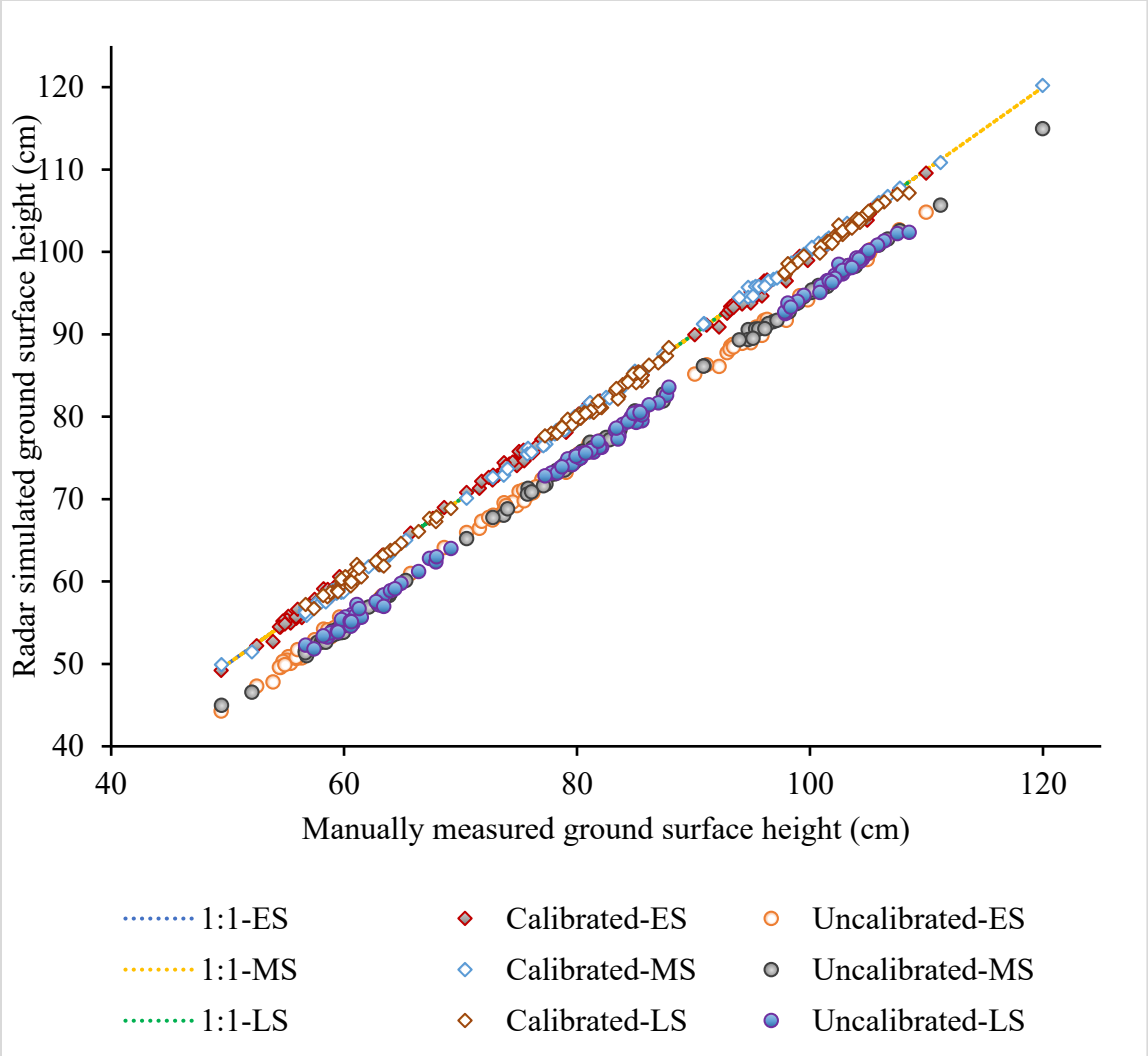

(b)

Figure 3-26: Simulated ground surface height values vs manually measured ground surface height corresponding to Field-A (a) and Field-B (b). In the graph body, ES represents the early-summer data, MS represents the mid-summer data, and LS represents the late-summer data.

Another problem was to estimate the ground surface height corresponding to the respective radar FOV. The radar algorithm under study accounted for reflected waves of 4 mm apart along the transect for estimating the ground surface height, which is extremely challenging to reconstruct manually. To address this issue while keeping in mind the narrow window for data collection, three manual readings were collected along with the transect understudy, and estimates were made based on the average height readings.

This research study was focused to evaluate the feasibility of radar sensor in wild blueberry fields for ground surface detection and height measurement. Pre-evaluation testing of the radar sensor revealed that the radar sensor works best in dynamic conditions as compare to standstill conditions. It was observed that if the radar sensor is kept in stationary condition for a longer period (>12 seconds), waves tend to penetrate the material under study which raises the erroneous output. Although this penetration problem was not faced under the dynamic condition and for metallic surfaces. Following this observation, each application of the radar sensor for data collection purposes lasted twelve seconds during this research study.

3.5 Conclusion

A novel ground surface detection system was developed and analyzed using a low frequency ultrawide band microwave radar sensor for non-destructive ground surface height measurement in wild blueberry fields. Multiple statistical analyses resulted in a significant correlation (R^2 = 0.92-0.99) between calibrated radar output and true ground surface height irrespective of the mounting height, stem characteristics, and fruit characteristics. Calibrated radar output showed a high degree of agreement (d = 0.96-0.99) to estimate the true ground surface height which proposed a high degree of accuracy related to the Terrahawk® radar to measure true ground surface height. Radar under study showed great potential in ground surface height detection in standstill conditions, but further studies are required to determine its real-time application for automation of wild blueberry harvester on-the-go (dynamic conditions). Overall, the developed system measured the ground surface with a high degree of accuracy and showed great potential in real-time ground surface detection in wild blueberry fields.

CHAPTER 4: EFFECT OF HARVESTER GROUND SPEED ON MICROWAVE RADAR GROUND SURFACE DETECTION SYSTEM

ABSTRACT

Mechanical harvesting of the wild blueberries is significantly impacted by machine parameters, plant characteristics, and topographic variation. Efficient harvesting operation highly depends on the operator's skills for manipulating the harvester parameters. These parameters include adjusting the harvester head height with varying topography and controlling the ground speed with changing density of fruit-bearing stems, which can increase profitability and yield. Spatial variation in wild blueberry fields creates a severe challenge for the operators to maintain the optimum machine parameters. The full automation of the harvester head requires precise feedback of the picking height. A non-destructive foliage penetration ground detection technique is required to provide the feedback of head height referenced to varying topography to automate the harvester head height for optimum berry picking operation and reduce operator stress. A ground surface detection system was developed, calibrated, and evaluated in static at the Dalhousie Mechanized Systems Research Lab in Truro, Nova Scotia. This research's primary focus was to analyze the combined effect of traditional wild blueberry harvester ground speed (1.2, 1.6, and 2.0 km h^{-1}) and mounting height (0.60, 0.80, and 1.00 m) on the performance of developed ground surface detection system. Two wild blueberry fields were selected in central Nova Scotia and a total of 36 areas of interest were defined within each field using an inverted W pattern. A specialized farm motorized vehicle (SFMV) was fabricated using a DC motor with advanced features to attain constant ground speed from 0 to 2.9 km h^{-1}. A unique mounting frame was designed and built to provide the developed system with a selected height clearance from the flat ground. The output of the developed system was compared with actual ground surface height using paired t-test (H_0: $\mu_d = 4.5$ mm, p-value > 0.05). Heights predicted by the developed system were strongly correlated with manually measured ground surface heights ($R^2 = 0.99$). Factorial analysis of variance was utilized to analyze the significance of ground speed (p-value $> \alpha$), mounting height (p-value < 0.001), and their interaction effect (p-value $> \alpha$) on the real-time performance of the developed system at a 5% level of significance ($\alpha = 0.05$). The developed ground surface detection system resulted in a highly precise and accurate prediction of actual ground surface height with a mean discrepancy of 4.5 mm. Results suggested that the developed system, if incorporated with the real-time harvesting operation, can provide accurate ground surface height feedback for automation of wild blueberry harvester head regardless of the variable ground speed.

4.1 Introduction

Wild blueberries (*Vaccinium angustifolium Ait.*) are perennial fruit crop native to Northeastern North America, which first originated from burned-over native stands in barren fields (Agriculture and Agri-Food Canada, 2017; Strik & Yarborough, 2005). Wild blueberry crop distinguishes itself from other fruit crops due to its native existence in barren deforested farmlands (Wood, 2004). Wild blueberry fields undergo a two-year management cycle with extensive vegetation growth in the first year followed by fruit growth in the second (Hall, 1955). Wild blueberry plants usually spread through underground rhizomes with existing seeds in the established fields (Glass & Percival, 2000). Over the past years, improved management practices such as pruning, mowing, application of fertilizers, pesticides, herbicides, and mechanical harvesting have significantly increased wild blueberry fruit production (Yarborough, 2004). The wild blueberry crop is a low-growing shrub with a stem height ranging between 5-30 cm (Farooque et al., 2020). Improving fruit quality, increasing berry yields, and production cost reduction has always been the key objectives among industry and researchers (Farooque, 2015). Fields in fruit year are usually harvested in August when approximately 90% of the berries are ripe (Farooque et al., 2014). Fields are typically harvested using the traditional hand raking technique or by using a mechanical harvester (Kinsman, 1993; Hall et al., 1967).

Over the past 100 years, traditional harvesting techniques were practiced for picking the wild blueberries using a handheld metal rake similar in design to the cranberry scoops (Farooque et al., 2014). Today, this technique is still used in approximately 20% of

the fields where the topography is extremely rough (Agriculture and Agri-Food Canada, 2017). Traditional harvesting techniques resulted in significant berry losses during harvesting operations, which varied from crew to crew, with overall harvesting losses of 20% (Kinsman, 1993). Underlying factors that initiated the transition from traditional harvesting techniques to mechanized harvesting include the significant increase in blueberry yields in recent years (Esau et al., 2018), the increase in labour wages (Government of Nova Scotia, 2019), the short harvesting season (Farooque et al., 2014), and the shortage of labour (Yarborough, 2001).

The pursuit of developing a wild blueberry mechanical harvester began in the 1950s but a viable machine was not built until the 1980s (Dale et al., 1994). This pursuit led to the development of the first mechanical harvester, which was initially modified from a cranberry picking machine in 1956. Unfortunately, this type of harvester caused significant fruit losses and further modification in the design had to be implemented to make the harvesting process more efficient (Rhodes, 1961). Mckiel (1958) developed a machine using the concept of stationary combs with a 30º inclination to the ground for detaching the berries and vacuum to transport the berries to storage bins. However, the concept was discarded due to extreme losses caused by berry detaching combs digging into the soil. Rhodes (1961) developed a mechanical harvester with a rotating raking mechanism, which was further modified by Soule (1967). Unfortunately, later evaluations of this prototype indicated that the collected berries were imbedded with the sand, making them inedible. Gary (1970) came up with the design of a hollow raking mechanism employing a rotating picking head, which serves as the basis of the currently used harvester design. Doug Bragg Enterprises (DBE), being the only large-scale producers of wild blueberry harvesters, has

served the industry as the potential driving force behind modern-age modifications in harvester machines including hydraulic head height control leading to better performance in rough terrains and higher fruit yields (Esau et al., 2020).

Harvesting wild blueberries using a mechanical harvester has proven to be the most cost-effective method in the past (Yarborough et al., 2017). However, efficient berry picking operation requires constant manipulations from the operator in head height adjustment, regulating the rotational speed of raking combs and maintaining the proper ground speed to ensure the maximum berry recovery (Farooque et al., 2014). Wild blueberry fields exhibit substantial spatial variation in plant characteristics and topographic features (Farooque et al., 2012; Farooque, 2015). Ground slope in wild blueberry fields can vary from 0.8º to 31º (Zaman et al., 2010a; Esau et al., 2021), which can cause an imbalance of the picking head, leading to poor berry recovery during the harvesting operation (Farooque, 2015). Continuous input by the operator to adjust the head height with respect to the field's topography is a demanding task (Chang et al., 2017). To make this process more user-friendly, an automated system to detect the real-time ground surface and back feed the controller for head height adjustments in real-time is necessary (Esau et al., 2020).

Various factors affecting the wild blueberry harvest efficiency have been delineated by several researchers and the potential of different precision agricultural techniques were analyzed (Chang et al., 2017; Farooque et al., 2013, 2014, 2016a, 2016b, 2020; Jameel et al., 2016; Zaman et al., 2009, 2010a, 2010b). Interestingly, research is still needed to analyze microwave radar technology's potential in real-time ground surface detection within wild blueberry fields. Although microwave radar technology's potential is still yet to be determined in wild blueberry cropping systems, researchers have successfully

employed microwave radar technology for non-destructive through foliage ground surface detection in various cropping systems (Noyman & Shmulevich,1996; Woods et al., 1999). In this research, a novel ground surface detection system comprised of UWB microwave radar technology was utilized for real-time detection of the ground surface within wild blueberry fields and its performance was analyzed at different ground speeds. Since the machine parameters, including the ground speed, can affect the harvesting operation in wild blueberry fields (Farooque et al., 2014; Farooque et al., 2020), this research focuses on analyzing the combined effect of traditional ground speeds (1.2, 1.6, and 2.0 km h^{-1}) and selected mounting heights (0.60 m, 0.80 m, 1.00 m) on the performance developed ground surface detection system.

4.2 Materials and Methods

4.2.1 Research sites

Two commercial wild blueberry fields were selected in central Nova Scotia for real-time performance evaluation of developed ground surface detection system. Selected fields include Slack Farm site (Field-A: 45°25'28.9"N, 63°28'56.2"W; 3.91 hectares) and Wild Blueberry Producers Association of Nova Scotia's research site (Field-B: 45°25'37.6"N 63°28'55.2"W; 2.14 hectares). Selected fields have been under commercial biennial management over the past decade and were in crop year during data collection.

4.2.2 Ground Surface Detection System

Developed ground surface detection system comprised a microwave radar coupled with ruggedized field laptop running the data visualization and acquisition software (**Figure 4-1**). The Terrahawk® radar (Headsight Inc., Bremen, Indiana, USA; Model: HT5230) was used as the main building block of the developed ground surface detection

system. It is a FMCW radar that employs an UWB of microwave frequencies, ranging from 1.5 to 6.4 GHz with a centered operating frequency of 3.97 GHz. The radar used in the ground surface detection system had a pulse repetition rate of 41.66 Hz. It offered a 90º field of view with an adjustable resolution of 4 mm or 8 mm. Signal processing and data acquisition were carried out using an external processing unit via USB 2.0 communication. A ruggedized field laptop (MSI Model: WS65 9TM-1410CA) was employed as an external processing unit (Micro-Star International Co., Ltd., Taipei, Taiwan) which was powered by an Intel Core i9-9880H/2.3-4.8 GHz chipset (Intel Co., California, USA) with a dedicated Nvidia Quadro RTX 5000/16GB GDDR5 (Nvidia Co., California, USA) graphic processing unit. An executable program named *TerrahawkBuddyLite* (Version: 1.20) was used for visualizing the outputs and declaring operating parameters of the developed ground surface detection system (**Figure 4-1**).

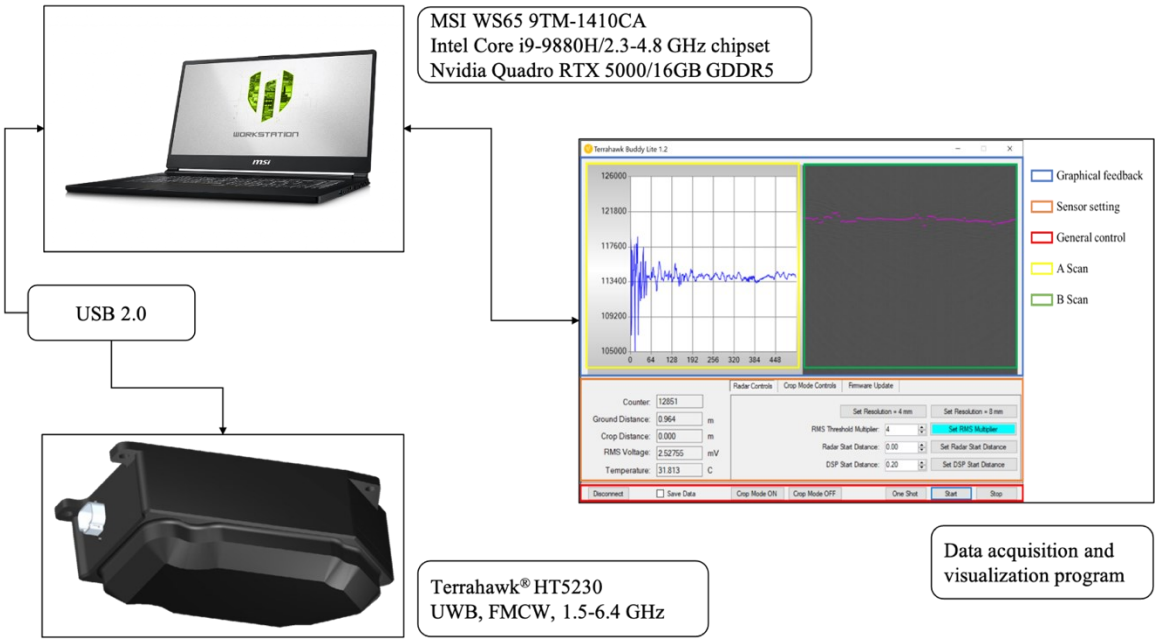

Figure 4-1: Components of developed ground surface detection system along with the *TerrahawkBudyLite*'s graphical user interface (GUI).

4.2.2.1 Radar Operating Parameters

Operating parameters related to the radar of the developed ground surface detection system can be categorized into two types: a) Output parameters and b) Input parameters. Output parameters include a clock to count sensed values, distance from the ground and potential distance from the crop canopy surface in meters, root mean square (RMS) voltage value (mV), sensor temperature (°C), and radar connection status. Input parameters include resolution, sensitivity RMS threshold multiplier, radar start distance, and digital signal processing (DSP) start distance. Radar can be operated in continuous mode where it senses the ground distance continuously or on a one-shot mode where it senses the ground distance when a user initiates a trigger. To detect the target ground surface, the radar start distance introduces the delay in initializing the first scan as a function of distance, while the DSP start distance determines the portion of the conical section of the radar beam to be considered for signal processing in meters. Trials for this research study were carried out in the continuous mode of operation by setting the resolution to default (4 mm), the RMS threshold multiplier to 4, the radar start distance to 0.00 m, and the DSP start distance to 0.10 m. Continuous mode of operation allowed the developed system to trans-receive the waves continuously as the buggy traverse over the selected areas of interest, which in turn allowed the radar to estimate the ground surface height better.

4.2.3 Specialized Farm Motorized Vehicle (SFMV)

A Specialized Farm Motorized Vehicle (SFMV) was developed by Precision Agriculture (PA) research team at Dalhousie AC, which had been extensively used in the fields for performance evaluation of multiple sensor-based systems and data collection purposes (Zaman et al., 2009; Chang et al., 2012). The SFMV was originally equipped with

a 190-cc gasoline engine (Honda Motor Co. Ltd., Tokyo, Japan) with the capacity of generating 4.47 kW at a maximum speed of 3600 rpm. The engine was linked to the wheels via a chain-sprocket power transmission system that provided the vehicle's required power for its operation in real-time. Slim bicycle wheels were used in SFMV to minimize the crop damage during field operation/testing of sensors. The SFMV could be driven at 0 - 10 km h^{-1} ground speed (Zhang et al., 2010). Since this research required the field operation to be carried out at constant speed, the SFMV was modified by replacing the gasoline engine with the permanent magnet direct current (PMDC) electric motor of 0.55 kW (0.75 hp) and 1800 rpm (**Figure 4-2**). The motor was powered using two 12V batteries, which were placed in the designed metallic brackets at the back end of the SFMV. The motor's direction and speed were controlled by a Sabertooth (Dual 2 x 32 A, 6-24 V) regenerative motor driver (Dimension Engineering, Ohio, USA). A gear reducer was introduced with the motor and chain sprocket transmission to reduce the original motor revolution by an overall ratio of 60:1. To prevent the SFMV from free-wheeling during down-hill tracks and to enable regenerative braking, modifications were made at the sprockets' bearing ends to provide propulsions to the wheels. The installation of the electric motor (PMDC), gear reducer, and motor driver controller, along with the necessary modifications, enabled the SFMV to travel at a constant and very low ground speed (0.1 - 2.9 km h^{-1}).

The modified SFMV was equipped with multiple new features for ease of control and monitoring the speed of SFMV, including a small potentiometer knob for speed control and a digital odometer using a magnetic proximity sensor for speed monitoring. A custom-made metallic mount assembly was designed and installed on the SFMV for mounting the sensor. The mounting plate was built to provide a 1.00 m clearance to the back of the radar

from the front frame of the SFMV. This installation aimed to mitigate the possibility of interferences between the metal frame and the radar projected beam. The mounting assembly was designed to have an infinite number of grasping points between the hollow metallic tube of the mounting assembly and the mounting rod using simple screws. This configuration enabled the mounting plate to have an adjustable height between 0.30 - 1.20 m from the flat ground.

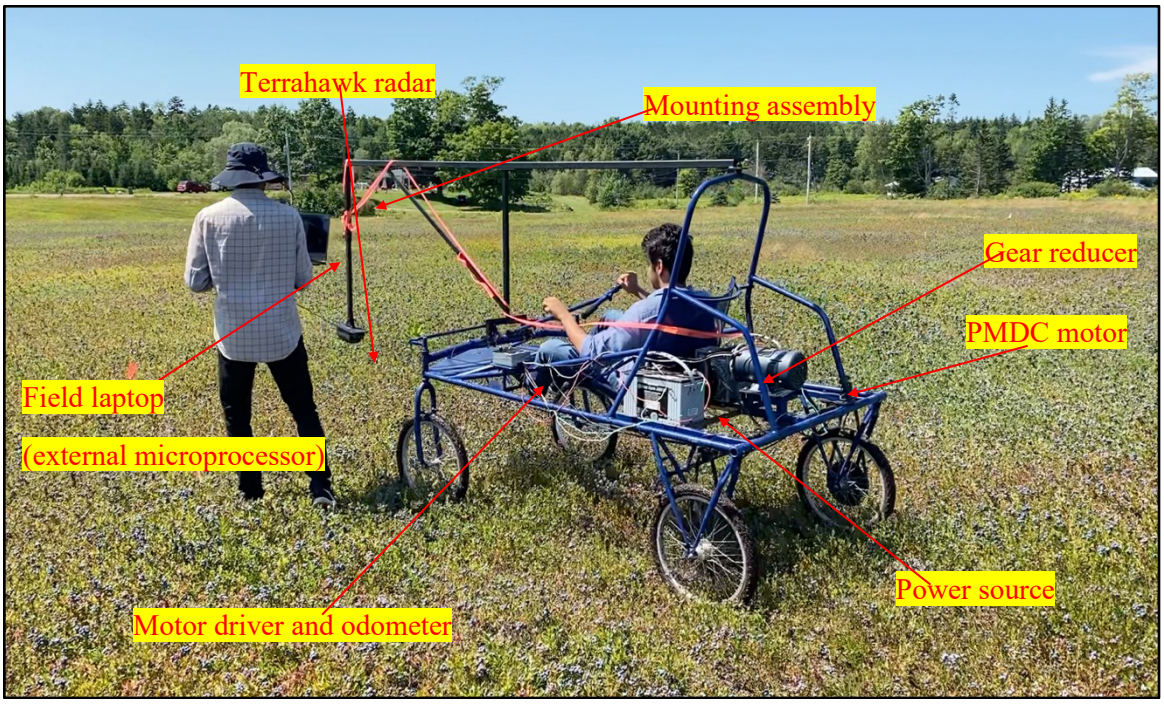

Figure 4-2: SFMV with developed ground surface detection system mounted and modified features labelled (during pre-harvest data collection in Field-A, 2020).

4.2.4 Data Collection

4.2.4.1 Experimental Variables

The designed experiment for this research study was focused on analyzing the individual and interaction effect of two main factors of interest: a) Mounting height (0.60, 0.80, and 1.00 m); and b) Ground speed (1.2, 1.6, and 2.0 km h^{-1}). Wild blueberries exhibit a large degree of variation in stem height with a maximum height approaching up to 0.40

m approximately (Farooque, 2015). The ground slope is another substantially variable factor ranging from 0.8-31.0º (Zaman et al., 2010a, Esau et al., 2021). Spatial variation caused by these factors led to the selection of the lowest mounting height of at least 0.60 m for non-destructive sensor operation. Commercial wild blueberry harvester manufactured by DBE is 0.91 m wide (Esau et al., 2020), which necessitated the developed system to be mounted at 1.00 m height from the flat ground to cover a complete field of view of 0.91 m. The developed system operation was also evaluated at 0.80 m height to cover more variability in the designed experiment. Farooque et al. (2014) quantified the effect of three traditional berry picking ground speeds (1.2, 1.6, and 2.0 km h^{-1}) on the picking efficiency of the mechanical wild blueberry harvester. The developed ground surface detection system was evaluated at similar ground speed settings using the modified SFMV. A total of nine treatments were generated from the interaction between the selected mounting height level and the ground speeds (0.60 m – 1.2 km h^{-1}, 0.60 m – 1.6 km h^{-1}, 0.60 m – 2.0 km h^{-1}, 0.80 m – 1.2 km h^{-1}, 0.80 m – 1.6 km h^{-1}, 0.80 m – 2.0 km h^{-1}, 0.80 m – 2.0 km h^{-1}, 1.00 m – 1.2 km h^{-1}, 1.00 m – 1.6 km h^{-1}, and 1.00 m – 2.0 km h^{-1}). These treatments were assigned randomly to the sampling units with four replications each.

4.2.4.2 Experimental Setup

Data were collected at 36 sampling locations in each selected field for performance evaluation of developed ground surface detection system. To ensure unbiased randomized selection of the sampling locations in both fields, the sampling points were selected randomly using the inverted-W pattern sampling technique (McCully et al., 1991; Thomas, 1985; Tamado & Milberg, 2000) (**Figure 4-3**). Starting points of the inverted W-pattern in both fields were chosen by walking 100 paces along the boundary of the fields facing West

and then walking 100 paces into the field by taking a right-angle turn. Different starting points (North facing end in Field-A and South facing end in Field-B) were selected in both fields to cover a maximum of variability. Each leg of the inverted W-pattern comprised a total of 9 sampling locations separated by 20 steps each.

Coordinates of the field boundaries and inverted W-pattern tracks were recorded using handheld DGPS. Digital Elevation Models (DEMs) indicating the digital elevation profile of selected fields were developed using ArcMap 10.5 (Esri Inc., California, USA). Elevation data for the selected fields were obtained from a database maintained by the government of Nova Scotia, namely GeoNOVA (GeoNOVA, 2019). The data obtained from a handheld DGPS were integrated with the DEMs using ArcMap 10.5 (**Figure 4-3**).

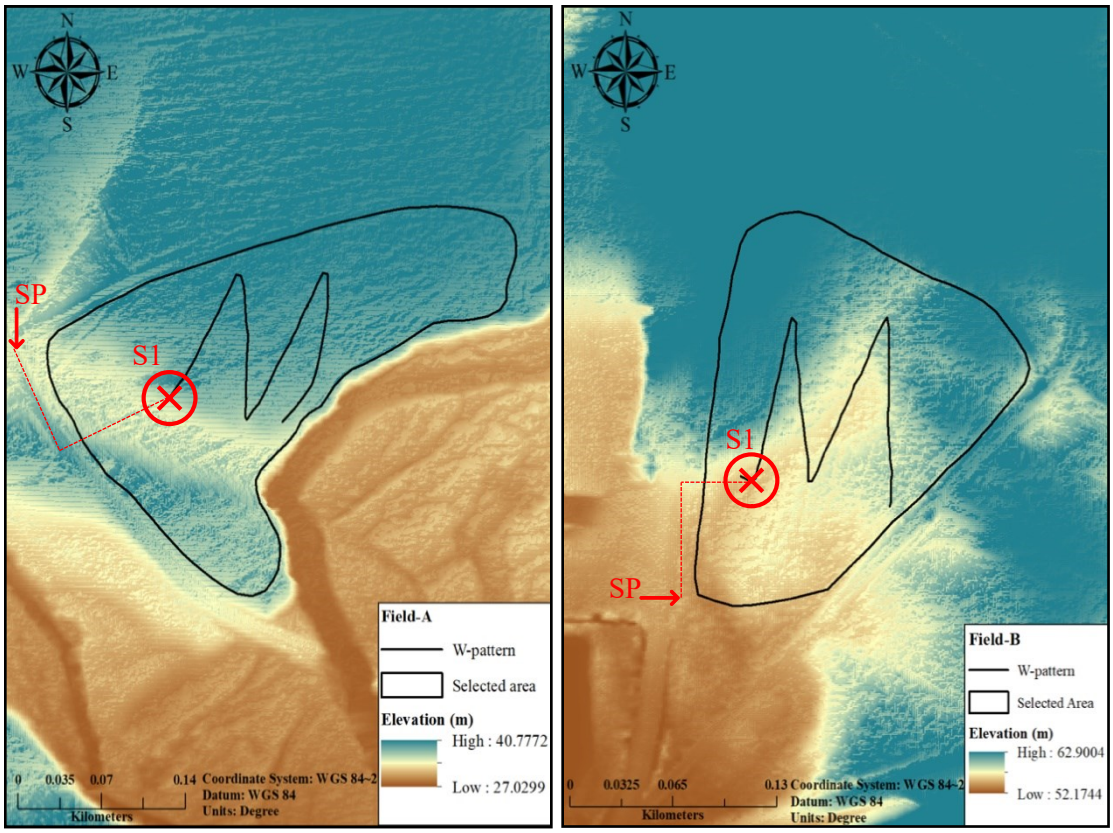

(a) (b)

Figure 4-3: Digital Elevation Models (DEMs) representing elevation profile of selected sites: (a) Field-A; (b) Field-B. The arrow indicates the starting point (SP) of selecting the first sampling location following the W-pattern technique and encircled cross sign represent the first sampling location in each field.

A wooden quadrat 0.81 m^2 was placed at each selected sampling point to define the area of interest for data collection. The center of the defined area of interest was flagged using a small metallic flag poles (**Figure 4-4**). Each flag was numbered and assigned randomly to a selected treatment. For each experimental treatment, a total of four replications were carried out, and radar output were recorded accordingly. Within the defined area of interest (0.81 m^2), manual ground surface heights were measured three times from the bottom of the radar sensor to the ground using a measuring scale. An average of three readings was recorded for each sampling area of interest. The mounting height of the radar sensor and ground speed of the SFMV were adjusted before reaching

each flagged position. The radar outputs were recorded each time that the radar travelled over the flagged location (center of the area of interest).

(a) (b)

Figure 4-4: Sampling location in Field-A (a) and Field-B (b) with an area of interest (labelled using red dotted square) and corresponding flag poles.

4.2.5 Statistical Analysis

The developed ground surface detection system's accuracy was analyzed in a dynamic state. This was accomplished by calculating the difference between manually measured and radar recorded ground surface heights at selected treatment conditions (ground speed and mounting height) using Eq. 1.

$$y_d = y - y^* \qquad \text{Eq. 1}$$

Where, y^* represents the ground surface height predicted by the developed system, y represents corresponding manually measured ground surface height, and y_d represents the difference. The developed system indicated the highest mean discrepancy of 4.5 mm

during standstill operation in the statistical analysis included in previous chapters. To analyze the performance accuracy of developed system in dynamic state operation, the calculated mean difference was compared with the known mean discrepancy value of 4.5 mm using paired t-test. The output of the developed system was correlated with manually measured ground surface height using linear regression analysis.

A 3x3 factorial analysis of variance (ANOVA) was used to analyze the joint effect of selected treatments on the real-time performance of a developed ground surface detection system. The significant factor of interest in factorial ANOVA was further analyzed using Fisher Least Significant Difference (LSD) to determine which specific mean significantly differs from others in selected treatment conditions. All statistical analyses were carried out using Minitab 19 (Minitab Inc., USA) at a 5% level of significance.

4.3 Results and Discussion

The developed ground surface detection system's outputs were compared with the manually measured ground surface height in both fields. Paired t-test analyses were performed separately for each field against known mean discrepancy (4.5 mm) (**Table 4-1**).

Table 4-1: Results of paired mean comparison between radar recorded and manually measured ground surface height in both fields.

Description	N	p-value	95% CI for μ^* (cm)
Field-A	36	0.51	(0.25, 0.55)
Field-B	36	0.11	(0.21, 0.47)

*Range where the mean difference (between radar predicted and actual ground surface height) resided with 95% certainty; CI – Confidence Interval; N – Total number of sampling points

Paired t-test resulted in non-significant results (**Table 4-1**) when the mean difference between radar predicted and actual ground surface height in both fields were compared to the known hypothesized mean offset of 4.5 mm. The results suggested that

mean discrepancy was not significantly different than the expected discrepancy value of 4.5 mm (p-value > 0.05). Confidence Interval at a 5% level of significance indicated the range in which the mean difference lied with 95% certainty. The performance of the developed radar system was slightly better in Field-B as 95% confidence interval range resulted in relatively smaller mean values as compared to Field-A. However, the performance of developed system in both fields was statistically not significantly different, as 95% confidence interval for both fields included the known mean discrepancy (4.5 mm) within the calculated range.

The paired t-test indicated that the developed radar system operated with similar accuracy in dynamic and static state operation for both fields. Overall, paired t-test results showed that the developed system could successfully read the actual ground surface height with a 4.5 mm maximum offset in both dynamic and static states of operation.

Table 4-2: Results of regression analyses for both fields along with the regression equation expressions for predicting the actual ground surface height using a developed system.

Description (Selected fields)	**Regression Equation (cm)**	**N**	**Co-efficient of determination (R^2)**
Field-A	$^{**}PGSH = {}^{*}AGH + (0.32)$	36	0.99
Field-B	$^{**}PGSH = {}^{*}AGH + (0.07)$	36	0.99

*AGH – Actual ground surface height measured manually; **PGSH – Predicted ground surface height by the developed system

Predicted ground surface heights were correlated with manually measured (actual) ground surface heights in both fields using linear regression analyses (**Table 4-2**; **Figure 4-5**; **Figure 4-6**). A significant correlation was found between the predicted and actual ground surface height in both fields ($R^2 = 0.99$). This implies that the 99% variability in predicted ground surface height can be explained using a single factor of actual ground surface height. The linear regression analyses implied that a developed ground surface

detection system could be used to predict the actual ground surface height efficiently in a non-destructive manner.

Scatter plots were developed between predicted and actual ground surface height to visualize the developed system's real-time performance in both fields (**Figure 4-5**; **Figure 4-6**), where a straight red line represented the 1:1 values of actual ground surface heights. A cluster of predicted values was observed at three distinct sections of the plots: between 50-66 cm, between 70-86 cm, and between 90-106 cm, which represented the ground surface heights at 60 cm, 80 cm, and 100 cm mounting heights respectively. Field-A indicated a more compact cluster of predicted values (**Figure 4-5**) compared to Field-B (**Figure 4-6**) at selected mounting height levels. This indicates that Field-B had a more variable topography than Field-A.

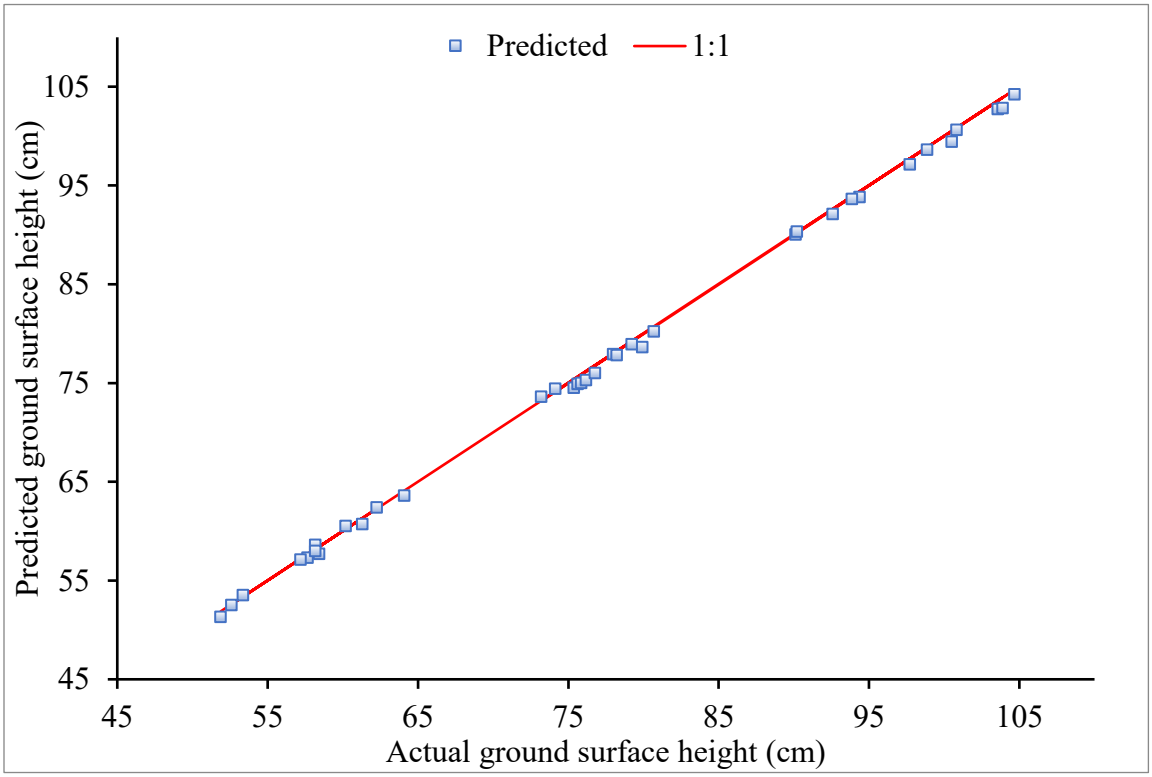

Figure 4-5: Relationship between actual and predicted ground surface heights at selected treatment conditions in Field-A.

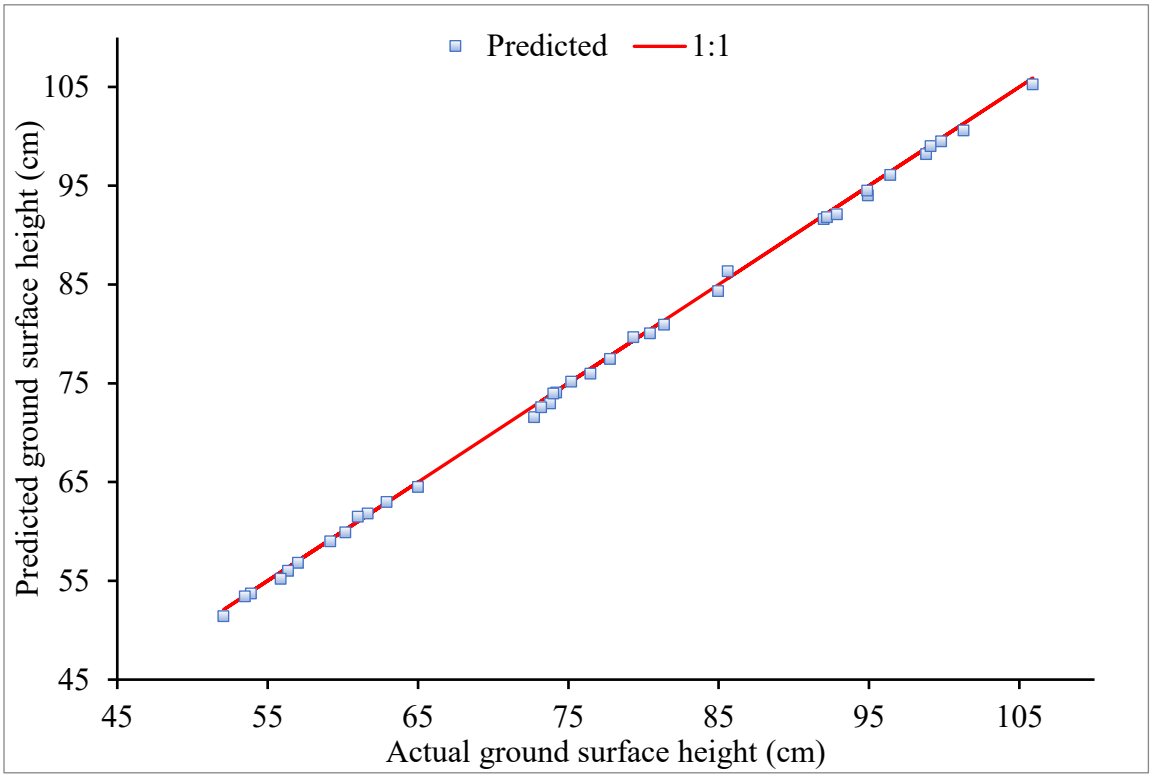

Figure 4-6: Relationship between actual and predicted ground surface heights at selected treatment conditions in Field-B.

Ground surface height values predicted by the developed system were found to be in close agreement with manually recorded ground surface height with slight constant offset (Field-A: 2.7 mm; Field-B: 0.3 mm) in predicted expressions (**Table 4-2**). Since the mean discrepancy in dynamic state operation was not significantly different from the mean discrepancy in static state operation, the developed system's re-calibration was not required for its application in dynamic state operation.

Table 4-3: Results of 3x3 factorial ANOVA including two factors of interest: i) Mounting height (0.60, 0.80, and 1.00 m); and ii) Ground speed (1.2, 1.6, 2.0 km h^{-1}).

Source Variables	Field-A	Field-B
Mounting height	*	*
Ground speed	NS	NS
Mounting height * Ground Speed	NS	NS

NS – Non-significant; * – Significant at 95% confidence interval

Factorial ANOVA was carried out to analyze the effect of two main factors of interest: i) selected mounting height levels from the flat ground (0.60, 0.80, and 1.00 m), and ii) traditional harvester ground speeds (1.2, 1.6, and 2.0 km h^{-1}). The 3x3 factorial ANOVA for both fields resulted in a non-significant effect of ground speed (Field-A: p-value = 0.760; Field-B: p-value = 0.221) on the performance of the developed system. Results from ANOVA implied that the developed system could detect the ground surface height in real-time operation regardless of ground speed (**Table 4-3**). Interaction effect of ground speed and mounting height was also added in the evaluation model to analyze the combined effect on radar's output, which was deemed statistically non-significant by ANOVA results (**Table 4-3**) in both fields (Field-A: p-value = 0.976; Field-B: p-value = 0.407).

Results of ANOVA suggested that factor including mounting height was the only significant factor in both fields (Field-A and Field B: p-value < 0.001). The significance of this factor was expected as mounting height level delineates a reference point for the developed system to detect and measure ground surface height correctly.

Table 4-4: Mean predicted height resulted by Fisher LSD and mean actual height of the detected ground surface at selected mounting heights.

Mounting Height (cm)	**Mean PGSH (cm)**	**Mean AGH (cm)**
Field-A		
100	97.10a*	97.60
80	76.42b*	76.94
60	57.75c*	57.94
Field-B		
100	95.74a**	96.15
80	76.54b**	76.95
60	58.01c**	58.22

*Letter grouping resulted by Fished LSD analyses of Field-A mean predicted heights; **Letter grouping resulted by Fished LSD analyses of Field-B mean predicted heights; AGH – Actual ground surface height measured manually; PGSH – Predicted ground surface height by the developed system

To determine that the developed system successfully distinguished the ground surface heights captured at selected reference levels of mounting height (0.60, 0.80, and 1.00 m), the significant factor of interest was further analyzed for multiple mean comparisons using the Fisher LSD method. The result of multiple mean comparisons suggested that the developed system successfully detected and measured the ground surface height at the selected mounting height level in both fields (**Table 4-4**). Letter groupings resulted by Fisher LSD analyses implied that any of the selected mounting height levels could be used for the correct operation of the developed system. It also indicated that there was no occurrence of erroneous overlapping readings between selected mounting heights (Fished LSD resulted in letter grouping which was not shared between means at different mounting height) (**Figure 4-7**).

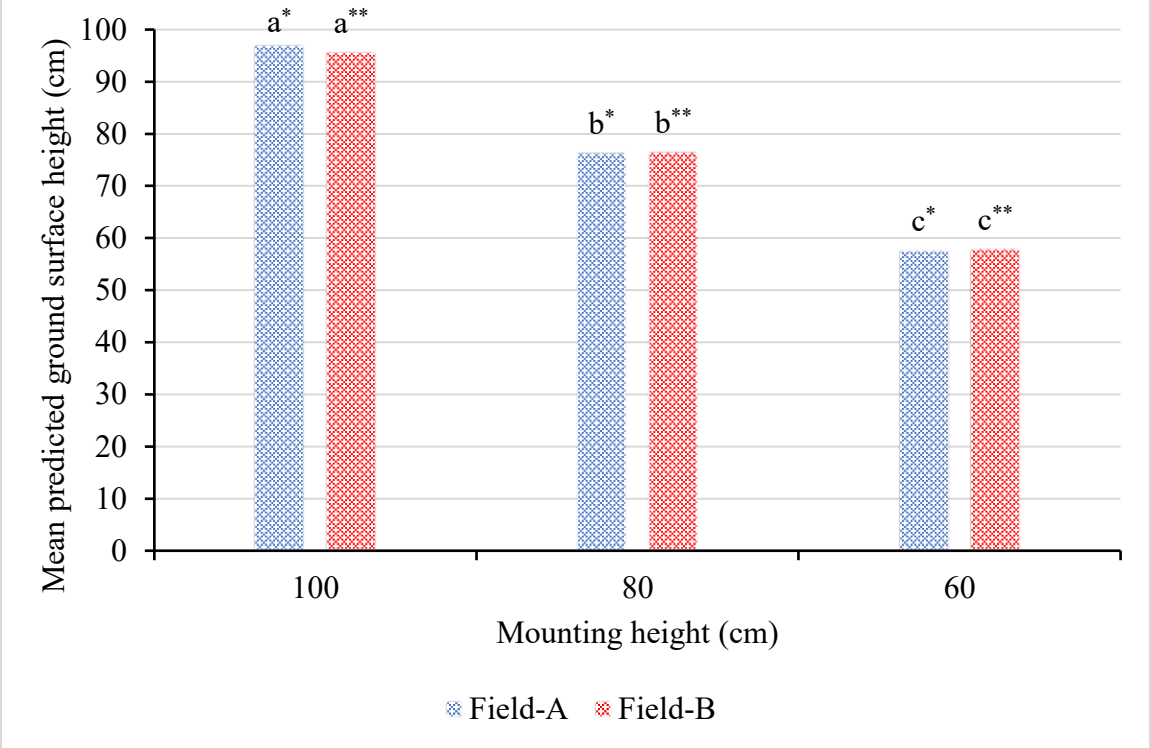

Figure 4-7: Letter grouping assigned by Fisher LSD method to groups representing different mounting heigh levels for both fields. Means not sharing the same letter is significantly different from each other. * represents Field-A letter grouping and ** represents Field-B letter grouping.

4.4 Conclusion

This research study's primary goal was to examine the impact of machine parameters, including ground speed and sensor mounting height, on the real-time performance of ground surface detection systems through field testing in commercial wild blueberry field. The mean predicted height at a selected speed and the mounting height level were compared to the developed system's maximum known discrepancy (4.5 mm) using a paired t-test at a 95% confidence interval. Paired t-test led to non-significant results implying that the mean discrepancy of the developed system remained unaffected by ground speed and mounting height level (p-value > 0.05). The predicted ground surface heights were strongly correlated to the actual ground surface height measured manually (R^2 = 0.99). A 3x3 factorial ANOVA suggested that ground detection was not affected significantly by the combined effect of travel speed and mounting height (p-value > 0.05). Multiple means comparison (MMC) of mounting height indicated that mean height measured at three selected heights were significantly different from each other. Results from MMC suggested that the developed system had an optimum performance at all selected mounting height levels. All three mounting heights were found to be equally accurate for measuring ground surface height using the developed system with a vertical resolution of approximately 4.5 mm at a 5% level of significance.

CHAPTER 5: CONCLUSIONS AND RECOMMENDATIONS

5.1 Conclusions

Mechanical harvesting of wild blueberries is highly dependent on operator proficiency for maximizing the fruit yield and profit margins. Adjusting the harvester head height with reference to variable topography in addition to avoid the contact between harvester picking teeth and potentially harmful objects hidden below the crop canopy (i.e., rocks etc.) defines a few most crucial factors determining the overall efficiency of the berry picking operation. Parallel tasks including head height adjustment, picking reels rotational speed regulation, ground speed manipulation, and fruit bin handling can make the operator's job very difficult. Alleviated operator fatigue can adversely affect the berry picking operation which demands the automation of wild blueberry harvester for achieving optimum harvesting efficiency. This research focused on the development and evaluation of a non-destructive ground surface detection system to aid the automation of harvester head height with reference to the variable ground surface.

Initially, three radars employing distinct microwave frequency bands (Acconeer: 60 GHz, Walabot: 3.3-10 GHz, and Terrahawk®: 1.5-6.5 GHz) were selected, and their feasibility to detect the ground surface was evaluated under controlled conditions in the Lab environment. The main factors of interest included in the designed experiments during Lab evaluations were three mounting height levels (i.e., 0.60, 0.80, and 1.00 m), vegetation covers (control, alfalfa hay, and grass clippings), and the three selected ground surfaces (aluminum sheets, wooden boards, and soil samples). The response variable in all the designed experiments was simulated ground surface height by the selected radars. The performance of selected radar sensors was compared in terms of precision, accuracy, and

bias. Statistical measures including standard deviation (SD), interquartile range (IQR), root mean square error (RMSE), and mean bias error (MBE) were utilized to calculate and compare the selected performance parameters during Lab evaluations (i.e., precision, accuracy, and bias).

During the initial Lab evaluations, the Terrahawk® radar was identified as the best performing radar with the highest precision (SD < 1.27 cm) and accuracy (RMSE: 4.45-5.62 cm) among the selected radars. Preliminary evaluations also suggested that Terrahawk® radar showed positive bias (underestimation) in all the trials as compared to other selected radars which lacked this consistency and resulted in positive and negative bias randomly in different trials. It was suggested from the preliminary evaluation results that calibration of Terrahawk® radar was required to compensate the mean offset in the predicted heights. Following the preliminary evaluations, the Terrahawk® radar was then subjected to calibration to enhance the performance efficiency and reducing the offset in ground surface height measurement.

The calibration was completed in both Lab and field environments using suitable regression models. Regression analyses indicated the best fitted model was linear for both Lab (R^2 = 0.99) and field (R^2 = 0.99) conditions. The data collected for the calibration purpose also indicated that offset was significantly reduced using the developed calibration models in both the selected environments (Lab: RMSE = 0.21-0.48 cm; Field: RMSE = 0.37-0.45 cm). A ground surface detection system was then developed using the Terrahawk® radar as a primary building block with best fitted linear regression model and a field laptop acting as an external processing and display unit for data acquisition for real-time field evaluations.

To determine the real-time performance efficiency of the developed system, evaluations were carried out in two wild blueberry fields selected in central Nova Scotia. Overall field evaluations were alienated into two objectives: the first was to analyze the performance of developed system under steady-state (standstill) conditions, and the second objective analyzed the performance of developed system under dynamic state conditions. Specifically, the first objective analyzed the effect of plant and fruit characteristics on the performance of the developed system and the second objective evaluated the effect of machine parameters (i.e., ground speed) on the performance of the developed ground surface detection system.

During the standstill conditions, the output of the developed system significantly correlated (R^2 = 0.92-0.99) with manually measured ground surface heights from the base of the radar sensor. Stepwise multiple linear regression models included the radar output only as a significant factor of interest. Results from the stepwise multiple linear regression indicated that plant characteristics (i.e., stem height, stem thickness, stem density, fruit zone height, and fruit density) did not significantly affect the system's performance. The newly developed system was successful in detecting the ground surface height irrespective of the plant characteristics. Output of the developed ground surface detection system showed a high degree of agreement (d = 0.96-0.99) with the ground truth data to estimate the true ground surface height non-destructively, which proposed a high degree of accuracy related to the Terrahawk® radar. The developed system resulted in the mean discrepancy of 0.37-0.45 mm between simulated and manually measured ground surface heights.

During the dynamic state conditions, the radar performance at selected mounting heights (0.60, 0.80, and 1.00 m) was evaluated under traditional harvester ground speeds

(1.2, 1.6, and 2.0 km h^{-1}). The mean predicted height at selected ground speed and mounting height level were compared with the maximum known discrepancy (4.5 mm) of the developed system using paired t-test at a 95% confidence interval. Paired t-test led to non-significant results implying that the mean discrepancy of the developed system remained unaffected by ground speed and mounting height level (p-value > 0.05). Predicted ground surface heights were strongly correlated to the actual ground surface height measured manually (R^2 = 0.99). A 3x3 factorial ANOVA suggested that ground detection was not affected significantly by the combined effect of travel speed and mounting height (p-value > 0.05). Overall, the developed system measured the ground surface with a high degree of accuracy and showed great potential in real-time ground surface detection in wild blueberry fields.

5.2 Recommendations

Mechanical harvesting has been proven to be the most cost-effective method to harvest wild blueberries. However, the harvest efficiency is highly dependent on the operator's skill to adjust the machine parameters according to the spatial variability encountered in the fields. A non-contact radar-based ground surface detection and height measurement system was developed and analyzed for its application in wild blueberry fields. Results of this study emphasize on consideration of the following recommendations:

- The system developed during this research is recommended for consideration as a basis for the automation of wild blueberry harvester as it provides real-time feedback of ground surface height.
- It is further recommended to develop a closed-loop feedback controller for the integration of the developed system with a mechanical harvester to

autonomously adjust the harvester head height with variable ground topography.

- The new system involving the closed loop feedback from the developed ground surface detection system must be evaluated for its application, preferably, during real-time harvesting operation in wild blueberry fields.
- The harvest efficiency of the manually operated mechanical wild blueberry harvester should be compared with the harvester integrated with the newly developed system to analyze the viability of autonomous operation.
- Complete and reliable automation of harvester head height requires the real-time feedback of plant characteristics (canopy height and fruit zone height) in addition to ground surface height. Therefore, the feasibility of microwave radar technology should be further explored to detect the fruit zone height, canopy height, and ground surface height simultaneously. Feedback from plant canopy and fruit zone heights in addition to ground surface height would help to develop a more efficient and accurate controller to automate the harvester head positioning.
- For safe operation and handling of Terrahawk® radar, the two radars must be 1.5 m apart all the time if both are operational at the same instant.

REFERENCES

Acconeer. (2019). A111 - Pulsed Coherent Radar (PCR). Online Datasheet. Retrieved December 21, 2019, from https://media.digikey.com/pdf/Data%20Sheets/Acconeer%20PDFs/A111_Datasheet_v0.8_PRELIMINARY.pdf

Adamski, W., & Kitlinski, M. (2001). On measurements applied in scientific researches of microwave heating processes. *Measurement Science Review, 1*(1), 199-203.

Agriculture and Agri-Food Canada. (2016). *Canadian Blueberries*. Online Database. http://www.agr.gc.ca/eng/industry-markets-and-trade/buying-canadian-food-products/canadian-blueberries/?id=1426167712421

Agriculture and Agri-Food Canada. (2017). *Crop Profile for lowbush blueberry in Canada, 2014.* Online Database. http://publications.gc.ca/collections/collection_2017/aac-aafc/A118-10-31-2014-eng.pdf

Ali, S. (2016). *Effects of harvesting time on berry losses during mechanical harvesting of wild blueberries* [Master's Thesis, Dalhousie University, NS, Canada]. http://hdl.handle.net/10222/72041

Ali, S., Zaman, Q. U., Farooque, A. A., Schumann, A. W., Udenigwe, C. C., Esau, T., & Chang, Y. K. (2018). Potential use of digital photographic technique to examine wild blueberry ripening in relation to time of harvest. *Applied Engineering in Agriculture, 34*(2), 299-308. https://doi.org/fxsn

Astatkie, T. (2006). Absolute and relative measures for evaluating the forecasting performance of time series models for daily streamflows. *Hydrology Research, 37*(3), 205-215. https://doi.org/10.2166/nh.2006.008

Aziz, S. A., Steward, B. L., Birrell, S. J., Kaspar, T. C., & Shrestha, D. S. (2004). Ultrasonic sensing for corn plant canopy characterization. ASAE Annual International Meeting 2004. https://doi.org/fxrm

Baghdadi, N., Boyer, N., Todoroff, P., El Hajj, M., & Bégué, A. (2009). Potential of SAR sensors TerraSAR-X, ASAR/ENVISAT and PALSAR/ALOS for monitoring sugarcane crops on Reunion Island. *Remote Sensing of Environment, 113*(8), 1724-1738. https://doi.org/10.1016/j.rse.2009.04.005

Ballester-Berman, J. D., Lopez-Sanchez, J. M., & Fortuny-Guasch, J. (2005). Retrieval of biophysical parameters of agricultural crops using polarimetric SAR interferometry. *IEEE Transactions on Geoscience and Remote Sensing, 43*(4), 683-694. https://doi.org/10.1109/TGRS.2005.843958

Barker, W. G., Hall, I. V., Aalders, L. E., & Wood, G. W. (1964). The lowbush blueberry industry in eastern Canada. *Economic Botany, 18*(4), 357-365. https://doi.org/10.1007/BF02862721

Bausch, W. C., & Delgado, J. A. (2003). Ground-based sensing of plant nitrogen status in irrigated corn to improve nitrogen management. In *Digital imaging and spectral techniques: Applications to precision agriculture and crop physiology* (pp. 151-163). ASA Speical Publications. https://doi.org/10.2134/asaspecpub66.c12

Bietresato, M., Carabin, G., Vidoni, R., Gasparetto, A., & Mazzetto, F. (2016). Evaluation of a LiDAR-based 3D-stereoscopic vision system for crop-monitoring applications. *Computers and Electronics in Agriculture, 124*, 1-13. https://doi.org/10.1016/j.compag.2016.03.017

Borden, K. A., Isaac, M. E., Thevathasan, N. V., Gordon, A. M., & Thomas, S. C. (2014). Estimating coarse root biomass with ground penetrating radar in a tree-based intercropping system. *Agroforestry systems, 88*(4), 657-669. http://dx.doi.org/10.1007/s10457-014-9722-5

Borjas, G. J. (2003). The labor demand curve is downward sloping: Reexamining the impact of immigration on the labor market. *The quarterly journal of economics, 118*(4), 1335-1374. https://doi.org/10.1162/003355303322552810

Brakke, T. W., Kanemasu, E. T., Steiner, J. L., Ulaby, F. T., & Wilson, E. (1981). Microwave radar response to canopy moisture, leaf-area index, and dry weight of wheat, corn, and sorghum. *Remote Sensing of Environment, 11*, 207-220. https://doi.org/10.1016/0034-4257(81)90020-1

Bramley, R. G. V. (2005). Understanding variability in winegrape production systems 2. Within vineyard variation in quality over several vintages. *Australian Journal of Grape and Wine Research, 11*(1), 33-42. https://doi.org/10.1111/j.1755-0238.2005.tb00277.x

Brodie, G., Jacob, M. V., & Farrell, P. (2016). A Brief Overview of Radio Frequency and Microwave Applications in Agriculture. In *Microwave and Radio-Frequency Technologies in Agriculture: An Introduction for Agriculturalists and Engineers* (pp. 19-31). Walter de Gruyter GmbH & Co KG. http://hdl.handle.net/11343/58280

Bruder, J. A. (2013). IEEE Radar standards and the radar systems panel. *IEEE Aerospace and Electronic Systems Magazine, 28*(7), 19-22. https://doi.org/fxsv

Bush, T. F., & Ulaby, F. T. (1978). An evaluation of radar as a crop classifier. *Remote Sensing of Environment, 7*(1), 15-36.

Butnor, J. R., Doolittle, J. A., Kress, L., Cohen, S., & Johnsen, K. H. (2001). Use of ground-penetrating radar to study tree roots in the southeastern United States. *Tree physiology, 21*(17), 1269-1278. https://doi.org/10.1093/treephys/21.17.1269

Carrière, S. D., Chalikakis, K., Sénéchal, G., Danquigny, C., & Emblanch, C. (2013). Combining electrical resistivity tomography and ground penetrating radar to study geological structuring of karst unsaturated zone. *Journal of Applied Geophysics, 94*, 31-41. https://doi.org/10.1016/j.jappgeo.2013.03.014

Chang, Y. K., Zaman, Q. U., Farooque, A. A., Rehman, T. U., & Esau, T. J. (2016). An on-the-go ultrasonic plant height measurement system (UPHMS II) in the wild

blueberry cropping system. 2016 ASABE Annual International Meeting. https://doi.org/fxrh

Chang, Y. K., Zaman, Q. U., Farooque, A. A., Schumann, A. W., & Percival, D. C. (2012). An automated yield monitoring system II for commercial wild blueberry double-head harvester. *Computers and electronics in agriculture, 81*, 97-103. https://doi.org/10.1016/j.compag.2011.11.012

Chang, Y. K., Zaman, Q. U., Rehman, T. U., Farooque, A. A., Esau, T. J., & Jameel, M. W. (2017). A real-time ultrasonic system to measure wild blueberry plant height during harvesting. *Biosystems engineering, 157*, 35-44. https://doi.org/10.1016/j.biosystemseng.2017.02.004

Colaço, A. F., Molin, J. P., Rosell-Polo, J. R., & Escolà, A. (2018). Application of light detection and ranging and ultrasonic sensors to high-throughput phenotyping and precision horticulture: current status and challenges. *Horticulture research, 5*(1), 35. https://doi.org/10.1038/s41438-018-0043-0

Collins, M. E., & Doolittle, J. A. (1987). Using Ground-Penetrating Radar to Study Soil Microvariability 1. *Soil Science Society of America Journal, 51*(2), 491-493. https://doi.org/10.2136/sssaj1987.03615995005100020045x

Collins, M. E., Schellentrager, G. W., Doolittle, J. A., & Shih, S. F. (1986). Using Ground-penetrating Radar to Study Changes in Soil Map Unit Composition in Selected Histosols 1. *Soil Science Society of America Journal, 50*(2), 408-412. https://doi.org/10.2136/sssaj1986.03615995005000020030x

Cunha, F., & Youcef-Toumi, K. (2018, May). Ultra-Wideband Radar for Robust Inspection Drone in Underground Coal Mines. *2018 IEEE International Conference on Robotics and Automation (ICRA), Australia* (pp. 86-92). https://doi.org/gh3stg

Daian, G., Taube, A., Birnboim, A., Shramkov, Y., & Daian, M. (2005). Measuring the dielectric properties of wood at microwave frequencies. *Wood Science and Technology, 39*(3), 215-223. https://doi.org/10.1007/s00226-004-0281-1

Dale, A. E., Hanson, J., Yarborough, D. E., McNicol, R. J., Stang, E. J., Brenan, R., Morris, J., & Hergert, G. B. (1994). Mechanical harvesting of berry crops. In J. Janick (Eds.), *Horticultural Reviews* (Vol. 16, pp. 255-382). John Wiley & Sons. http://dx.doi.org/10.1002/9780470650561.ch8

Davis, J. L., & Annan, A. P. (1989). Ground-penetrating radar for high-resolution mapping of soil and rock stratigraphy 1. *Geophysical prospecting, 37*(5), 531-551. https://doi.org/10.1111/j.1365-2478.1989.tb02221.x

Dirac, P. A. M. (1927). The quantum theory of the emission and absorption of radiation. *Proceedings of the Royal Society of London. Series A, Containing Papers of a Mathematical and Physical Character, 114*(767), 243-265. https://doi.org/10.1098/rspa.1927.0039

Dobson, M. C., & Ulaby, F. T. (1986). Active microwave soil moisture research. *IEEE Transactions on Geoscience and Remote Sensing,* (1), 23-36. https://doi.org/dk27z4

Doolittle, J. A. (1987). Using Ground-penetrating Radar to Increase the Quality and Efficiency of Soil Surveys 1. *Soil survey techniques, 20*, 11-32. https://doi.org/10.2136/sssaspecpub20.c2

Doolittle, J. A., Rebertus, R. A., Jordan, G. B., Swenson, E. I., & Taylor, W. H. (1988). Improving soil-landscape models by systematic sampling with ground-penetrating radar. *Soil Horizons, 29*(2), 46-54.

Du, Y., Ulaby, F. T., & Dobson, M. C. (2000). Sensitivity to soil moisture by active and passive microwave sensors. *IEEE Transactions on Geoscience and Remote Sensing, 38*(1), 105-114. https://doi.org/bbgqrc

Eaton, L. J. (1988). *Nitrogen Cycling in Lowbush Blueberry Stands* [Doctoral Dissertation, Dalhousie University, NS, Canada].

Eaton, L. J. (1994). Long-term effects of herbicide and fertilizers on lowbush blueberry growth and production. *Canadian Journal of plant science, 74*(2), 341-345. https://doi.org/10.4141/cjps94-066

Eaton, L. J., & Nams, V. O. (2006). Second cropping of wild blueberries—effects of management practices. *Canadian Journal of plant science*, *86*(4), 1189-1195. https://doi.org/10.4141/P05-134

Einstein, A. (1951). The advent of the quantum theory. *Science, 113*(2926), 82-84.

Engman, E. T., & Chauhan, N. (1995). Status of microwave soil moisture measurements with remote sensing. *Remote Sensing of Environment, 51*(1), 189-198. https://doi.org/10.1016/0034-4257(94)00074-W

Esau, K., Esau, T. J., Zaman, Q. U., Farooque, A. A., & Schumann, A. W. (2018). Effective use of a variable speed blower fan on a mechanical wild blueberry harvester. *Applied Engineering in Agriculture*. https://doi.org/10.13031/aea.12818

Esau, T. J., MacEachern, C. B., & Zaman, Q. U. (2020). Development and Evaluation of a Closed-Loop Control System for Automation of a Mechanical Wild Blueberry Harvester's Picking Reel. *AgriEngineering, 2*(2), 322-335. https://doi.org/10.3390/agriengineering2020022

Esau, T. J., MacEachern, C. B., Farooque, A. A., & Zaman, Q. U. (2021). Evaluation of Autosteer in Rough Terrain at Low Ground Speed for Commercial Wild Blueberry Harvesting. *Agronomy, 11*(2), 384. https://doi.org/10.3390/agronomy11020384

Esau, T. J., Zaman, Q. U., Chang, Y. K., Schumann, A. W., Percival, D. C., & Farooque, A. A. (2014). Spot-application of fungicide for wild blueberry using an automated prototype variable rate sprayer. *Precision agriculture, 15*(2), 147-161. http://doi.org/10.1007/s11119-013-9319-4

Esau, T. J., Zaman, Q. U., MacEachern, C., Farooque, A. A., & Mohamed, M. (2019). Precise Picking Height Positioning on Wild Blueberry Harvesters using Electric Linear Actuators. 2019 ASABE Annual International Meeting. https://doi.org/fxrc

Escolà, A., Planas, S., Rosell, J. R., Pomar, J., Camp, F., Solanelles, F., Gracia, F.,

Llorens, J., & Gil, E. (2011). Performance of an ultrasonic ranging sensor in apple tree canopies. *Sensors, 11*(3), 2459-2477. https://doi.org/10.3390/s110302459

Farooque, A. A, Chang, Y. K., Zaman, Q. U., Nguyen-Quang, T., Groulx, D., & Schumann, A. W. (2016a). Development of a predictive model for wild blueberry harvester fruit losses during harvesting using artificial neural network. *Applied Engineering in Agriculture, 32*(6), 725-738. https://doi.org/f9k3kc

Farooque, A. A. (2015). *Performance evaluation of a commercial wild blueberry harvester using precision agriculture technologies and mathematical modeling* [Doctoral Dissertation, Dalhousie University, NS, Canada]. http://hdl.handle.net/10222/58860

Farooque, A. A., Chang, Y. K., Zaman, Q. U., Groulx, D., Schumann, A. W., & Esau, T. J. (2013). Performance evaluation of multiple ground based sensors mounted on a commercial wild blueberry harvester to sense plant height, fruit yield and topographic features in real-time. *Computers and electronics in agriculture, 91*, 135-144. https://doi.org/10.1016/j.compag.2012.12.006

Farooque, A. A., Jameel, M. W., Zaman, Q. U., Esau, T. J., Schumann, A. W., & Abbas, F. (2020). Impact of Wild Blueberry Fruit Characteristics and Machine Parameters on Performance of a Mechanical Harvester: Basis for Automation. *Applied Engineering in Agriculture, 36*(3), 271-280. https://doi.org/fxst

Farooque, A. A., Zaman, Q. U., Chang, Y., Esau, T. J., Schumann, A. W., & Jameel, W. (2016b). Variation in harvesting losses in relation to fruit yield, plant height and slope: A basis for automation of harvester. 2016 American Society of Agricultural and Biological Engineers Annual International Meeting. https://doi.org/fxrf

Farooque, A. A., Zaman, Q. U., Esau, T. J., Chang, Y. K., Schumann, A. W., & Jameel, W. (2017). Influence of wild blueberry fruit yield, plant height, and ground slope on picking performance of a mechanical harvester: Basis for automation. *Applied engineering in agriculture, 33*(5), 655-666. https://doi.org/gcgtf4

Farooque, A. A., Zaman, Q. U., Groulx, D., Schumann, A. W., Yarborough, D. E., & Nguyen-Quang, T. (2014). Effect of ground speed and header revolutions on the picking efficiency of a commercial wild blueberry harvester. *Applied engineering in agriculture, 30(*4), 535-546. 10.13031/aea.30.10415

Farooque, A. A., Zaman, Q. U., Schumann, A. W., Madani, A., & Percival, D. C. (2012). Response of wild blueberry yield to spatial variability of soil properties. *Soil Science, 177*(1), 56-68. https://doi.org/dcnx69

Fleming, J. A. (1910). *The Principles of Electric Wave Telegraphy and Telephony*. Longmans, Green & Co.

Fricke, T., & Wachendorf, M. (2013). Combining ultrasonic sward height and spectral signatures to assess the biomass of legume–grass swards. *Computers and Electronics in Agriculture, 99*, 236-247. https://doi.org/10.1016/j.compag.2013.10.004

Fricke, T., Richter, F., & Wachendorf, M. (2011). Assessment of forage mass from grassland swards by height measurement using an ultrasonic sensor. *Computers and electronics in agriculture, 79*(2), 142-152. https://doi.org/10.1016/j.compag.2011.09.005

Friesen, J., Steele-Dunne, S. C., & van de Giesen, N. (2012). Diurnal differences in global ERS scatterometer backscatter observations of the land surface. *IEEE Transactions on Geoscience and Remote Sensing, 50*(7), 2595-2602. https://doi.org/gg3npp

Frolking, S., Milliman, T., Palace, M., Wisser, D., Lammers, R., & Fahnestock, M. (2011). Tropical forest backscatter anomaly evident in SeaWinds scatterometer morning overpass data during 2005 drought in Amazonia. *Remote Sensing of Environment, 115*(3), 897-907. https://doi.org/10.1016/j.rse.2010.11.017

GeoNOVA. (2019). *Data Locator-Elevation Explorer.* Online Database. Retrieved February 25, 2021, from https://nsgi.novascotia.ca/datalocator/elevation/

Glass, V. M., & Percival, D. C. (2000). Challenges facing pollination and fruit set in indigenous blueberries (Vaccinium angustifolium Ait.). *Journal-American Pomological Society*, 54, 44-47.

Goodman, D. (1994). Ground-penetrating radar simulation in engineering and archaeology. *Geophysics, 59*(2), 224-232. https://doi.org/10.1190/1.1443584

Government of Nova Scotia (2019). *Minister accepts minimum wage increase recommendations*. Retrieved December 13, 2020, from https://novascotia.ca/news/release/?id=20190108002.

Gray, L. G. (1970). *Development of a hollow reel raking mechanism for harvesting lowbush blueberries* [Doctoral Dissertation, University of Maine, Maine, United States of America].

Hall, I. V. (1955). Floristic changes following the cutting and burning of a woodlot for blueberry production. *Canadian Journal of Agricultural Science, 35*(2), 143-152. https://doi.org/10.4141/agsci-1955-0020

Hall, I. V., Aalders, L. E., Jackson, L. P., Wood, G. W., & Lockhart, C. L. (1967). Lowbush blueberry production in Canada. Publ. 1278. Ottawa, Ontario: Canadian Dep. Agric.

Hall, I. V., Aalders, L. E., Nickerson, N. L., & Vander Kloet, S. P. (1979). Biological flora of Canada. I. Vaccinium angustifolium Ait., sweet lowbush blueberry. *Canadian field-naturalist*, *93*(4), 415-430. http://pascal-francis.inist.fr/vibad/index.php?action=getRecordDetail&idt=PASCAL8010243753

Hall, I. V., Craig, D. L., & Lawrence, R. A. (1983). A comparison of hand raking and mechanical harvesting of lowbush blueberries. *Canadian Journal of plant science, 63*(4), 951-954. https://doi.org/10.4141/cjps83-119

Headsight Inc. (2019). *Terrahawk Horizon Manual 09062203a*. Online Datasheet. Retrieved December 23, 2019, from

http://www.headsight.com/sites/default/files/manuals/09062203a_terrahawk_horizon_0.pdf

Hepler, P. R., & Yarborough, D. E. (1991). Natural variability in yield of lowbush blueberries. *HortScience, 26*(3), 245-246. https://doi.org/10.21273/HORTSCI.26.3.245

Holland, K. H., Schepers, J. S., & Shanahan, J. F. (2006). Configurable multi-spectral active sensor for highspeed plant canopy assessment. In D. J. Mulla (Ed.), *Proceedings of the 8th International Conference on Precision Agriculture (CD)*. Minneapolis, MN, USA: University of Minnesota.

Houldcroft, C. J., Campbell, C. L., Davenport, I. J., Gurney, R. J., & Holden, N. (2005). Measurement of canopy geometry characteristics using LiDAR laser altimetry: A feasibility study. *IEEE Transactions on Geoscience and Remote Sensing, 43*(10), 2270-2282. https://doi.org/bdr4cv

Hruska, J., Čermák, J., & Šustek, S. (1999). Mapping tree root systems with ground-penetrating radar. *Tree Physiology, 19*(2), 125-130. https://doi.org/10.1093/treephys/19.2.125

Hutchings, N. J., Phillips, A. H., & Dobson, R. C. (1990). An ultrasonic rangefinder for measuring the undisturbed surface height of continuously grazed grass swards. *Grass and Forage Science, 45*(2), 119-127. https://doi.org/10.1111/j.1365-2494.1990.tb02192.x

Jackson, T. J., Le Vine, D. M., Hsu, A. Y., Oldak, A., Starks, P. J., Swift, C. T., Isham, J., D., & Hakem, M. (1999). Soil moisture mapping at regional scales using microwave radiometry: The Southern Great Plains Hydrology Experiment. *IEEE transactions on geoscience and remote sensing, 37*(5), 2136-2151. https://doi.org/fpn6sp

Jameel, M., Zaman, Q., Schumann, A., Farooque, T., Brewster, G., Nguyen-Quang, H., & Chattha. (2016). Effect of plant characteristics on picking efficiency of the wild blueberry harvester. *Applied Engineering in Agriculture, 32*(5), 589-598. https://doi.org/f9cmfz

Jamieson, A. R. (2008). Developing seed-propagated lowbush blueberry families. *HortScience, 43*(6), 1686-1689. https://doi.org/10.21273/HORTSCI.43.6.1686

Jordan, W. C., & Eaton, L. J. (1995). A comparison of first and second cropping years of Nova Scotia lowbush blueberries (Vaccinium angustifolium) Ait. *Canadian Journal of plant science, 75*(3), 703-707. https://doi.org/10.4141/cjps95-120

Khan, A. H. (2019). *Economic Analysis of Alternative Mechanical Harvesting Systems for Wild Blueberries* [Master's Thesis, Dalhousie University, NS, Canada]. http://hdl.handle.net/10222/76266

Kinsman, G. (1993). *The history of the lowbush blueberry industry in Nova Scotia 1950-1990*. Nova Scotia Dept. of Agriculture & Marketing. http://hdl.handle.net/10222/28451

Kraszevvski, A. W., & Nelson, S. O. (2003). Microwave techniques in agriculture.

Journal of microwave power and electromagnetic energy, 38(1), 13-35. https://doi.org/10.1080/08327823.2003.11688485

Kraszewski, A. W., & Nelson, S. O. (1995). Application of microwave techniques in agricultural research. *Proceedings of 1995 SBMO/IEEE MTT-S International Microwave and Optoelectronics Conference* (Vol. 1, pp. 117-126). https://doi.org/db5hsd

Kumar, S., & Shukla, S. (2014). *Concepts and Applications of Microwave Engineering*. PHI Learning Pvt. Ltd.

Laymon, C. A., Crosson, W. L., Jackson, T. J., Manu, A., & Tsegaye, T. D. (2001). Ground-based passive microwave remote sensing observations of soil moisture at S-band and L-band with insight into measurement accuracy. *IEEE transactions on geoscience and remote sensing, 39*(9), 1844-1858. https://doi.org/fcghzm

Liu, H., Koyama, C. N., Takahashi, K., & Sato, M. (2014, June). High-resolution imaging of damaged wooden structures for building inspection by polarimetric radar. *Proceedings of the 15th International Conference on Ground Penetrating Radar* (pp. 423-428). https://doi.org/fxsz

Maierhofer, C. (2003). Nondestructive evaluation of concrete infrastructure with ground penetrating radar. *Journal of Materials in Civil Engineering, 15*(3), 287-297. https://doi.org/10.1061/(ASCE)0899-1561(2003)15:3(287)

Malay, W. J. (2000). *Spatial variability and yield monitor evaluation for carrots and wild blueberries* [Master's Thesis, Nova Scotia Agricultural College, NS, Canada].

McCully, K. V., Sampson, M. G., & Watson, A. K. (1991). Weed survey of Nova Scotia lowbush blueberry (Vaccinium angustifolium) fields. *Weed Science,* 180-185. http://dx.doi.org/10.1017/S0043174500071447

McKeand, P. (2014). Interpreting Ground-penetrating Radar for Archaeology. *Plains Anthropologist, 59*(229), 98-100. https://doi.org/10.1179/0032044714z.00000000010

McKiel, C. (1958). *The design and development of a pneumatic blueberry harvester* [Master's Dissertation, University of Maine, Orono, USA].

McKinley, K. (2007). Ground-Penetrating Radar for Archaeology. *Historical Archaeology, 41*(2), 173-174. https://doi.org/10.1007/BF03377017

McNairn, H., & Brisco, B. (2004). The application of C-band polarimetric SAR for agriculture: A review. *Canadian Journal of Remote Sensing, 30*(3), 525-542. https://doi.org/10.5589/m03-069

Meng, K., & Meng, Y. (2019). Through-Wall Pose Imaging in Real-Time with a Many-to-Many Encoder/Decoder Paradigm. *2019 18th IEEE International Conference On Machine Learning And Applications (ICMLA)* (pp. 14-21). https://doi.org/fxsr

Mohamed, M., Zaman, Q. U., Esau, T., & Farooque, A., A. (2018). Design of Ground Surface Sensing using RADAR. *Proceedings of 14th International Conference on*

Precision Agriculture. Montreal, Quebec: International Society of Precision Agriculture (ICAP), June 24th - 27th, 2018.

Montgomery, D., Holmén, G., Almers, P., & Jakobsson, A. (2019, October). Surface Classification with Millimeter-Wave Radar Using Temporal Features and Machine Learning. *2019 16th European Radar Conference (EuRAD)* (pp. 1-4). IEEE.

Naesset, E., & Bjerknes, K. O. (2001). Estimating tree heights and number of stems in young forest stands using airborne laser scanner data. *Remote sensing of Environment, 78*(3), 328-340. https://doi.org/10.1016/S0034-4257(01)00228-0

Nelson, S. O. (2005). Dielectric spectroscopy in agriculture. *Journal of Non-Crystalline Solids, 351*(33-36), 2940-2944. https://doi.org/10.1016/j.jnoncrysol.2005.04.081

Noyman, Y., & Shmulevich, I. (1996). Ground surface sensing through plant foliage using an FM-CW radar. *Computers and electronics in agriculture, 15*(3), 181-193. https://doi.org/10.1016/0168-1699(96)00015-4

Paget, A. C., Long, D. G., & Madsen, N. M. (2016). RapidScat diurnal cycles over land. *IEEE Transactions on Geoscience and Remote Sensing, 54*(6), 3336-3344. https://doi.org/f8q845

Passive. Vol. I: Microwave Remote Sensing Fundamentals and Radiometry. Artech House Publishers.

Paul, C. R. (2006). *Introduction to electromagnetic compatibility* (Vol. 184). John Wiley & Sons Publications Inc. Retrieved December 29, 2019, from https://cds.cern.ch/record/995029/files/9780471755005_TOC.pdf

Puckett, W. E., Collins, M. E., & Schellentrager, G. W. (1990). Design of soil map units on a karst area in West Central Florida. *Soil Science Society of America Journal, 54*(4), 1068-

Rhodes, R. B. (1961). The harvesting of lowbush blueberries. *American Society of Agriculture Engineers,* 61-206.

Richard, P. (1982). Development of a mechanical harvester for lowbush blueberries [Bachelor's Thesis, Nova Scotia Agriculture College, Truro, NS, Canada].

Scotford, I. M., & Miller, P. C. H. (2004). Combination of spectral reflectance and ultrasonic sensing to monitor the growth of winter wheat. *Biosystems Engineering, 87*(1), 27-38. https://doi.org/10.1016/j.biosystemseng.2003.09.009

Shih, S. F., & Doolittle, J. A. (1984). Using Radar to Investigate Organic Soil Thickness in the Florida Everglades 1. *Soil Science Society of America Journal, 48*(3), 651-656. https://doi.org/10.2136/sssaj1984.03615995004800030036x

Skriver, H., Mattia, F., Satalino, G., Balenzano, A., Pauwels, V. R., Verhoest, N. E., & Davidson, M. (2011). Crop classification using short-revisit multitemporal SAR data. *IEEE Journal of Selected Topics in Applied Earth Observations and Remote Sensing, 4*(2), 423-431. https://doi.org/bzm5fd

Soule, H. M. (1969). Developing a lowbush blueberry harvester. *Transactions of the ASAE*, *12*(1), 127-0129. https://doi.org/fxrb

Soule, H. M., & Gray, G. L. (1972). Performance tests for a lowbush blueberry harvester. *CSAE Paper*, 72-316.

Spaete, L. P., Glenn, N. F., Derryberry, D. R., Sankey, T. T., Mitchell, J. J., & Hardegree, S. P. (2011). Vegetation and slope effects on accuracy of a LiDAR-derived DEM in the sagebrush steppe. *Remote Sensing Letters, 2*(4), 317-326. https://doi.org/10.1080/01431161.2010.515267

Statistics Canada. (2018). *Blueberry area by census division (CD), 2016 Canada.* Online Database. https://www150.statcan.gc.ca/n1/pub/95-634-x/2017001/article/54905/catm-ctra-205-eng.htm

Statistics Canada. (2021). *Table 32-10-0364-01. Area, Production and Farm gate value of marketed fruits*. Online Database. https://doi.org/10.25318/3210036401-eng.

Stove, A. G. (1992). Linear FMCW radar techniques. *IEEE Proceedings F (Radar and Signal Processing)* (Vol. 139, No. 5, pp. 343-350). IET Digital Library. https://doi.org/cb2hn3

Strik, B. C., & Yarborough, D. (2005). Blueberry production trends in North America, 1992 to 2003, and predictions for growth. *HortTechnology, 15*(2), 391-398. https://doi.org/fxsw

Sui, R., & Thomasson, J. A. (2006). Ground-based sensing system for cotton nitrogen status determination. *Transactions of the ASABE, 49*(6), 1983-1991. https://doi.org/fxrk

Tamado, T., & Milberg, P. (2000). Weed flora in arable fields of eastern Ethiopia with emphasis on the occurrence of Parthenium hysterophorus. *Weed Research, 40*(6), 507-521. https://doi.org/10.1046/j.1365-3180.2000.00208.x

Thomas, A. G. (1985). Weed survey system used in Saskatchewan for cereal and oilseed crops. *Weed Science,* 34-43. http://dx.doi.org/10.1017/S0043174500083892

Toomay, J. C., & Hannen, P. J. (2004). *Radar Principles for the Non-specialist* (Vol. 2). SciTech Publishing.

Truman, C. C., Perkins, H. F., Asmussen, L. E., & Allison, H. D. (1988). Using ground-penetrating radar to investigate variability in selected soil properties. *Journal of soil and water conservation, 43*(4), 341-345.

Ulaby, F. T., & Jedlicka, R. P. (1984). Microwave dielectric properties of plant materials. *IEEE Transactions on Geoscience and Remote Sensing,* (4), 406-415. https://doi.org/cdkw3b

Ulaby, F. T., Dubois, P. C., & Van Zyl, J. (1996). Radar mapping of surface soil moisture. *Journal of Hydrology, 184*(1-2), 57-84. https://doi.org/10.1016/0022-1694(95)02968-0

Ulaby, F.T., Moore, R.K. and Fung, A.K. (1981). *Microwave Remote Sensing: Active and Passive (Volume 1*). Addison-Wesley, Reading, UK.

Vander Kloet, S. P. (1978). Systematics, distribution, and nomenclature of the polymorphic Vaccinium angustifolium. *Rhodora, 80*(823), 358-376. https://www.jstor.org/stable/23311154

Walabot (2019). *Walabot – Technical Brief*. Online Datasheet. Retrieved December 20, 2019, from https://walabot.com/docs/walabot-tech-brief-416?type=pdf.

Walabot (2020). *Walabot API: Overview of Walabot Application*. Online Database. Retrieved January 19, 2020, from https://api.walabot.com/.

Walther, B. A., & Moore, J. L. (2005). The concepts of bias, precision and accuracy, and their use in testing the performance of species richness estimators, with a literature review of estimator performance. *Ecography, 28*(6), 815-829. https://doi.org/10.1111/j.2005.0906-7590.04112.x

Wang, R., Xiang, S., Feng, C., Wang, P., Ergan, S., & Fang, Y. (2019). Through-wall object recognition and pose estimation. *Proceedings of the International Symposium on Automation and Robotics in Construction (ISARC)* (Vol. 36, pp. 1176-1183). https://doi.org/ggdsgw

WBPANS. (2018). *June 2018 Dispatch*. http://www.nswildblueberries.com/members/newsletters/download?path=June2018.pdf

Wilding, L. P. (1985). Spatial variability: its documentation, accomodation and implication to soil surveys. *Soil spatial variability Conference, Las Vegas NV, November 30th – December 1st, 1984* (pp. 166-194).

Willmott, C. J. (1981). On the validation of models. *Physical geography, 2*(2), 184-194. https://doi.org/10.1080/02723646.1981.10642213

Wood, G. W. (2004). The wild blueberry industry-past. *Small Fruits Review, 3*(1-2), 11-18. https://doi.org/10.1300/J301v03n01_03

Woods, G. S., Maskell, D. L., & Ruxton, A. B. (1999). Microwave ground level detection sensor. *1999 Asia Pacific Microwave Conference (APMC'99). Microwaves Enter the 21st Century* (Vol. 2, pp. 531-534). https://doi.org/cnx6g6

Yarborough, D. E. (1997). Production trends in the wild blueberry industry in North America. *Acta Horticulturae*, (446)*,* 33-36. https://doi.org/10.17660/ActaHortic.1997.446.1

Yarborough, D. E. (2001). *Progress Towards the development of a mechanical harvester for wild blueberries.* Wild Blueberry Fact Sheet No. 226, University of Maine Cooperative Extension, Orono, Maine, USA. Retrieved September 18, 2019, from https://extension.umaine.edu/blueberries/factsheets/production/progress-towards-the-development-of-a-mechanical-harvester-for-wild-blueberries/

Yarborough, D. E. (2004). Factors contributing to the increase in productivity in the wild

blueberry industry. *Small Fruits Review, 3*(1-2), 33-43. https://doi.org/10.1300/J301v03n01_05

Yarborough, D. E. (2009). *Wild Blueberry*. University of Maine Cooperative Extension. Retrieved September 11, 2019, from www.wildblueberries.maine.edu/

Yarborough, D. E. (2018). *Blueberry Production Around the Globe* [Annual Meeting Presentation]. WBPANS Annual General Meeting November 2018, NS, Canada.

Yarborough, D., Drummond, F., Annis, S., & D'Appollonio, J. (2017). Maine wild blueberry systems analysis. *Acta Hortic, 1180*, 151-160. https://doi.org/10.17660/ActaHortic.2017.1180.21

Yarborough, D.E. (2017). *Blueberry Enterprise Budget.* Wild Blueberry Fact Sheet No. 260, University of Maine Cooperative Extension, Orono, Maine, USA. Retrieved February 17, 2020, from https://extension.umaine.edu/blueberries/factsheets/marketing-and-business-management/260-blueberry-enterprise-budget/

Yuzugullu, O., Erten, E., & Hajnsek, I. (2015). Rice growth monitoring by means of X-band co-polar SAR: Feature clustering and BBCH scale. *IEEE Geoscience and Remote Sensing Letters, 12*(6), 1218-1222. https://doi.org/f68d85

Zaman, Q. U., & Salyani, M. (2004). Effects of foliage density and ground speed on ultrasonic measurement of citrus tree volume. *Applied Engineering in Agriculture, 20*(2), 173. https://doi.org/fxrj

Zaman, Q. U., Percival, D. C., Gordon, R. J., & Schumann, A. W. (2009). Estimation of wild blueberry fruit yield using digital color photography. *Acta Horticulturae*, (824), 57-65. https://doi.org/10.17660/ActaHortic.2009.824.6

Zaman, Q. U., Schumann, A. W., & Percival, D. C. (2010a). An automated cost-effective system for real-time slope mapping in commercial wild blueberry fields. *HortTechnology, 20*(2), 431-437. https://doi.org/10.21273/HORTTECH.20.2.431

Zaman, Q. U., Swain, K. C., Schumann, A. W., & Percival, D. C. (2010b). Automated, low-cost yield mapping of wild blueberry fruit. *Applied Engineering in Agriculture, 26*(2), 225-232. https://doi.org/fxrd

Zhang, F., Zaman, Q. U., Percival, D. C., & Schumann, A. W. (2010). Detecting bare spots in wild blueberry fields using digital color photography. *Applied engineering in agriculture, 26*(5), 723-728. https://doi.org/fxs3